



SATELLITE REENTRY CONTROL
VIA
SURFACE AREA AMPLIFICATION

THESIS

Salvador Alemán, Captain, USAF

AFIT/GSS/ENY/09-M01

DEPARTMENT OF THE AIR FORCE
AIR UNIVERSITY

AIR FORCE INSTITUTE OF TECHNOLOGY

Wright-Patterson Air Force Base, Ohio

APPROVED FOR PUBLIC RELEASE; DISTRIBUTION UNLIMITED.

The views expressed in this thesis are those of the author and do not reflect the official policy or position of the United States Air Force, Department of Defense, or the United States Government.

AFIT/GSS/ENY/09-M01

SATELLITE REENTRY CONTROL
VIA
SURFACE AREA AMPLIFICATION

THESIS

Presented to the Faculty
Department of Aeronautical and Astronautical Engineering
Graduate School of Engineering and Management
Air Force Institute of Technology
Air University
Air Education and Training Command
In Partial Fulfillment of the Requirements for the
Degree of Master of Science (Space Systems)

Salvador Alemán, BSME
Captain, USAF

March 2009

APPROVED FOR PUBLIC RELEASE; DISTRIBUTION UNLIMITED.

AFIT/GSS/ENY/09-M01

SATELLITE REENTRY CONTROL
VIA
SURFACE AREA AMPLIFICATION

Salvador Alemán, BSME
Captain, USAF

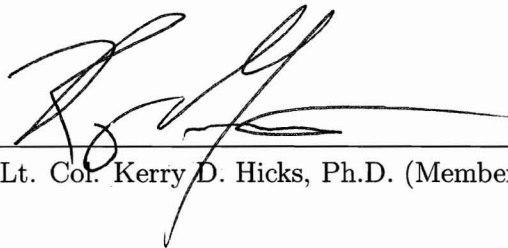
Approved:



William E. Wiesel, Ph.D. (Chairman)




Date



Lt. Col. Kerry D. Hicks, Ph.D. (Member)



Date



Robert B. Greendyke, Ph.D. (Member)



Date

Abstract

This project endeavors to find whether it is feasible to use an increase in surface area as a way of increasing the drag on an orbiting object, thus decreasing its orbital lifetime. The surface area increase can be achieved by an apparatus that deploys a balloon. The balloon will act as a parachute that will decrease the potential energy of the object through atmospheric drag. This is most effective by objects that reach the Low Earth altitudes of less than 500 kilometers, where an object is encountering a firmer atmospheric density.

The project is carried out through propagating three different element sets to reentry using STK[®]. The orbital paths generated by the software are then graphed in Microsoft Excel[®] and presented.

The analysis is divided into four main studies. The first study focuses on confirming the effects the atmospheric instability has on the long term predictions of a natural decay. The second study explores how an increase in the scale of the drag, at different points in the orbital path, affects the reentry time. The third study investigates a specific increase of area to mass ratio (A/M) at different points in the trajectory. This is to survey changes in the variability of the reentry time prediction and how the reentry location's variability is altered. To finish off, the last study examines how A/M manipulation affects the reentry time prediction.

The project discovered that an increase in A/M decreases the variability in reentry prediction. Furthermore, it discerns the exponential relationship between the time to reentry and the A/M .

AFIT/GSS/ENY/09-M01

To My Wife

Acknowledgements

First and foremost, I want to thank my Lord Jesus Christ for everything that I have been blessed with and this accomplished work. I owe a large debt of gratitude and pay my respects to Dr. William E. Wiesel for his guidance through this project. I also want to thank my reading committee, in particular Lt. Col. Hicks. Finally, I would not have been able to accomplish all this work without the support from my father, mother, and especially my wife.

Salvador Alemán

Table of Contents

	Page
Abstract	iv
Acknowledgements	vi
List of Figures	x
List of Tables	xv
List of Symbols	xvi
List of Abbreviations	xvii
 I. Introduction	 1
1.1 Space Environment	1
1.2 Removal of Space Debris Needed	1
1.3 Thesis Purpose	2
1.4 Atmospheric Instability	2
1.5 Previous Attempts at Enforced Reentry	3
 II. Problem Background and Review	 4
2.1 A Space Debris Problem	4
2.1.1 Science and Technology Council Update Report	5
2.1.2 United Nations Updates Their Report	6
2.1.3 IADC Publishes Guidelines	8
2.1.4 NASA Provides More Guidelines	9
2.1.5 Problem Wrap Up	11
2.2 Population Safety	12
2.2.1 Skylab Reentry	12
2.2.2 Cosmos 954 Reentry	13
2.2.3 USA 193 Destruction	13
2.2.4 Other Famous Reentries	14
2.3 Attempt to Enforce a Safe Reentry	16
2.3.1 Design Strategy	16
2.3.2 Tether Technology	16
2.4 Balloon Satellites	17
2.5 Atmospheric Unpredictability	19
2.6 Square Cube Law	22

	Page
III. Methodology	24
3.1 Initial Set Up and First Study: Variability in Reentry Prediction Due to the Atmosphere	24
3.1.1 Propagator	24
3.1.2 Reentry Criterion	25
3.1.3 Simulated Orbits	25
3.1.4 Object Parameters	26
3.1.5 Trajectory Data	26
3.1.6 Chosen Atmospheric Model	26
3.2 Second Study: Drag Scale Increase Study	27
3.2.1 Greater Scale Increase	28
3.3 Third Study: Single A/M Increase at Several Points in Orbital Path	28
3.4 Fourth Study: A/M Manipulation at a Single Point in Orbital Path	30
IV. Simulation Results & Analysis	31
4.1 Atmospheric Unpredictability	31
4.1.1 Debris Reentry Prediction	31
4.1.2 ISS Orbit Reentry Prediction	33
4.1.3 Terrasar-X Prediction	34
4.1.4 Atmospheric Unpredictability Conclusion	37
4.2 Drag Increase by a Factor	38
4.2.1 Debris Orbit Reentry	38
4.2.2 ISS Orbit Reentry	42
4.2.3 Terrasar-X Orbit Reentry	46
4.2.4 Drag Increase Conclusion	49
4.3 Reentry Prediction with a Single Increase to A/M at Several Points in Orbit Path	50
4.3.1 Debris Variability Change	50
4.3.2 ISS Element Variability Change	63
4.3.3 Terrasar-X Element Variability Change	65
4.3.4 Conclusion of Reentry Variability Due to A/M Change	65
4.4 Reentry Prediction Change by A/M Manipulation at a Single Point	67
V. Conclusions and Recomendations	71
5.1 Atmospheric Unpredictability	71
5.2 Drag Increase by a Factor	71
5.3 Decrease Variability in Reentry Prediction and Manipulation of A/M	71
5.4 Parachute Proposal	73
5.4.1 Design Parameters	73

	Page
5.4.2 Prototype Use	73
5.4.3 Further Research Needed	74
Appendix A. Orbital Element Sets	75
A.1 Orbital Element Sets Used For Simulations	75
Appendix B. STK Propagator Inputs	80
B.1 Set Up Inputs for Simulations	80
Appendix C. Graphs From Chapter Four	84
C.1 Graphs From Section Three and Four of Chapter Four	84
Bibliography	105

List of Figures

Figure		Page
2.1	Model values for current spatial density. [6]	7
2.2	Typical ranges for number of major collisions for three scenarios, 1995-2095. [6]	7
2.3	Protected regions. [8]	9
2.4	Debris count as of August 2007. [10]	9
2.5	On-orbit objects by type. [10]	10
2.6	Debris projections. [26]	11
2.7	Skylab workshop, May 14, 1973. [35]	12
2.8	Delta II rocket body in Texas. [24]	14
2.9	Delta II Rocket body in Saudi Arabia. [24]	15
2.10	Delta II Rocket body in South Africa. [24]	15
2.11	The Echo I team stand in front of their balloon. [21]	18
2.12	Pageos I inflation test. [16]	18
2.13	Atmosphere picture taken from the ISS. [12]	19
2.14	Solar wind disrupting earth's magnetic field. [30]	20
2.15	Solar's unusual activities during Solar Min. [32]	21
2.16	Increase in length demonstration. [19]	22
2.17	Drastic surface area comparison. [19]	23
4.1	Debris orbit reentry predictions by ten atmospheric models.	31
4.2	Summarized predicted reentry times for Debris orbit.	32
4.3	ISS orbit reentry predictions by ten atmospheric models.	33
4.4	Summarized predicted reentry times for ISS Orbit.	34
4.5	Terrasar-X orbit reentry predictions by seven atmospheric models.	35
4.6	Terrasar-X orbit reentry predictions by three atmospheric models.	36
4.7	Summarized predicted reentry times for Terrasar-X orbit.	37
4.8	Debris reentry predictions due to drag increase at several points in the orbit path.	38

Figure		Page
4.9	Predicted reentry times for Debris orbit; Original vs. New Time to Decay plot; New over Original Time to Decay Ratio plot.	39
4.10	Debris reentry predictions due to extreme drag increase at several points in the orbit path.	40
4.11	(Second) Predicted reentry times for Debris orbit; Original vs. New Time to Decay plot; New over Original Time to Decay Ratio plot.	41
4.12	ISS reentry predictions due to drag increase at several points in the orbit path.	42
4.13	Predicted reentry times for ISS orbit; Original vs. New Time to Decay plot; New over Original Time to Decay Ratio plot.	43
4.14	ISS reentry predictions due to extreme drag increase at several points in the orbit path.	44
4.15	(Second) Predicted reentry times for ISS orbit; Original vs. New Time to Decay plot; New over Original Time to Decay Ratio plot.	45
4.16	Terrasar-X reentry predictions due to drag increase at several points in the orbit path.	46
4.17	Predicted reentry times for ISS orbit; Original vs. New Time to Decay plot; New over Original Time to Decay Ratio plot.	47
4.18	Terrasar-X Reentry predictions due to extreme drag increase at several points in the orbit path.	48
4.19	(Second) Predicted reentry times for ISS orbit; Original vs. New Time to Decay plot; New over Original Time to Decay Ratio plot.	49
4.20	Debris orbit reentry predictions by ten atmospheric models with a single A/M increase 57 hours prior to original reentry.	51
4.21	Homed in Debris orbit reentry predictions by ten atmospheric models with a single A/M increase 57 hours prior to original reentry.	52
4.22	Summarized predicted Debris orbit reentry times and locations by ten atmospheric models with a single A/M increase 57 hours prior to original reentry.	53
4.23	Debris orbit reentry predictions by ten atmospheric models with a single A/M increase 24 hours prior to original reentry.	55

Figure		Page
4.24	Homed in Debris orbit reentry predictions by ten atmospheric models with a single A/M increase 24 hours prior to original reentry. .	56
4.25	Summarized predicted Debris orbit reentry times and locations by ten atmospheric models with a single A/M increase 24 hours prior to original reentry.	57
4.26	Debris orbit reentry predictions by ten atmospheric models with a single A/M increase 10 hours prior to original reentry.	59
4.27	Homed in Debris orbit reentry predictions by ten atmospheric models with a single A/M increase 10 hours prior to original reentry. .	60
4.28	Summarized predicted Debris orbit reentry times and locations by ten atmospheric models with a single A/M increase 10 hours prior to original reentry.	61
4.29	Summarized Debris orbit orbit reentry time spreads with a single A/M increase at 57, 24, and 10 hours prior to original reentry. . . .	62
4.30	Summarized ISS orbit reentry time spreads with a single A/M increase at 180, 24, and 10 hours prior to original reentry.	64
4.31	Summarized Terrasar-X orbit reentry time spreads with a single A/M increase at 72, 24, and 10 hours prior to original reentry. . . .	66
4.32	Reentry predictions as A/M changes between 0.01 and 1.00 at a single point in orbit path.	68
4.33	Summarized reentry prediction times as A/M changes between 0.001 and 1.000 at a single point in orbit path.	69
4.34	Comparison: Time to reentry as a function of A/M vs Neutral Density profile	70
A.1	Orbital element set for Debris orbit.	76
A.2	Orbital element set for ISS orbit.	77
A.3	Orbital element set Terrasar-X orbit.	78
A.4	Orbital element set keys.	79
B.1	STK propagator inputs for Debris orbit simulation.	81
B.2	STK propagator inputs for ISS orbit simulation.	82
B.3	STK propagator inputs for Terrasar-X orbit simulation.	83

Figure		Page
C.1	ISS orbit reentry predictions by ten atmospheric models with a single A/M increase 180 hours prior to original reentry.	85
C.2	Homed in ISS orbit reentry predictions by ten atmospheric models with a single A/M increase 180 hours prior to original reentry. . . .	86
C.3	Summarized predicted ISS orbit reentry times and locations by ten atmospheric models with a single A/M increase 180 hours prior to original reentry.	87
C.4	ISS orbit reentry predictions by ten atmospheric models with a single A/M increase 24 hours prior to original reentry.	88
C.5	Homed in ISS orbit reentry predictions by ten atmospheric models with a single A/M increase 24 hours prior to original reentry. . . .	89
C.6	Summarized predicted ISS orbit reentry times and locations by ten atmospheric models with a single A/M increase 24 hours prior to original reentry.	90
C.7	ISS orbit reentry predictions by ten atmospheric models with a single A/M increase 10 hours prior to original reentry.	91
C.8	Homed in ISS orbit reentry predictions by ten atmospheric models with a single A/M increase 10 hours prior to original reentry. . . .	92
C.9	Summarized predicted ISS orbit reentry times and locations by ten atmospheric models with a single A/M increase 10 hours prior to original reentry.	93
C.10	Terrasar-X orbit reentry predictions by ten atmospheric models with a single A/M increase 72 hours prior to original reentry.	94
C.11	Homed in Terrasar-X orbit reentry predictions by ten atmospheric models with a single A/M increase 72 hours prior to original reentry.	95
C.12	Summarized predicted Terrasar-X orbit reentry times and locations by ten atmospheric models with a single A/M increase 72 hours prior to original reentry.	96
C.13	Terrasar-X orbit reentry predictions by ten atmospheric models with a single A/M increase 24 hours prior to original reentry.	97
C.14	Homed in Terrasar-X orbit reentry predictions by ten atmospheric models with a single A/M increase 24 hours prior to original reentry.	98

Figure		Page
C.15	Summarized predicted Terrasar-X orbit reentry times and locations by ten atmospheric models with a single A/M increase 24 hours prior to original reentry.	99
C.16	Terrasar-X orbit reentry predictions by ten atmospheric models with a single A/M increase 10 hours prior to original reentry.	100
C.17	Homed in Terrasar-X orbit reentry predictions by ten atmospheric models with a single A/M increase 10 hours prior to original reentry.	101
C.18	Summarized predicted Terrasar-X orbit reentry times and locations by ten atmospheric models with a single A/M increase 10 hours prior to original reentry.	102
C.19	Homed in Reentry predictions as A/M changes between 0.10 and 1.00 at a single point in orbit path.	103
C.20	All reentry predictions as A/M changes between 0.001 and 1.000 at a single point in orbit path.	104

List of Tables

Table		Page
2.1	Estimated debris population. [5]	5
2.2	Catalogued objects by altitude ranges. [5]	6
2.3	Tether table performance. [17]	16
3.1	Satellite's inertial matrix.	26

List of Symbols

Symbol		Page
\mathbf{a}_d	Acceleration Due to Drag	28
C_d	Object's Coefficient of Drag	28
ρ	Atmospheric Density	28
A	Object's Cross-sectional Area Perpendicular to Velocity	28
m	Object's Mass	28
\mathbf{v}	Object's Velocity	28

List of Abbreviations

Abbreviation		Page
US	United States of America	4
IADC	Inter-Agency Space Debris Coordination Committee	4
NASA	National Aeronautics and Space Administration	4
STD 8719.14	NASA Technical Standard 8719.14	5
NPR	NASA Procedural Requirements-8715.6	5
NHDBK	NASA Handbook 8719.14	5
NSTC	National Science and Technology Council	5
ISS	International Space Station	5
LEO	Low Earth Orbit	8
GEO	Geosynchronous	8
DoD	Department of Defense	13
EST	Eastern Standard Time	13
ATP	Area-Time-Product	17
GTO	Geotransfer	17
MSIS	Mass Spectrometer and Incoherent Scatter Radar	20
CIRA	COSPAR International Reference Atmosphere	20
COSPAR	Committee on Space Research	20
NRLMSISE-00	Navy Research Lab MSIS-Exosphere 2000	20
STK	Satellite Tool Kit	24
AGI	Analytical Graphics, Inc	24
SI	International System of Units	24
LLA	Latitude, Longitude, Altitude	26
ISS	International Space Station	27
A/M	Area to Mass Ratio (meters squared per kilogram)	28

SATELLITE REENTRY CONTROL VIA SURFACE AREA AMPLIFICATION

I. Introduction

Since the launch of Sputnik I the space community has placed every possible object into orbit, from animals to sophisticated satellites. These activities have had important missions but there has not been a strong and consistent worldwide effort into mitigating the space debris problem we are facing today. Understandably, the space debris problem was left alone with the purpose of benefiting the advancement of technology, as well as not adding another burden to the space acquisitions and budgets of the world. Nonetheless, space operational regions are a limited resource that must be protected.

1.1 *Space Environment*

Currently the total debris amount hovers about the twelve thousand mark, which includes objects in all orbits. Projections (using current trends and not accounting for mitigation measures) for Low Earth Orbiting debris only are in the eleven thousand range by the year 2010. To make things worse, some satellites' missions never even get started. In the last few decades, total satellite failures have happened with an almost predictable regularity. These failures have left the objects floating in orbit to naturally decay back to the earth. Some of these failures have been of objects close to earth with periods small enough to reenter the earth's atmosphere within a few years or even months.

1.2 *Removal of Space Debris Needed*

Objects in orbit that have no control system are, in essence, kinetic weapons with hypervelocities in the range of kilometers per second. For this reason, it is

advantageous to have the objects reenter since it lessens the possibility of orbital collisions amongst debris and decreases the danger of damage or destruction of active satellites. The root concept behind this thesis is the basic principal that drag causes an object to decrease in orbital period, eventually making it reenter.

Another reason to have an object reenter in a controlled manner is the safety of the population. There are satellites that carry large payloads such as the Skylab reentry on July 11, 1979, which was around one hundred tons. There are dangerous satellites such as Cosmos 954 that reentered on January 24, 1978, which had a nuclear reactor and spread radioactive fuel on a 600 kilometer path. Other failed payloads include USA 193, which was shattered to pieces by a missile on February 21, 2008, in the interest of population safety.

1.3 Thesis Purpose

The goal of this thesis is to bring forth and establish the idea that we can gain a certain amount of control over reentering objects that have no control. The idea would be implemented by a small independent system that will only manipulate the drag of the object. Consequently, the time and place of reentry within a particular window may be chosen. Fundamentally, this thesis presents the proposal of increasing the atmospheric drag of an object through the increase in the object's surface area, thus increasing its area-to-mass ratio. The surface area increase will be through the inflation of a balloon that will act as a parachute on the object. The new area-to-mass ratio is what will directly increase the atmospheric drag on the object, decreasing its period, and ultimately speeding its reentry.

1.4 Atmospheric Instability

One huge problem of reentry prediction is the amount of instability in the earth's atmosphere. This instability makes the atmosphere difficult to model, making any type of prediction that is further than two days into the future extremely unreliable.

In effect, another thing gained from decreasing the time the object is left in orbit is that we can make the reentry prediction much more reliable.

1.5 Previous Attempts at Enforced Reentry

Intentional reentry caused by an increase in drag has been proposed before, but through using tethers on satellites. Such proposal did not include gaining control over the time and place of reentry. The use of a tether has very much the same effect as the proposed parachute with the distinct difference that a parachute will increase the radius of the object's cross-sectional area by, at most, tens of meters. A tether, on the other hand, will typically have the length of several kilometers and a width of millimeters. These last details increase the possibility of something going wrong during the orbital lifetime of the object.

II. Problem Background and Review

This section will address the increasing problem of debris build, the rising hazard to the population from debris reentering the earth, and how the unpredictability of the atmosphere makes it difficult for us to deal with reentry prediction. It will also mention how balloon satellites were already used in the 1960s. To conclude, it will bring up the “square-cube” law may be used to help with the space debris problem.

2.1 *A Space Debris Problem*

For the last few decades the United States (US), as well as other nations, has launched into space satellites, experiments, and even parts for a laboratory, i.e. the International Space Station, leaving a trail of debris that is now becoming a greater concern for the safety of future space missions. In November of 1995, the White House published the Interagency Report on Orbital Debris [5] through the Office of Science and Technology Policy, which is a technical assessment of the orbital debris that has accumulated in space. This report brought forth a new sense of urgency to the space debris problem in the US.

A few years later, the international community looked forward to the particular dangers of all the debris left in space and the United Nations released a technical report in 1999 highlighting some of their concerns for the possible outcomes. After many years of conferencing and technical consulting, the international forum of governmental bodies called The Inter-Agency Space Debris Coordination Committee (IADC) published the IADC Space Debris Mitigation Guidelines in September of 2007, where they outline best practices for the space community to follow. These will reduce the probability of an undesirable collision of space debris with an operating satellite.

Although the National Aeronautics and Space Administration (NASA) had been looking at the debris problem since at least the late 1980s, they finally made mandatory some of the widely accepted practices in the last couple of years with the publica-

tion of the NASA Technical Standard 8719.14 (STD 8719.14), the NASA Procedural Requirements 8715.6 (NPR), and the NASA Handbook 8719.14 (NHDBK).

2.1.1 Science and Technology Council Update Report. During 1995, the National Science and Technology Council (NSTC) reviewed the US Government’s 1989 Interagency Report on Orbital Debris to update its findings and recommendations, as well as to depict the progress and comprehension of the orbital debris environment.

Later in November they released the 1995 Interagency Report on Orbital Debris, where they reemphasized the growing problems. They noted that the International Space Station (ISS) had taken steps to maximize protection from debris penetration through implementing state-of-the-art shielding, avoiding larger debris, and developing operational/design options that minimize the risk to the station. [5]

According to the review, there was a fairly clear picture of the debris environment in low earth orbit. The review also stated that a particular concern was the sustained rate of fragmentation regardless of what everybody’s “mitigation efforts” were.

Another important point was that the NSTC brought forth the prerequisite of expected development of technical cooperation and consensus amongst nations prior to international agreement on any regulatory regimes. The concern for this was the possible competitive disadvantage resulting from any unilateral action by the US in trying to diminish debris when nobody else is willing to follow it or has the technical information to do it.

Table 2.1: Estimated debris population. [5]

Size	Number of Objects	%number	%Mass
>10 cm	8,000	0.02%	99.93%
1-10 cm	110,000*	0.031%	0.035%*
0.1-1 cm	35,000,000*	99.67%*	0.035%*
Total	35,117,000*	100.0%*	2,000,000 kg#

* statistically estimated values

calculated value from reported data

Table 2.2: Catalogued objects by altitude ranges. [5]

Orbit Type	LEO	MEO	GEO	Other	Total
Cataloged Objects	55747	134	601	1447	7929

The estimated debris numbers as of November 1995 are described by Table 2.1. It is important to note that at the time of this report there were a total of about 8,000 catalogued objects in space depicted in Table 2.2

2.1.2 United Nations Updates Their Report. Years later, the United Nations released the Technical Report on Space Debris [6] in 1999. It described the measuring, modeling, and mitigation measures of space debris for the international community.

The Scientific Technical Subcommittee, who handled the report, articulates that it was important to have a firm scientific and technical basis for future actions on the complex attributes of space debris. They later noted there was already ongoing research in some countries that helped the understanding of the problem as a whole. This research included sources of debris, areas where the amount of debris was increasing, and collision probability as well as its effects. At last, this brought to the front the necessity to diminish the production of debris. However, the report conceded that there was not even a consensus for the definition of space debris. [6]

The report goes into a summary of how the community measures space debris. An important nugget of information was that there was no available information on the submillimeter debris population above 600 kilometers. Of particular importance is that there was no information available in the highest debris density regions of 800-1,000 kilometers or the geostationary orbit. When trying to model the debris in space, the report used six different debris environment models. Figure 2.1 shows the findings of the different models in spatial density. Figure 2.1 has these models showing that the smaller the object the more objects you have in space at a set altitude. However, an even more important graph is shown later in the report on Figure 2.2.

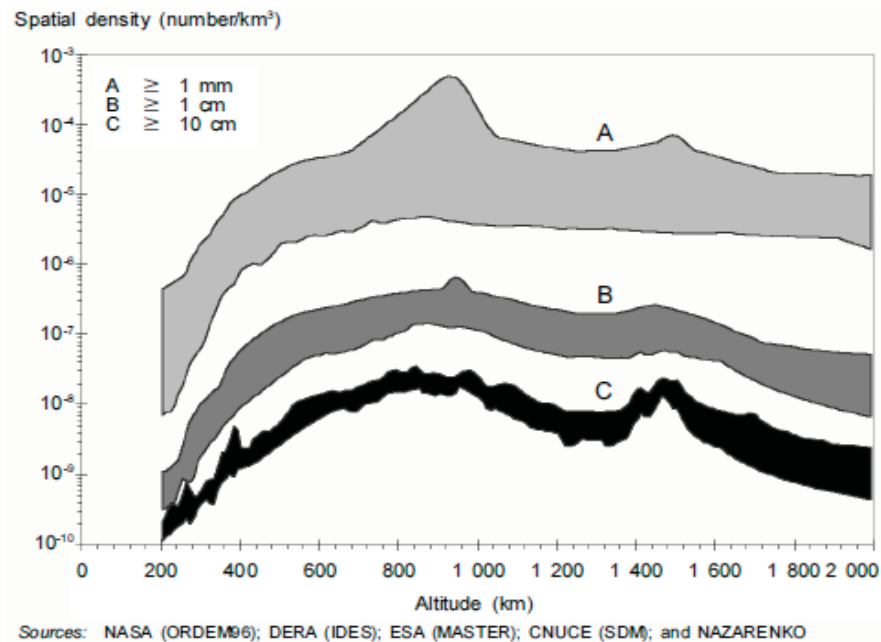


Figure 2.1: Model values for current spatial density. [6]

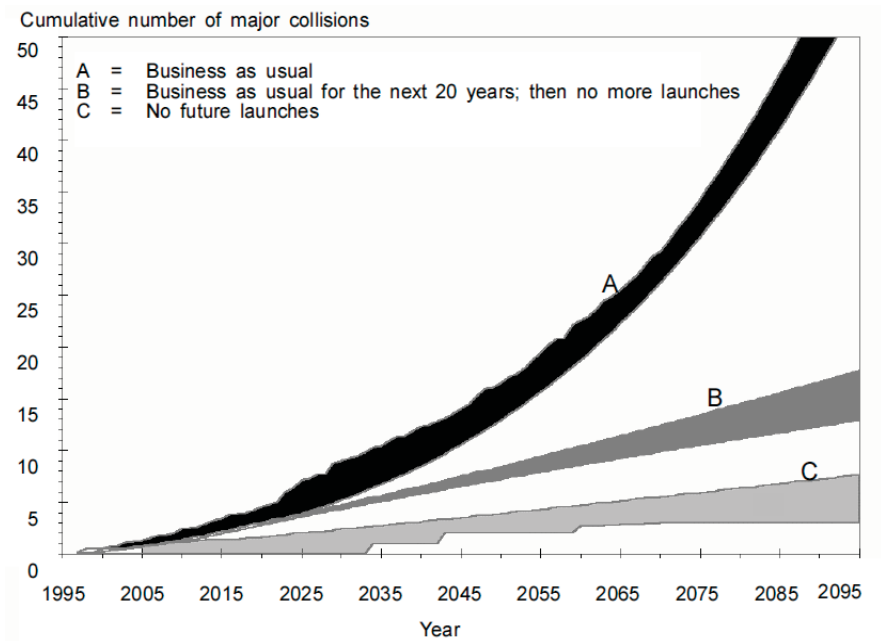


Figure 2.2: Typical ranges for number of major collisions for three scenarios, 1995-2095. [6]

The results of the long term debris models do not agree quantitatively because of differences in assumption and initial conditions. However, the basic trends and tendencies obtained by the models agree qualitatively. With the continued implementation of debris mitigation measures, the “business as usual” scenario could be avoided.

This last graph shows all models having the same trends, an increase of collisions in space. We can safely deduce that debris will dramatically increase as collisions increase. The debris mitigation measure presented can be summarized as lessening debris generation practices under normal operations, prevention of on orbit break ups, and finally deorbiting and reorbiting of space objects.

According to this report, the biggest mitigation measure of the space debris problem was the mere increase in awareness amongst nations. The report ends with a somewhat anticlimactic tone when, in the last paragraph, it states that “manmade space debris poses little risk to . . . approximately 600 active spacecraft now in Earth Orbit.” [6]

2.1.3 IADC Publishes Guidelines. Officially founded in 1993, the Inter-Agency Space Debris Coordination Committee used the United Nations 1999 report, as well as many ongoing proposals and space community practices, to generate and publish in September of 2007 the IADC Space Debris Mitigation Guidelines for the international community. The fundamental principles this publication follows are the prevention of on-orbit breakups, the removal of all debris (including dead satellites) from useful regions, and the limiting of debris objects released during normal operations. [8]

An interesting part of the guidelines are the protected regions that must be ensured for safe use. These are the Low Earth Orbit region (LEO) and the Geosynchronous (GEO) region. [8] The LEO region, Region A in Figure 2.3, consists of the spherical region from the surface of the Earth all the way out to 2,000 kilometers in altitude.

The GEO region is the a spherical shell described by Figure 2.3:

lower altitude = geostationary altitude minus 200 km

upper altitude = geostationary altitude plus 200 km

-15 degrees \leq latitude \leq +15 degrees

geostationary altitude (Z_{GEO}) = 35,786 km (the altitude of the geostationary Earth orbit)

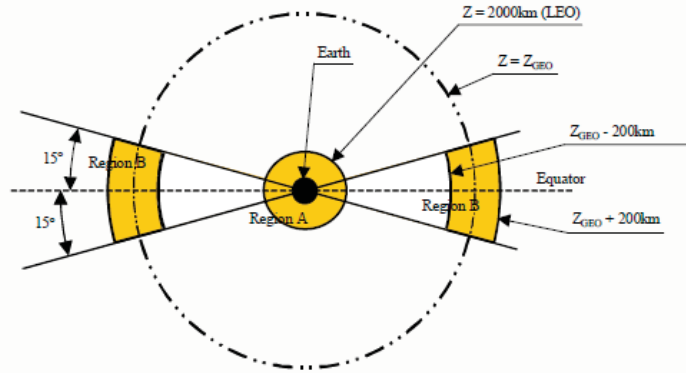


Figure 2.3: Protected regions. [8]

2.1.4 *NASA Provides More Guidelines.* As late as July 2008, NASA approved the Handbook for Limiting Orbital Debris. [10] This book is designed to accompany the previously published NASA STD 8719.14 [9] and the NPR 8715.6A. [11]

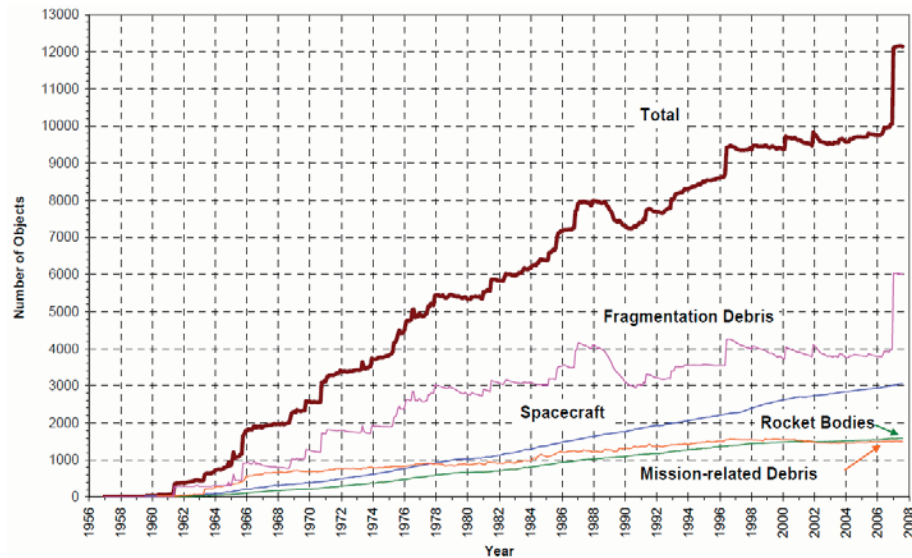


Figure 2.4: Debris count as of August 2007. [10]

This latest update to the guidance on NASA’s orbital debris mitigation is a refinement and also amplifies some of its applicability to resolve the problem. It goes into detail and updates some of the previous projections on the amount of debris and the primary components depicted previously in Figure 2.4.

The regulation updates have mandatory requirements on design and implementation of the mitigation measures, hence showing a much better commitment to help with this problem. [5] It is noteworthy to see how the debris of breakups in space (whether from system separations, collisions, or unintentional/intentional detonations, shown in Figure 2.5) are really starting to take charge of the overall picture:

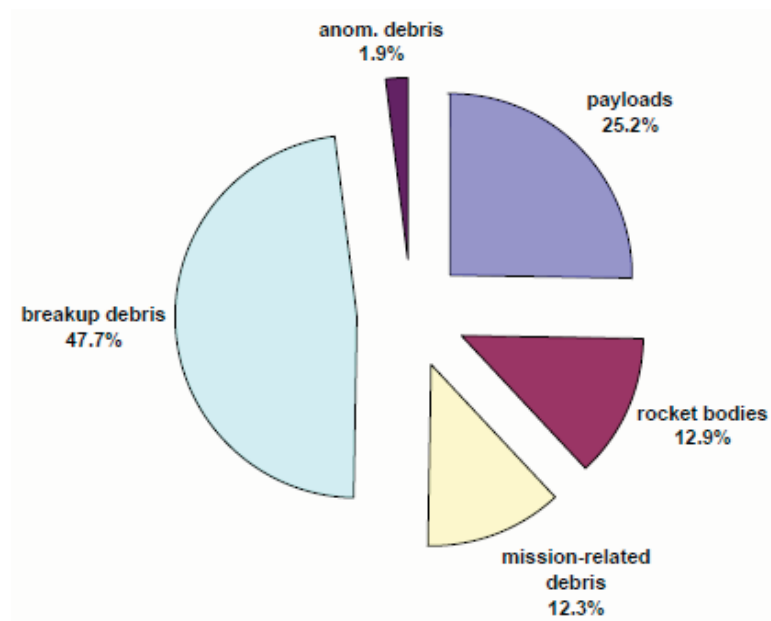


Figure 2.5: On-orbit objects by type. [10]

As of October 2008 there are a total of over 12,800 objects in space, with less than 25 percent of them being payloads, according to Orbital Debris Quarterly News. This currently amounts to over 2,000 tons of debris in space. At the present there are models showing it is no longer possible to eliminate the space debris due to the collision probability (that will produce more debris) even if we stop launching altogether. Figure 2.6 clearly shows these projected increases in debris.

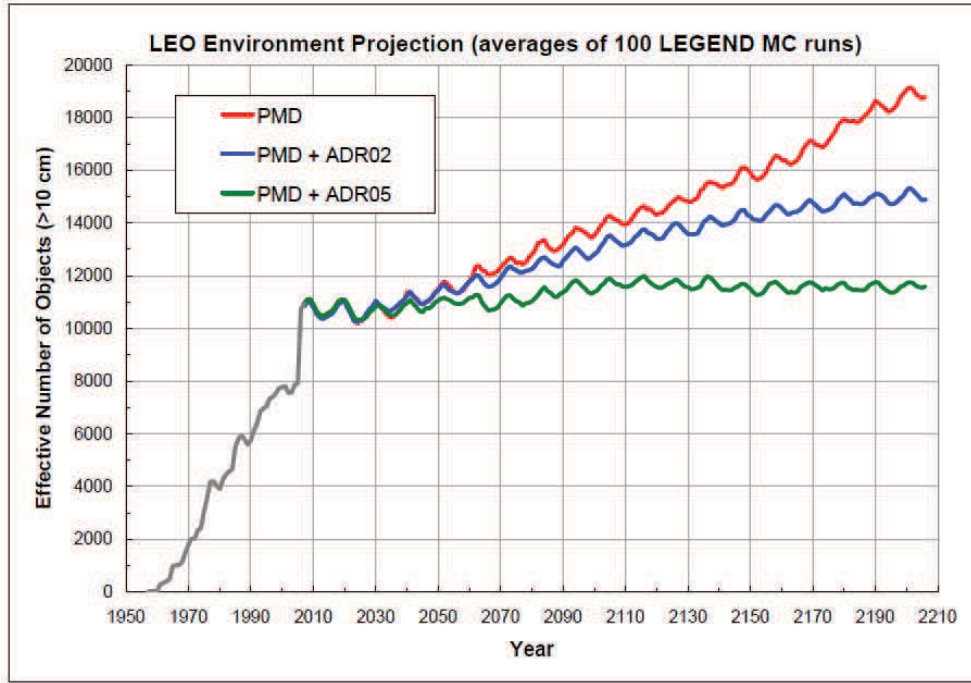


Figure 1. Comparison of three different scenarios. From top to bottom: postmission disposal (PMD) only, PMD and ADR of two objects per year, and PMD and ADR of five objects per year, respectively.

Figure 2.6: Debris projections. [26]

2.1.5 Problem Wrap Up. Throughout the years, the space community has launched every possible object into space, from animals to sophisticated satellites, all with very important missions, but there has not been a very strong effort into mitigating the space debris problem we are now facing. It was left alone to benefit the advancement of technology and the purpose of not adding another burden to the space acquisition and budgets of the world. Except, space operational regions are a limited resource that must be protected.

Good ideas that try to affect our design and acquisition of new systems have been proposed. It is well understood that the hypervelocities of space objects make them true weapons and could eventually have disastrous consequences to our heavily technology dependant society. A better effort seems to be brought forth by the US with the latest regulations.

2.2 *Population Safety*

The safety of the population has been put in jeopardy when reentering objects carrying dangerous payloads don't get incinerated by the extreme heat of reentry and make it to the ground.

2.2.1 Skylab Reentry. The very first American Space Station was called Skylab (Figure 2.7). It was launched on May 14, 1973. It had many goals such as to prove humans can live in space, to expand astronomic knowledge, to detail earth's resources, and to conduct experiments, among others. After the end of the last mission in 1974 and after completing engineering tests, Skylab was placed in a stable orbit where it would remain for eight to ten years. Tragically, the increase in solar activity greatly increased the drag and the station reentered back to Earth on July 11, 1979. The station might have been over ninety tons in mass; therefore, pieces of the station survived reentry and, like a display of huge fireworks, scattered debris over the Indian Ocean and Western Australia. [35]

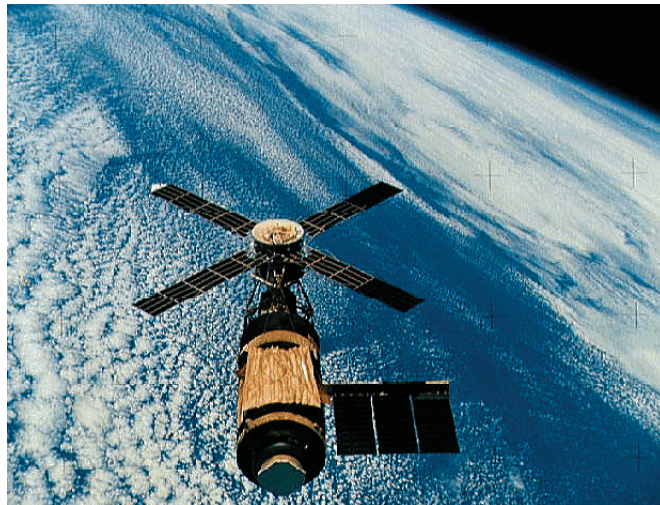


Figure 2.7: Skylab workshop, May 14, 1973. [35]

2.2.2 Cosmos 954 Reentry. The dangerous reentry on January 24, 1978 of Cosmos 954 occurred over Northwest Canada and marked a new sense of concern over objects falling from the darkness of space. It became a high profile reentry for the US and Canadian governments. The extreme importance was not because the satellite was designed to scan the oceans for surface ships, but because it was powered by a small nuclear reactor. The reactor was ninety percent enriched Uranium-235 and it was “hot and alive.” The name “Operation Morning Light” was the code for the joint operation the two governments performed to clean up the spread of radioactive fuel. [36]

The path of debris covered hundreds of kilometers. Dozens of radioactive objects, as well as about four thousand particles, were spread over a wide area ranging from Great Slave Lake to Saskatchewan and Northern Alberta. [13] As a settlement, Canada and the Union of Soviet Socialist Republics agreed on a payment of three million Canadian dollars for all matters relating with the incident. [25]

2.2.3 USA 193 Destruction. According to the US Department of Defense (DoD) an experimental satellite had to be shot down by a single modified Standard Missile-3 (SM-3) in February of 2008. The satellite never became operational after it was launched in December of 2006. According to the DoD’s news releases, the satellite could have had over 11,000 kilograms of its mass survive the reentry which included 435 kilograms of hazardous hydrazine propellant fuel. The successful destruction of the satellite at 10:26pm EST, February 20, 2008, was widely publicized. [1, 7, 14]

The event brought a diplomatic problem to the forefront. The incident was criticized by Russia as a test of US’s capability to destroy other nation’s satellites and accusing the US of causing a space arms race. It even prompted the Bush Administration to inform diplomats that the event should not be seen under the same light as China’s destruction of its satellite the previous year. [2, 3, 29, 31]

2.2.4 Other Famous Reentries. At the current time, there is an average of one large piece of debris falling back to the earth each day. Most of them fall on the oceans or deserts, but not all. Such are the cases in the following occurrences of a few Delta II rocket bodies. [24]



Figure 2.8: Delta II rocket body in Texas. [24]

Figure 2.8 “... is the main propellant tank of the second stage of a Delta 2 launch vehicle which landed near Georgetown, TX, on 22 January 1997. This approximately 250 kg tank is primarily a stainless steel structure and survived reentry relatively intact.” [24]

“On 21 January 2001, a Delta 2 third stage, known as a PAM-D (Payload Assist Module - Delta), reentered the atmosphere over the Middle East. The titanium motor



Figure 2.9: Delta II Rocket body in Saudi Arabia. [24]

casing of the PAM-D, weighing about 70 kg, landed in Saudi Arabia about 240 km from the capital of Riyadh.” (Figure 2.9) [24]



Figure 2.10: Delta II Rocket body in South Africa. [24]

“Another Delta 2 second stage reentered on 27 April 2000 over South Africa. In this incident, three objects were recovered along a path nearly 100 km long: the main stainless steel propellant tank, a titanium pressured tank, and a portion of the main engine nozzle assembly.” (Figure 2.10) [24]

2.3 Attempt to Enforce a Safe Reentry

2.3.1 Design Strategy. Satellite developers have been under scrutiny to include a better design that will have satellites disintegrate easier upon reentry. There have been many objects that have survived reentry because they were made with materials that have high melting points. Some examples of these materials are stainless steel, titanium, and beryllium. The satellite design must include parts that have lower melting points, and in addition, be formulated for the system to easily break upon reentry, making it easier for the parts to melt on their way down. On the other hand, if the break up allows objects to evade high melting points then the design must incorporate a method that keeps those survivable objects together longer so that they experience the high melting temperatures. Either one of these answers must be found through the study of breakup reentry phenomenon. [18]

2.3.2 Tether Technology. Studies have been done to discover whether the use of electrodynamic drag can be used to decrease the orbital lifetime of debris. These studies have focused on objects with an altitude of 400 kilometers and higher, as shown in Table 2.3.

Table 2.3: Tether table performance. [17]

Initial Height [km]	Orbit Inclination			
	0°	25°	50°	75°
	DE-ORBIT TIME [days]			
1400	170	220	325	EDT not used
1300	140	185	280	
1200	120	155	230	
1100	95	125	185	
1000	70	95	140	375
900	55	70	110	280
800	45	55	80	200
700	30	40	55	140
600	20	30	40	80
500	15	20	25	40
400	10	15	15	20

Time to de-orbit a 1500 kg spacecraft from a given initial altitude to 250 km with a 7.5 km Terminator $Tether^{TM}$ with a mass of 1% of the S/C.

According to a summary report of IADC AI 19.1, the benefits of using tethers may be significant. The first is that spacecraft may only require between one and five percent of their total mass on a typical tether system, making them extremely attractive. A second benefit is that tethers may decrease the de-orbit time. A final benefit is that they reduce the Area-Time-Product (ATP) of LEO orbiting objects, resulting in lessening their opportunity for collision with other objects. [17]

Nonetheless, tethers are very long and thin. Tethers may be between 5 and 7.5 kilometers in length and between 0.5 and 2.5 centimeters wide. This increases the possibilities of problems due to their large increase in collision cross-sectional area. Also, the severing of the tethers can be attributed to many culprits such as meteors, vibration, other debris, and even manufacturing defects, with an end result of providing more debris. [17]

Most of the studies done were under the assumption of circular orbits, where tethers can be stable, but not for any highly eccentric orbits such as Geotransfer (GTO). Furthermore, the studies done in IADC AI 19.1 were performed using different particle flux models, creating the need for a common model where a firm standard may be defined. Therefore, tether technology is in need of further study on: materials that may survive impacts, prolonged wear (currently are supposed to be up there for years), and better space particle flux models for collision probability studies. [17]

2.4 Balloon Satellites

The idea of an object with a balloon that is dozens of meters in diameter is not new. The satellite Echo I was launched in August of 1960. The mission of the satellite was designed as a passive communications deflector. The object weighed 180 kilograms. It was launched into an orbit with a 118 minute period and an altitude of over 1,500 kilometers. The balloon was proven to work at that altitude even with micrometeoroids affecting it. [27]

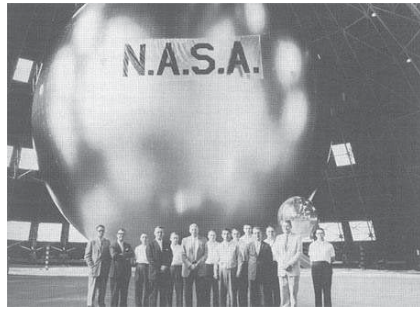


Figure 2.11: The Echo I team stand in front of their balloon. [21]

A second satellite balloon with an even bigger diameter of 41 meters was launched in January of 1964 into an orbit with an inclination of 81 degrees. [4] One last balloon was sent into space in the 1960s. The Pageos I was launched in June of 1966, but it had the diameter of Echo I and was placed at an 87 degree inclination, with an altitude of over 4,200 kilometers. This satellite's mission was to be a target for geodetic purposes. It reentered in July of 1975. [34]



Figure 2.12: Pageos I inflation test. [16]

2.5 *Atmospheric Unpredictability*

The atmosphere is extreme in its variability; it is in constant motion as it is affected by solar heating. As air warms up it moves into the higher parts of the atmosphere. At the same time, cooler air drops in altitude. This boiling-type effect happens vertically as well as horizontally. All this merging of different air temperatures and the rotation of the earth, coupled with the filtering of the different atmospheric component weights (as altitude increases over 120 kilometers) makes for very erratic atmospheric profiles. [30,33]



Figure 2.13: Atmosphere picture taken from the ISS. [12]

There are many different atmospheric models that may be used when solving for an object's path in earth's orbit. These models state the atmosphere's density at a certain location. The commonly used Standard 1976 atmospheric density model is an updated version that was originally published in 1958 with updates in 1962, 1966, and finally 1976. It consists of tables that state the temperature, pressure, and mass densities of the different atmospheric components as a function of altitude. [15,30]

Most atmospheric density models go through updates because of the complicated wavering nature of the atmosphere and our continuous renewing of atmospheric education. A model that went through the update phases (and is still going through them) is the Mass Spectrometer and Incoherent Scatter Radar (MSIS) model. For this reason, the family of models for this type came to be known as the MSIS-77,-83,-86, with the last one being combined with the CIRA-1986. The CIRA models were first produced by the Committee on Space Research (COSPAR). The latest MSIS-E 1990, where the “E” was added because it covered from the ground to 1,000 kilometers in altitude, is an update that is still very widely used. [22,28] One last permutation of the MSIS model is the Navy Research Lab MSISE 2000 (NRLMSISE-00). This latest model has updated databases and uses inputs as solar flux and geomagnetic heating to report the atmospheric densities. [23]

These never ending studies and updates of atmospheric density profiles clearly depict how complicated and difficult is to even have an accurate model of atmospheric density. As stated before, all fluctuations are directly related to the sun’s activities which create differential solar winds affecting our atmosphere. See Figure 2.14. [15,30]

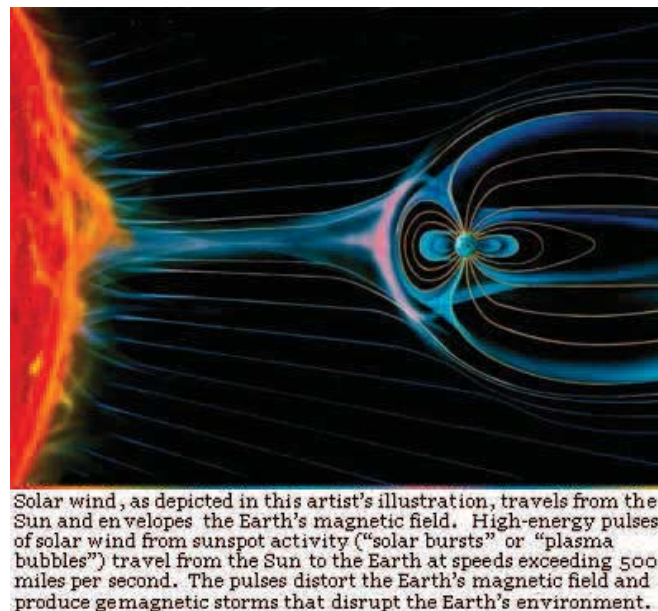


Figure 2.14: Solar wind disrupting earth’s magnetic field. [30]

The sun has its own disturbances and the activities seem to have a cycle of about eleven years. When the sun is most active, it is said to be in “solar max” and when the activity slows down it is called “solar min.” These changes in activity have marked effects on our atmosphere. During these activities the sun releases tremendous amounts of energy and mass, producing strong winds. These winds change the earth’s atmosphere making it compressed and changing the drag satellite systems perceive. Thus, the sun’s activities have a great effect on the true atmospheric drag that objects orbiting the earth “feel” and our current models can only try to predict what an orbiting path will look like. [30]

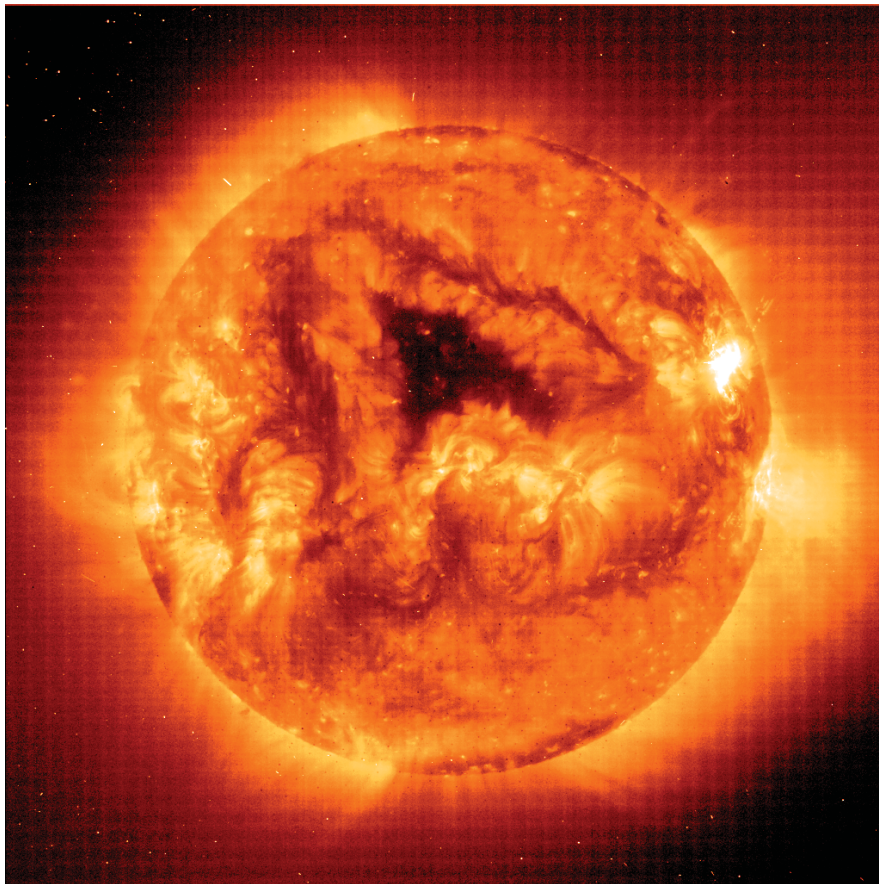


Figure 2.15: Solar’s unusual activities during Solar Min. [32]

2.6 Square Cube Law

The square cube law was first introduced by Galileo Galilei in his writings called *Two New Sciences*. He discusses how an object that increases proportionally in size will not have the same proportional increase in strength. This phenomenon has to do with the area to volume ratio, which is commonly used as the area to mass ratio, since it is assumed to keep a constant density. Therefore, when you increase the size of an object the surface area is increased by the square of its length while the mass is increased by the cube of its length. This means the object will become heavier much faster than the surface area it will cover. [19,20]

This can be seen by the simple illustration of a cube. A cube with a length L will have the surface area of $SA = 6 * L^2$ and a volume of $V = L^3$. Therefore, if the length of the object is increased by an order of magnitude, the cube will have a length of $L = 10$, a surface area equal to $SA = 6 * (10 * 10) = 600$, and a volume of $V = (10 * 10 * 10) = 1000$. This shows that the object increased its length by a factor of ten, its surface area by a factor of one hundred, and its volume (or mass) by one thousand. [19,20]

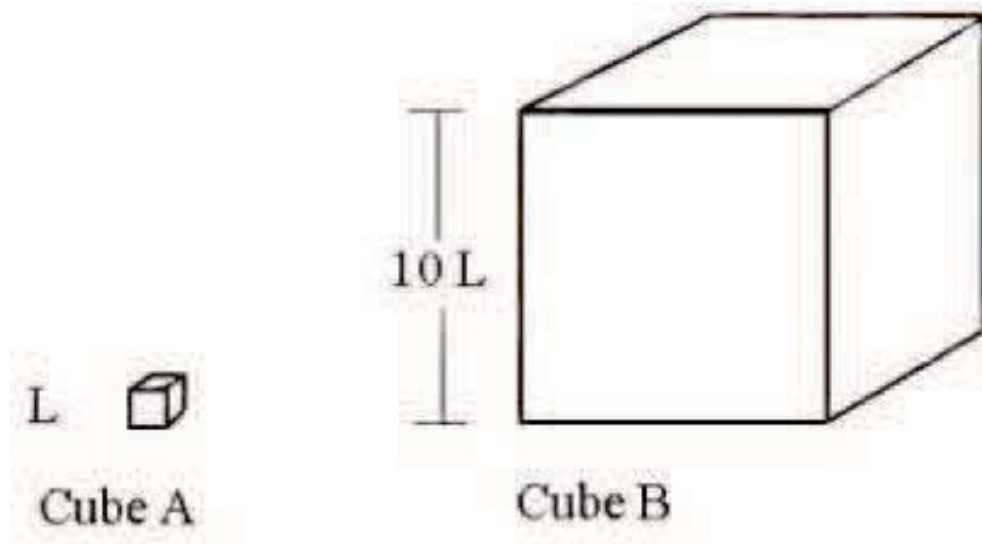


Figure 2.16: Increase in length demonstration. [19]

This law explains many phenomenon, including the size of animals, how they cope with the need to keep warm, and even their ability to move around. An elephant is not capable of jumping because its weight prohibits it, but an ant falling from a skyscraper will survive and go on to carry fifty times its own weight. Even biological cells stay at the microscopic size levels, because the high efficiency required to transfer nutrients and waste across their membranes occurs at those sizes. Consequently, cells just multiply, keeping their high surface area to mass ratio instead of growing. [19,20]

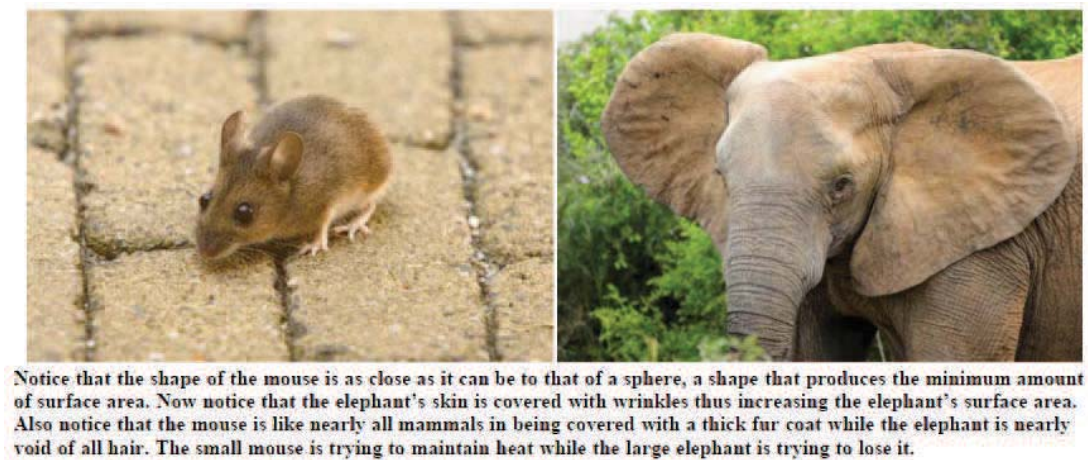


Figure 2.17: Drastic surface area comparison. [19]

This thesis will use the fact that when inflating a balloon, the surface area increases by the square of the radius while at the same time decreasing the actual density of the object as a whole. Although a balloon is the geometric figure with the smallest surface area to volume ratio, it is also the most consistent when viewed from any angle. This means that it does not have to be oriented for it to use its maximum cross-sectional area when it is being used as the agent to increase drag.

III. Methodology

All simulations for this thesis were performed using the Satellite Tool Kit (STK) software produced by Analytical Graphics, Inc (AGI). This entire project will use the International System of Units (SI).

STK is a commercial off the shelf analysis software that may be used to depict scenarios in a very clean and clear format. The software is capable of using three-dimensional visualization and using many kinds of integration algorithms to answer problems. It solves fundamental location and inter-visibility problems associated with land, sea, air, and space scenarios. The overall purpose for each of the procedures will be stated first, followed by the specific simulation set up including parameters used along with the rationality behind them.

3.1 Initial Set Up and First Study: Variability in Reentry Prediction Due to the Atmosphere

The atmosphere's unpredictability is an important factor that must be taken into account in any kind of analysis dealing with an object's reentry. To explore the variability in reentry prediction due to atmosphere variation, a particular orbit was propagated using different atmospheric models. Furthermore, two additional orbits were used in the simulations to account for the reentry variability in different orbit types.

3.1.1 Propagator. All orbits were propagated using the High Precision Orbit Propagator in STK. The program has the option of setting an atmospheric model from ten different available models that have been used through the years. Thus, in order to get the best picture of what the reentry could look like, all ten atmospheric models were used. The mere fact that there are ten models to choose from shows the unpredictability of the atmosphere.

The available atmospheric density models in STK are the following:

1. 1976 Standard

2. CIRA 1972
3. Harris-Priester
4. Jacchia 1960
5. Jacchia 1970
6. Jacchia 1971
7. Jacchia-Roberts
8. MSIS 1986
9. MSISE 1990
10. NRLMSISE 2000

For the rest of the study, especially throughout the plots and analysis, they will mostly be referred to by the number they were assigned in this section instead of their whole name in order to add clarity to the visual results.

3.1.2 Reentry Criterion. A reentry criterion must be set for the study. The reason for this is because several atmospheric models are not capable of modeling below 90 kilometers. Air Force Space Command considers an object reentered at 120 kilometers. Using these two criterion, 100 kilometers was used as the point where an object will be considered reentered. Even though the reentry criterion was set, all simulations were executed all the way to the lowest atmospheric altitude limit set by their correspondent atmospheric model.

3.1.3 Simulated Orbits. Three different orbital element sets were chosen for the study in order to ensure a wide enough number of factors are covered. The particular element sets can be found in Appendix A.

1. The first propagated orbital element set was from a piece of debris that was left from the destruction of USA 193. This orbit has a 58.5 degree inclination with an eccentricity of .01687 and a period of 91.4 minutes. The specific numbers used to set up STK are on Figure B.1 in Appendix B.

2. The second orbital element set used was from the ISS and has a 51.7 degree inclination with an eccentricity of .00100 and a period of 91.6 minutes. The specific numbers used to set up STK are in Figure B.2 in Appendix B.
3. The third element set used was from a satellite named Terrasar-X in a polar orbit. It has a 97.4 degree inclination with an eccentricity of 0.00014 and a period of 94.8 minutes. The specific numbers used to set up STK are in Figure B.3 in Appendix B.

3.1.4 Object Parameters. To get uniform results, the same satellite dimensions were used for all simulations. The object has the default mass of 1,000 kilograms, with an area to mass ratio of 0.1 and an inertial matrix that looks like Table 3.1.

Table 3.1: Satellite's inertial matrix.

	X	Y	Z
X	4500 kg m ²	0	0
Y	0	4500 kg m ²	0
Z	0	0	4500 kg m ²

3.1.5 Trajectory Data. Once the orbit was propagated, STK provided positional data in Latitude, Longitude, Altitude (LLA) tables for the entire satellite trajectory. An LLA table includes the previously mentioned position parameters as well as corresponding times and rates of change. STK is able to provide these tables in a spreadsheet format. Using Microsoft Excel, all reentry path altitudes of the object were plotted against time to explore their reentry variability.

3.1.6 Chosen Atmospheric Model. Atmospheric model number 9, which is the MSISE 1990, was chosen to be used as the effective reference reentry path for the rest of the simulations. In other words, the reference reentry path will be used as if it was the actual path the satellite would follow to reentry. The rationalization for this was that the model predictions' were the closest to the median out of all models predictions.

In addition, this atmospheric model is capable of propagating to zero altitude. The STK program has an option to increase the drag by an input scale at an input time. This option was used for the following set of simulations. The goal for this part of the experiment is to investigate how a drag increase by a particular factor affects the overall reentry time.

3.2 Second Study: Drag Scale Increase Study

The drag in the propagator was increased by a factor of 10. The drag increment was set for 4 separate position points through the orbit. Once the drag was increased, the orbit was propagated all the way to whatever atmospheric limitation was set by the model. For every single simulation, STK provided data in spreadsheets that were later used to plot the reentry path altitudes as a function of time.

1. The first set of simulations for this study were using the element set of the debris from USA 193. The drag scale increase was set at the beginning of the day of the reference reentry, regardless of the time left to reentry. To observe how much the total time to reentry would change, the next 3 drag increments were set 24 hours apart.

One more set variable was the point in the orbit where the drag increments happen. In order to detect any blatant effect due to the location of the drag increment, the drag increments were alternated between perigee and apogee. The first drag increase happened at perigee which was closer to the reference reentry time.

2. The second set of simulations was on the element set from the ISS. This first drag scale increase also happened at the beginning of the day of reentry. Again, to observe how the reentry time between the drag increase and final reentry would change, the next drag increments were set even further apart, at 4 days.
3. The last set of simulation was on the Terrasar-X. The first drag scale increase was also at the beginning of the day of reentry. This time, in order to observe

the change in time left to reentry, the rest of the drag increments were about 24 hours apart.

3.2.1 Greater Scale Increase. To briefly explore what a larger increase in the drag scale would do to the time of reentry, the scale was increased to 100 and the same procedures as above were followed.

3.3 Third Study: Single A/M Increase at Several Points in Orbital Path

This thesis proposes to increase the drag force exerted on the object through the amplification of its surface area. It is a more intuitive way of thinking about the reentry process. The greater the surface area, the greater the acceleration (\mathbf{a}_d) due to drag the satellite will experience according to the basic equation:

$$\mathbf{a}_d = -\frac{1}{2}C_d\rho\frac{A}{m}\mathbf{v}^2 \quad (3.1)$$

[37, 38] where the symbols represent the following:

- C_d = Object's Coefficient of Drag
- ρ = Atmospheric Density
- A = Object's Cross-sectional Area Perpendicular to Velocity
- m = Object's Mass
- \mathbf{v} = Object's Velocity

Thus, when computing drag change, it is easier to visualize changing a specific parameter in the simulation. This factor would be the area to mass ratio (A/M) and STK has the capability to adjust it.

The area used in the equation is the cross sectional area perpendicular to the velocity vector of the orbiting object. Consequently, for the rest of the simulations,

the capability of modifying the area to mass ratio will be used instead of adjusting the drag by a certain factor.

This next set of simulations will look directly into the variability of the reentry time due to the atmospheric models. The A/M ratio will be increased from the default of 0.1 to 1.0 for all the different atmospheric models. The results will be compared against the reference orbit solved by the MSISE 1990 with a 0.1 A/M ratio.

The capability of STK to increase the drag by a certain factor had the option of inputting the specific time when the drag would increase. On the other hand, the capability to manipulate the A/M ratio is set for the whole propagation and cannot be made to change at a certain time. This prompted the use of an element set (that was solved for) from the reference orbit. Therefore, at the chosen time for the increase in A/M ratio, the element set from the reference orbit was used as the epoch of the orbit and the simulations began from that point to final decay.

For every single simulation, STK provided data in spreadsheets that were later used to plot the reentry path altitude against time.

1. The USA 193 debris orbital element was used first. The first increase in A/M ratio was a little more than 2 days and 9 hours before the reference reentry time. The second A/M ratio increase was done 24 hours prior to reference reentry. The last ratio increase was set 10 hours prior to reference reentry.
2. The next simulation was the ISS orbital element set. The first increase in A/M ratio was 7.5 days before the reference reentry time. The second A/M ratio increase was done 24 hours prior to reference reentry. The last ratio increase was set 10 hours prior to reference reentry.
3. The last simulation was the Terrasar-X element set. The first set to be propagated was 3 days before reentry. The second A/M ratio increase was 24 hours prior to reentry and the last ratio increase was 10 hours before reentry.

3.4 Fourth Study: A/M Manipulation at a Single Point in Orbital Path

The last set of simulations was focused on briefly exploring how the A/M ratio affected the reentry prediction time as it was manipulated. The only element set to be propagated for this part of the study is the original USA 193 debris orbital element set. The atmospheric model used throughout will be the MSISE 1990. Only the A/M ratio will be changed. Eleven different ratios were chosen, spread between 0.001 and 1.000. The reentry altitudes were plotted on 3 different plots to study their reentry behavior more clearly.

IV. Simulation Results & Analysis

The four different studies show firm results of the effects of atmospheric unpredictability, drag increase, and the amplification of the object's surface area.

4.1 Atmospheric Unpredictability

Here are the simulations results and discussions of the study on the variability of reentry predictions due to atmospheric instability.

4.1.1 Debris Reentry Prediction. The propagation path of the USA 193 debris element set using all atmospheric models is shown in Figure 4.1:

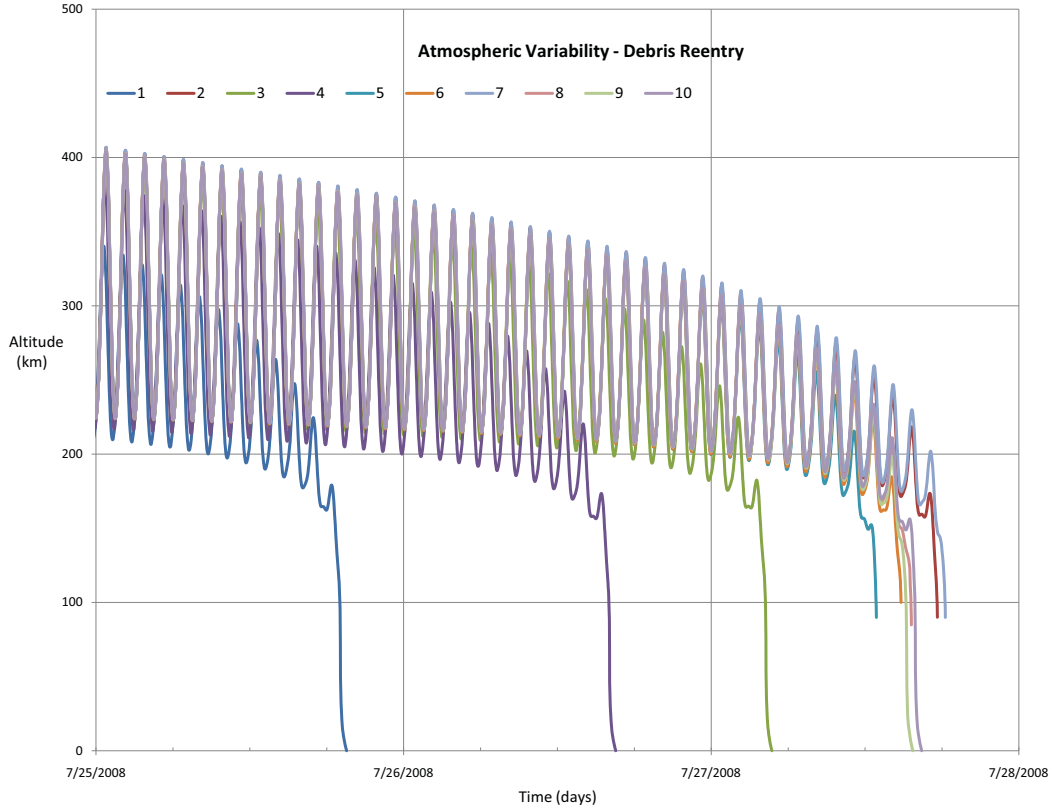


Figure 4.1: Debris orbit reentry predictions by ten atmospheric models.

The atmosphere’s variability showed it has a big impact on the reentry time prediction. The period between the epoch of the element set until the reference reentry time was almost 116 hours. This means that the element set was propagated almost 5 days before reentry. The result was a reentry prediction spread of over 47 hours among the ten different atmospheric models.

Taking out the predictions that are not within a few hours of the reference prediction (3 outliers) from the group, the time spread dropped down to almost 5.5 hours. Still, a 323 minute spread amounts to over 3.5 revolutions around the earth, making the predictions useless. The results are summarized in Figure 4.2:

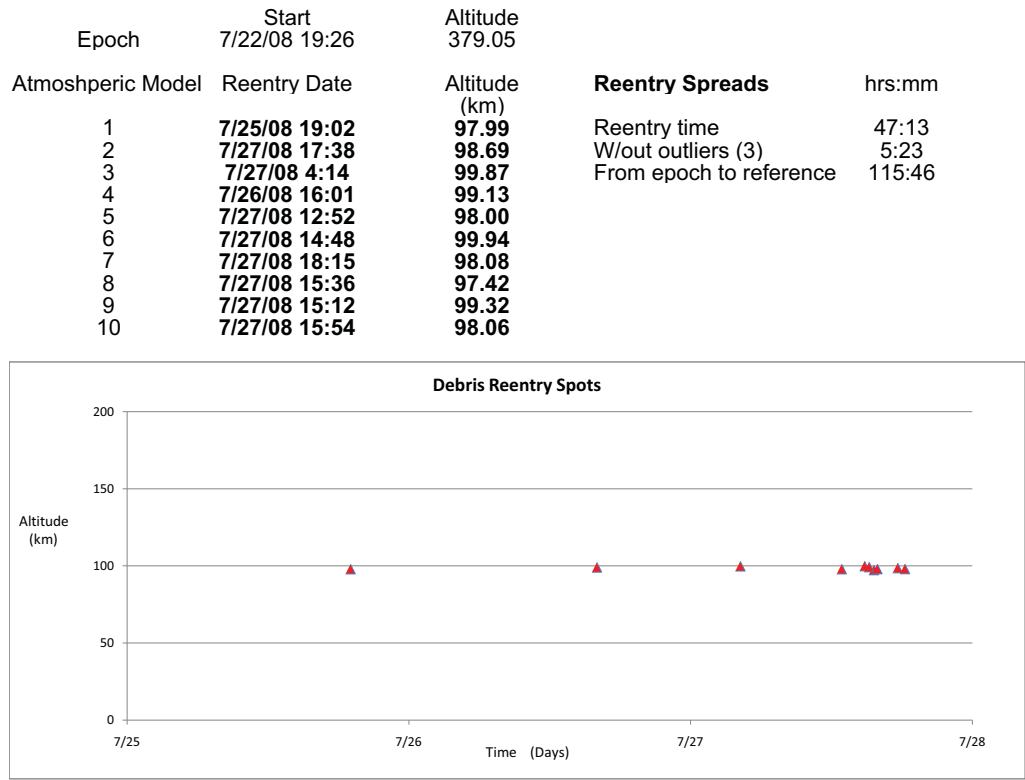


Figure 4.2: Summarized predicted reentry times for Debris orbit.

4.1.2 *ISS Orbit Reentry Prediction.* The propagation of the ISS orbit in all ten atmospheric models provided the reentries show in Figure 4.3:

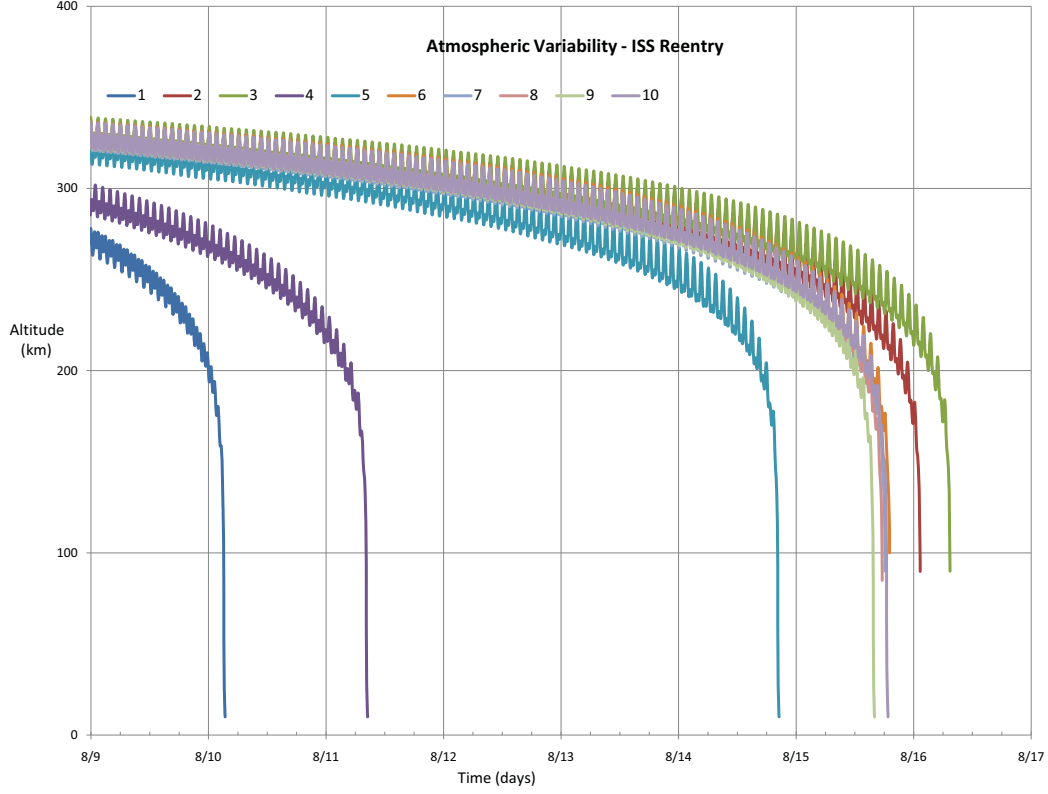


Figure 4.3: ISS orbit reentry predictions by ten atmospheric models.

The time from initial orbit propagation until reference reentry was approximately 13 days or almost 316 hours. The actual time span of all reentry predictions was over 6 days, or more than 148 hours, shown by the summarized results Figure 4.4:

	Epoch	Start 8/2/08 12:00	Altitude 357.12		
	Atmospheric Model	Reentry Date	Altitude (km)	Reentry Spreads	days hrs:mm
	1	8/10/08 3:05	100.23	Reentry time	6 4:18
	2	8/16/08 1:19	94.69	W/out outliers (3)	0 15:40
	3	8/16/08 7:23	99.08	From epoch to reference	13 3:43
	4	8/11/08 8:12	99.82		
	5	8/14/08 20:13	94.39		
	6	8/15/08 19:03	99.97		
	7	8/15/08 18:07	97.98		
	8	8/15/08 17:32	98.31		
	9	8/15/08 15:43	95.92		
	10	8/15/08 18:26	100.70		

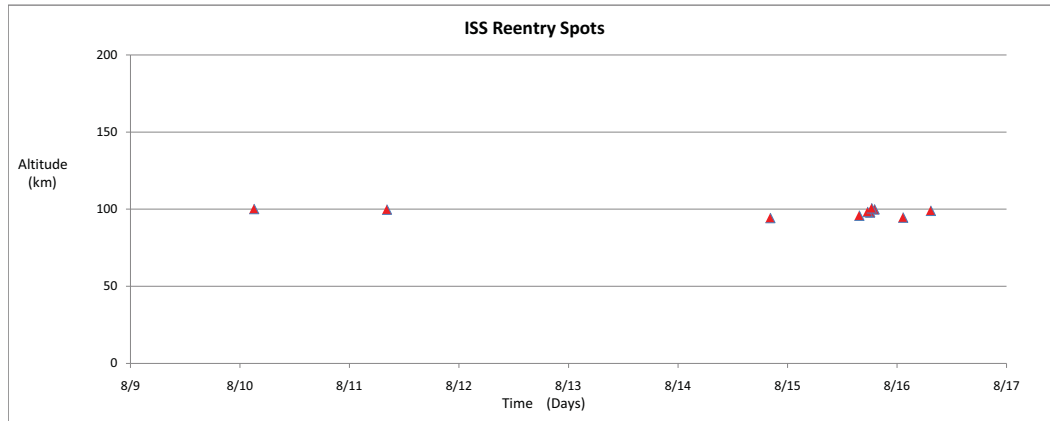


Figure 4.4: Summarized predicted reentry times for ISS Orbit.

Again, for this simulation, there seem to be 3 predictions that are outliers. These are the 3 earliest ones, which are separated by more than a few hours from the reference reentry. When taking these points out of the spread the window is reduced to almost 16 hours. This equals to over 10 revolutions around the earth, making the predictions hollow.

4.1.3 Terrasar-X Prediction. The last element set propagated for the study was that of the Terrasar-X satellite. There were some extreme results for these simulations as depicted in Figure 4.5 and Figure 4.6:

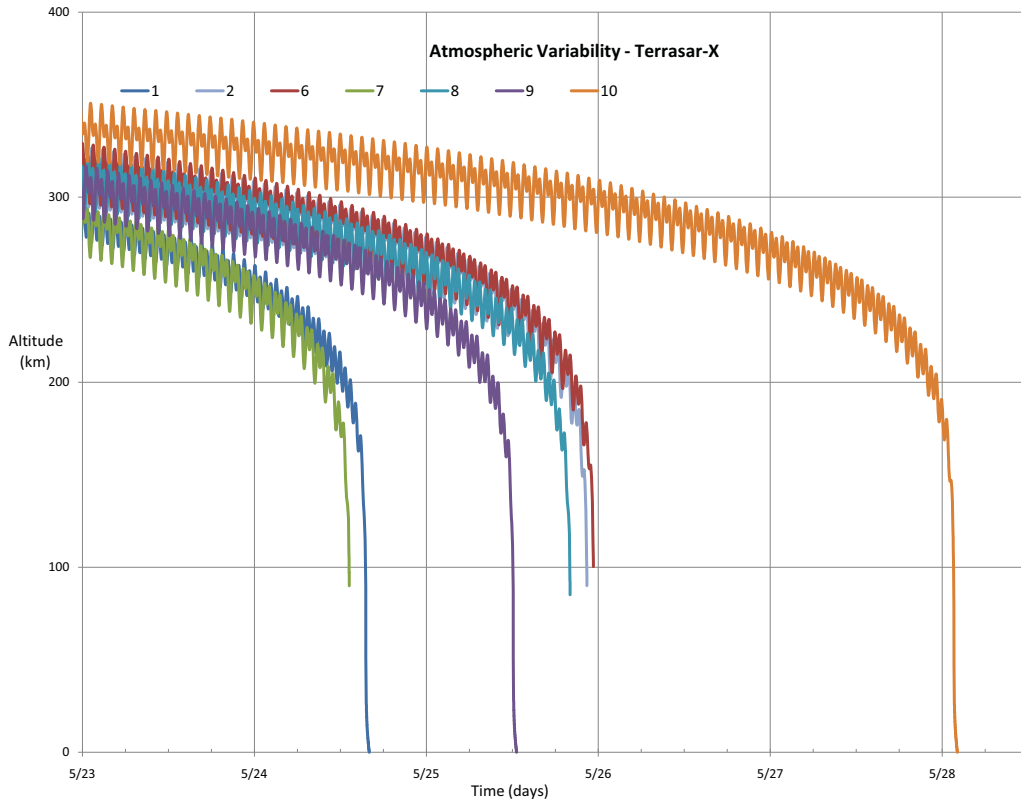


Figure 4.5: Terrasar-X orbit reentry predictions by **seven** atmospheric models.

In view of the fact that this is a very different orbit from those previously used, the reference prediction is more than 6 months apart from its initial propagation point. The reason for the extreme time to reenter is the orbits' low eccentricity and the much higher altitude of over 500 kilometers.

The long orbit propagation only increased the effect of the atmospheric variability in the reentries, increasing the prediction spread to almost 79 days. To see the reentries more clearly, the graph was split amongst the 2 groups.

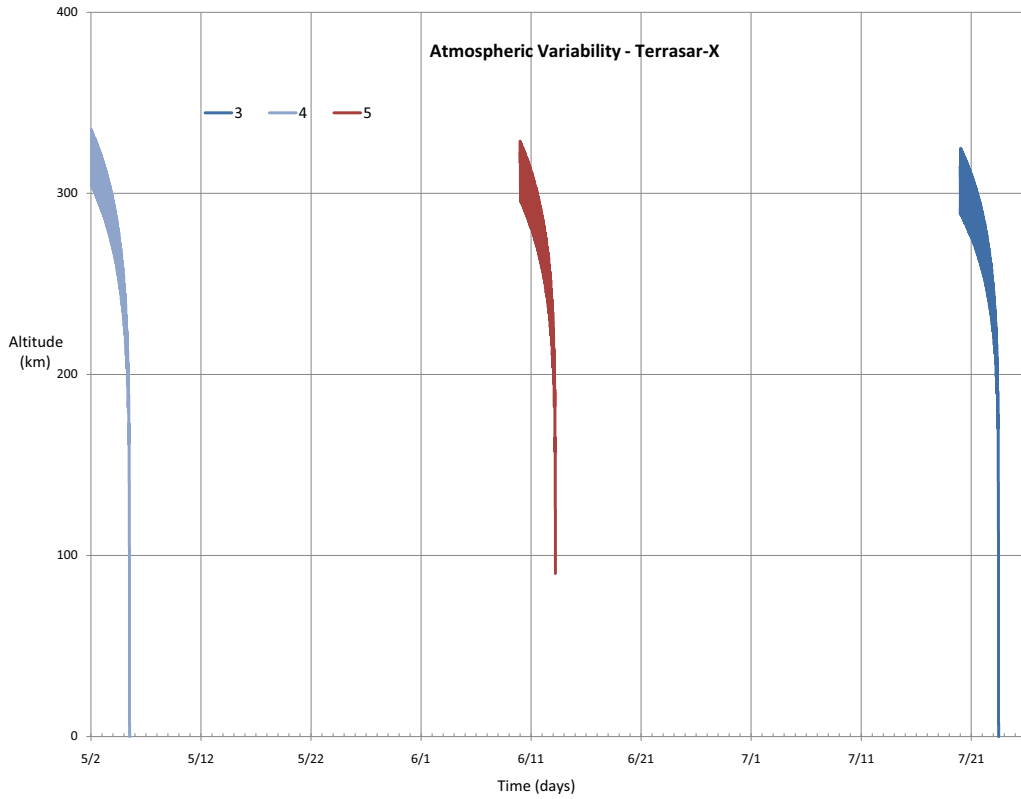


Figure 4.6: Terrasar-X orbit reentry predictions by **three** atmospheric models.

The first group of predictions (shown in Figure 4.5) are the predictions that are closer to each other. The second group of predictions in Figure 4.6 were considered to be outliers and are the ones that contribute the most to the prediction time spread.

When only considering the first group of predictions for the analysis, the reentry spread dropped down to over 3.5 days. Again, this 84 hour prediction spread is of almost no particular use. The specific numbers are summarized in the Figure 4.7:

Epoch	Start 12/2/08 4:42	Altitude 508.91		
Atmospheric Model	Reentry Date	Altitude (km)	Reentry Spreads	months days hrs:mm
1	5/24/09 15:30	99.93	Reentry time	3 18 23:15
2	5/25/09 22:22	100.04	W/out outliers (3)	1 3 12:22
3	7/23/09 11:15	100.06	From epoch to reference	6 22 7:21
4	5/5/09 11:59	100.55		
5	6/13/09 4:55	99.79		
6	5/25/09 23:19	100.37		
7	5/24/09 13:13	100.00		
8	5/25/09 20:01	99.51		
9	5/25/09 12:04	100.13		
10	5/28/09 1:35	100.10		

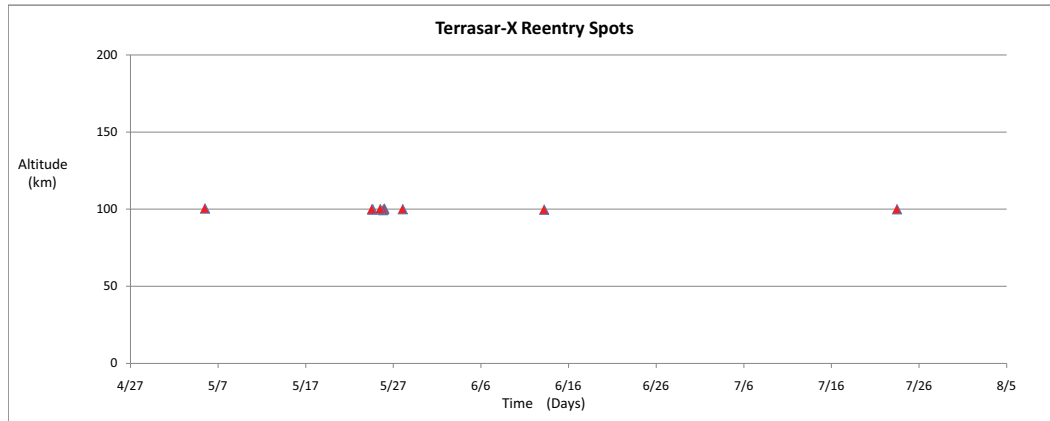


Figure 4.7: Summarized predicted reentry times for Terrasar-X orbit.

4.1.4 Atmospheric Unpredictability Conclusion. These simulations have confirmed the impracticality of any reentry prediction that is more than a few days into the future due to the unpredictability of the atmosphere. As a result, the study showed a variability increase in reentry prediction as the actual reentry was further into the future.

4.2 Drag Increase by a Factor

The STK software program provides the capability to increase drag by a certain factor at a certain point in time. This feature was used to explore the effects of increased drag, as in the case of solar panel deployments, at different points in the orbital path. This study focuses on the time reentry prediction only and not the location reentry prediction.

4.2.1 Debris Orbit Reentry. Figure 4.8 shows the dramatic change the object experiences in its reentry path when the drag is scaled up by a factor of ten. The drag is increased at a single point and propagated until reentry. This is done for four different points (not on the same simulation). Figure 4.8 shows all five simulations:

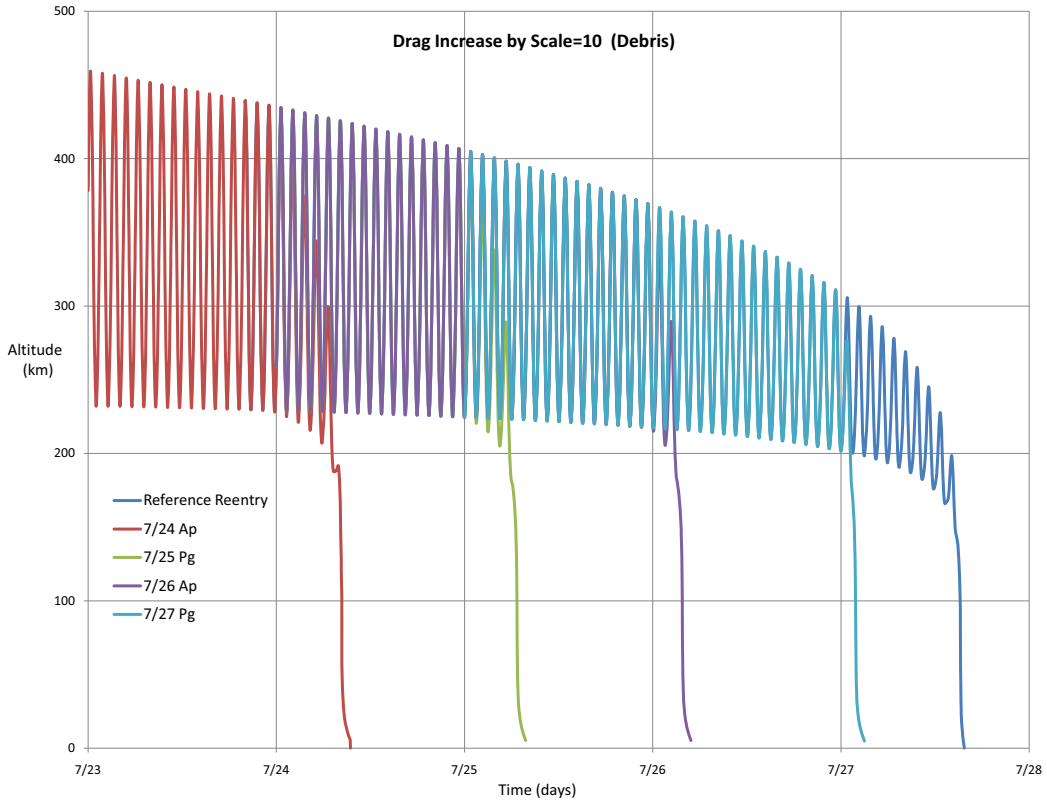


Figure 4.8: Debris reentry predictions due to drag increase at several points in the orbit path.

Each drag increase is set at the beginning of the calendar day. In the first drag scale, the object accelerated and took just over 9 hours to reenter with the reference reentry prediction almost 4 days into the future. Thus, the same thing happens for the rest of the points. It is important to note that the graph shows an increase in the objects' acceleration the closer to reentry the drag increase is set. This is depicted by the top graph in Figure 4.9:

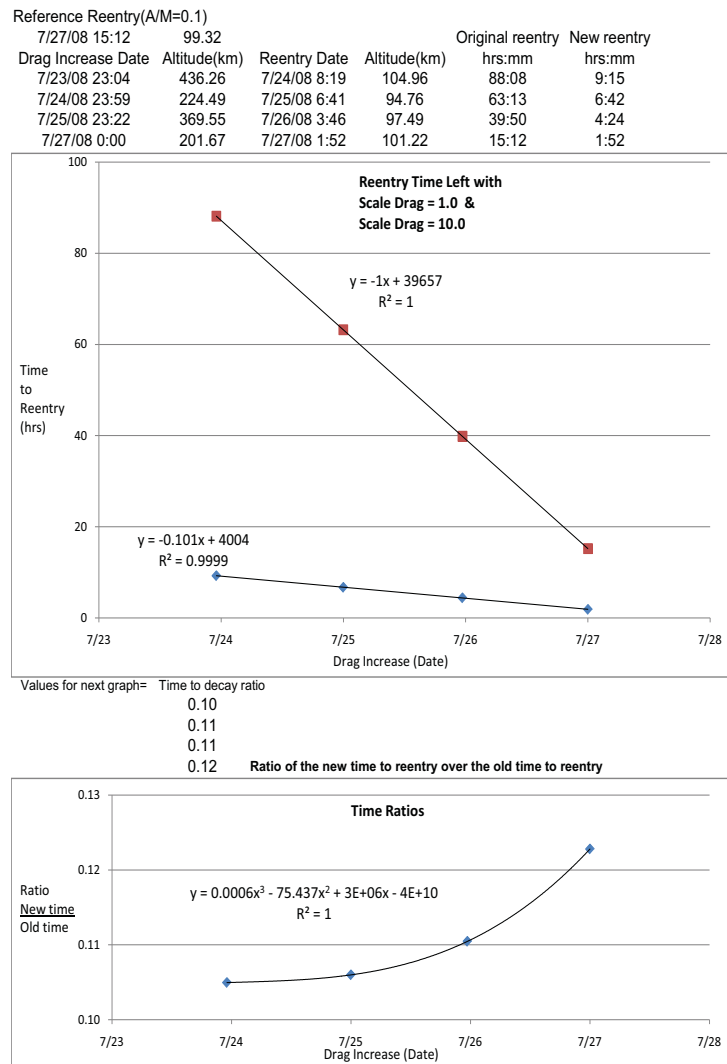


Figure 4.9: Predicted reentry times for Debris orbit; Original vs. New Time to Decay plot; New over Original Time to Decay Ratio plot.

In fact, the ratio of the new time to reentry over the reference time to reentry increases as you get closer to reentry. This means the closer the object is to reentry the more the new time to reentry approaches the original time to reentry. This is expected since it should approach one at the point of reentry. Still the ratio stays in the teens for the 4 chosen points.

To see how the reentries behaved with an extreme drag increase, the factor by which the drag was increased was set to 100 and path changes are depicted in Figure 4.10.

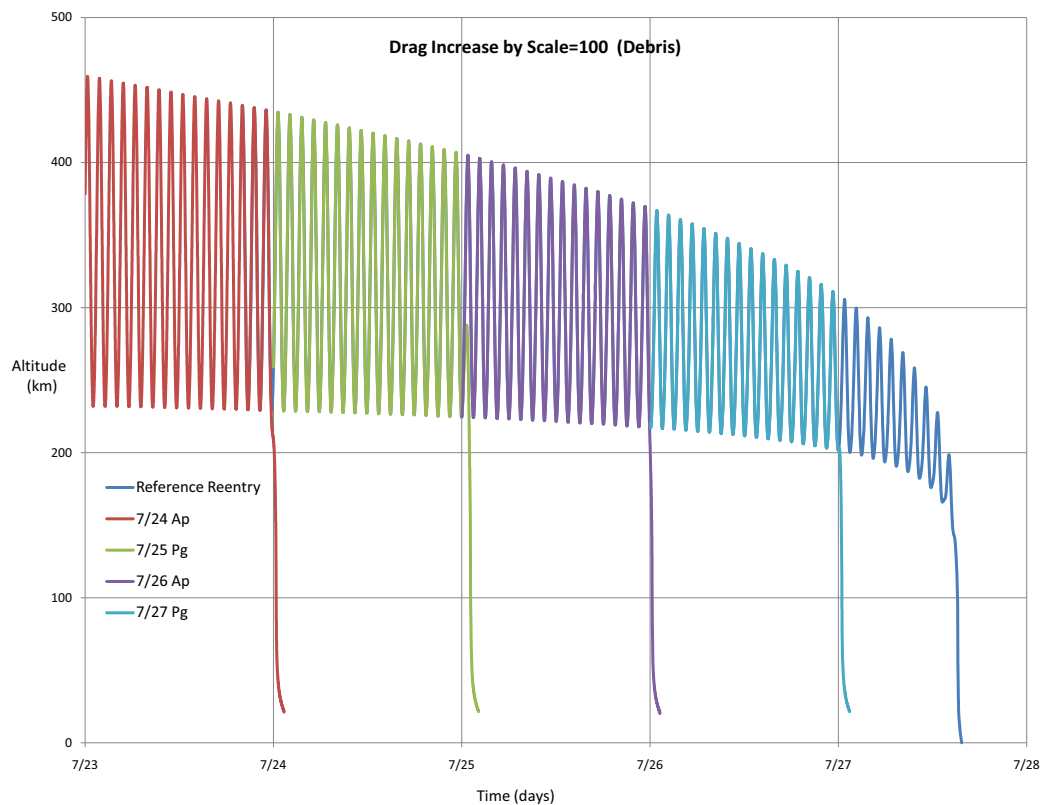


Figure 4.10: Debris reentry predictions due to extreme drag increase at several points in the orbit path.

It is obvious that with a drag increase of this magnitude the object was made to come in within 1 revolution.

Figure 4.11 shows the new time predictions to reentry and how the ratio between the new prediction and the old prediction did not increase as dramatically because of the already small ratio values:

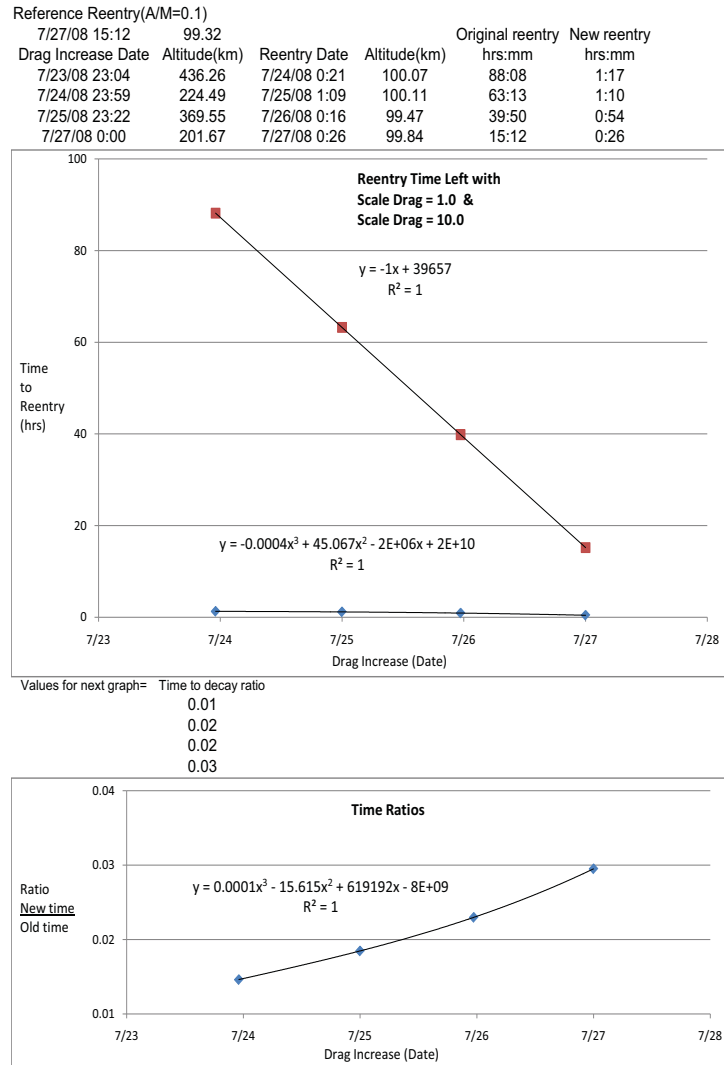


Figure 4.11: (Second) Predicted reentry times for Debris orbit; Original vs. New Time to Decay plot; New over Original Time to Decay Ratio plot.

4.2.2 ISS Orbit Reentry. This second set of simulations focuses on exploring the change in the time left to reentry by increasing the time in between points of drag increases from 24 hours in the previous set of simulations to 96 hours. Figure 4.12 illustrates the reentry paths:

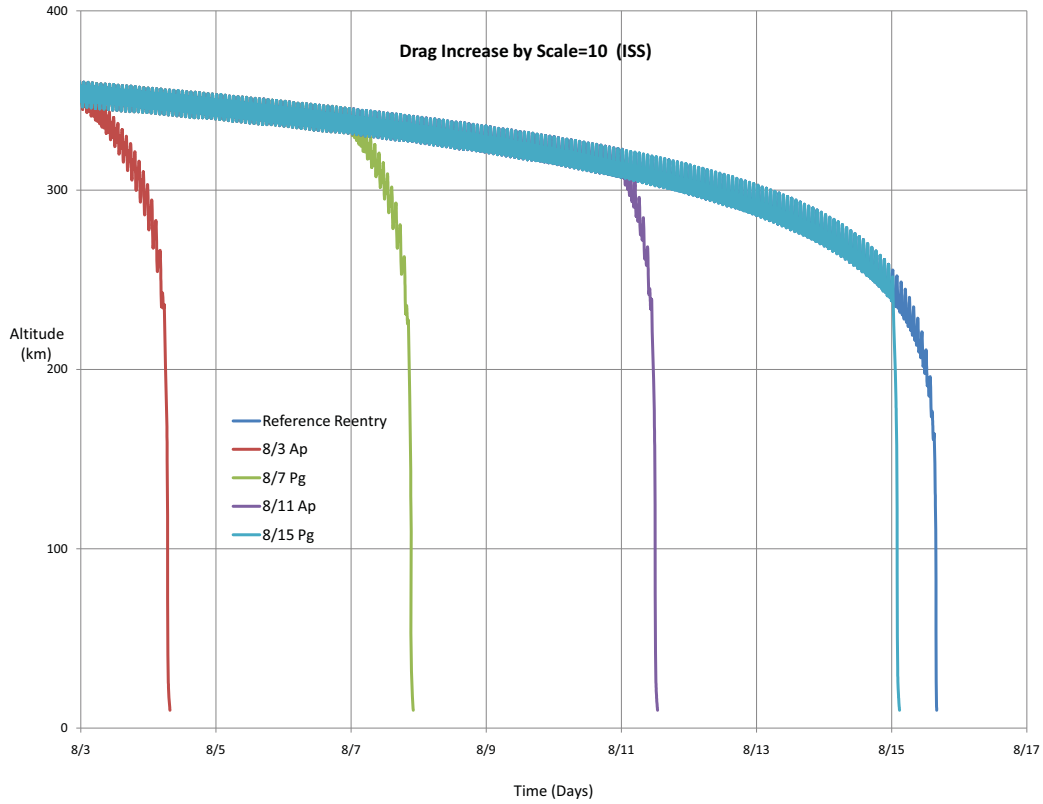


Figure 4.12: ISS reentry predictions due to drag increase at several points in the orbit path.

The first drag scale increase was set over 12.5 days prior to reentry and the time between drag increase points was set to 4 days. Figure 4.13 shows the same trends from the previous simulations:

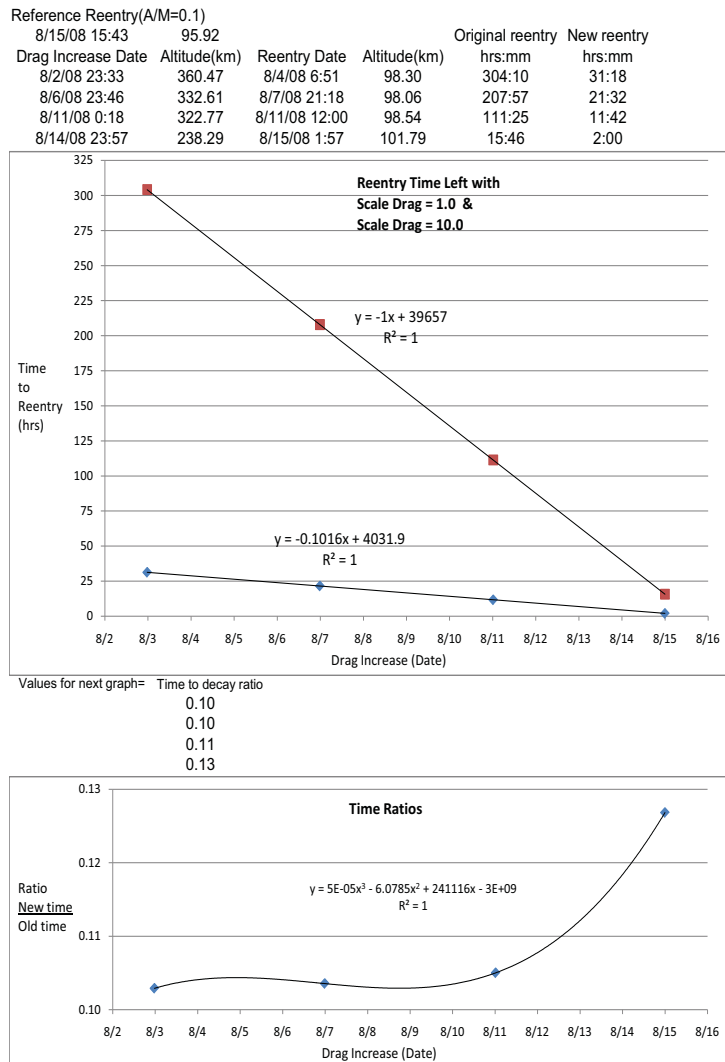


Figure 4.13: Predicted reentry times for ISS orbit; Original vs. New Time to Decay plot; New over Original Time to Decay Ratio plot.

The interesting change was that the ratio of the new time to reentry over the old time to reentry showed a little stagnation until the third point. The ratios are still in the 10 to 11 percent range of the original time left to reentry. Figure 4.14 shows

the reentry paths resulting from an increase in drag scale of 100:

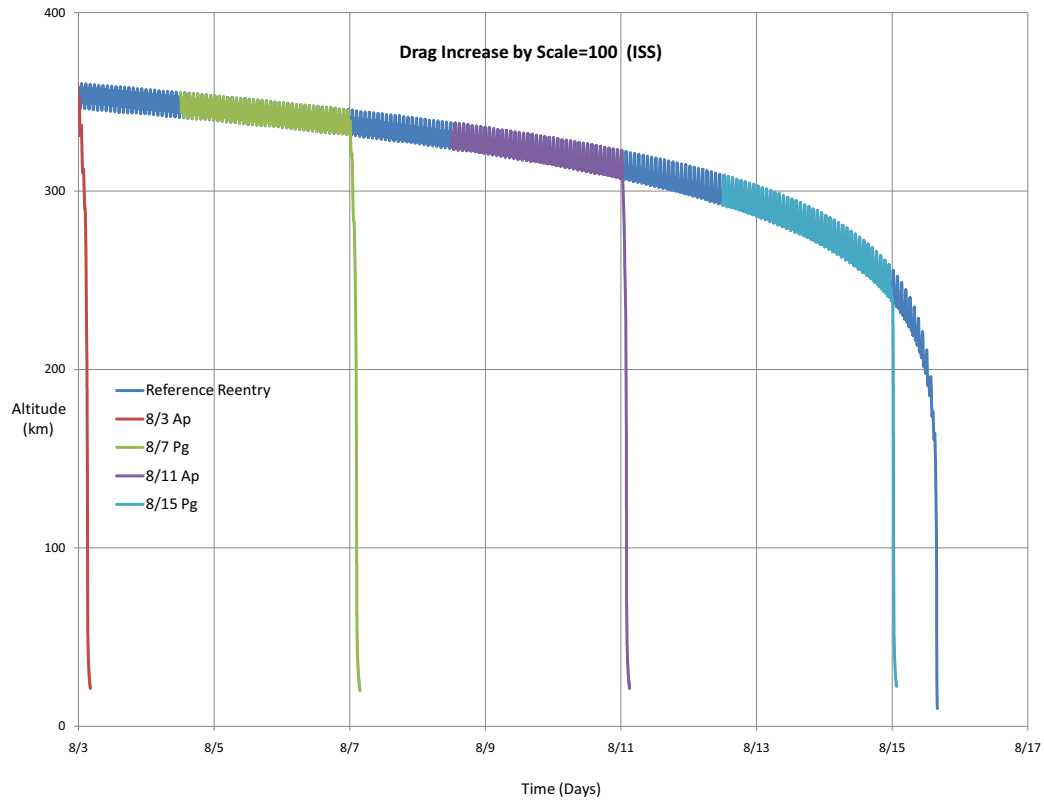


Figure 4.14: ISS reentry predictions due to extreme drag increase at several points in the orbit path.

Once more, the extreme increase in drag pulled the reentries to within 4 hours from the drag increase. The following summary shows the last one making it reenter in 36 minutes:

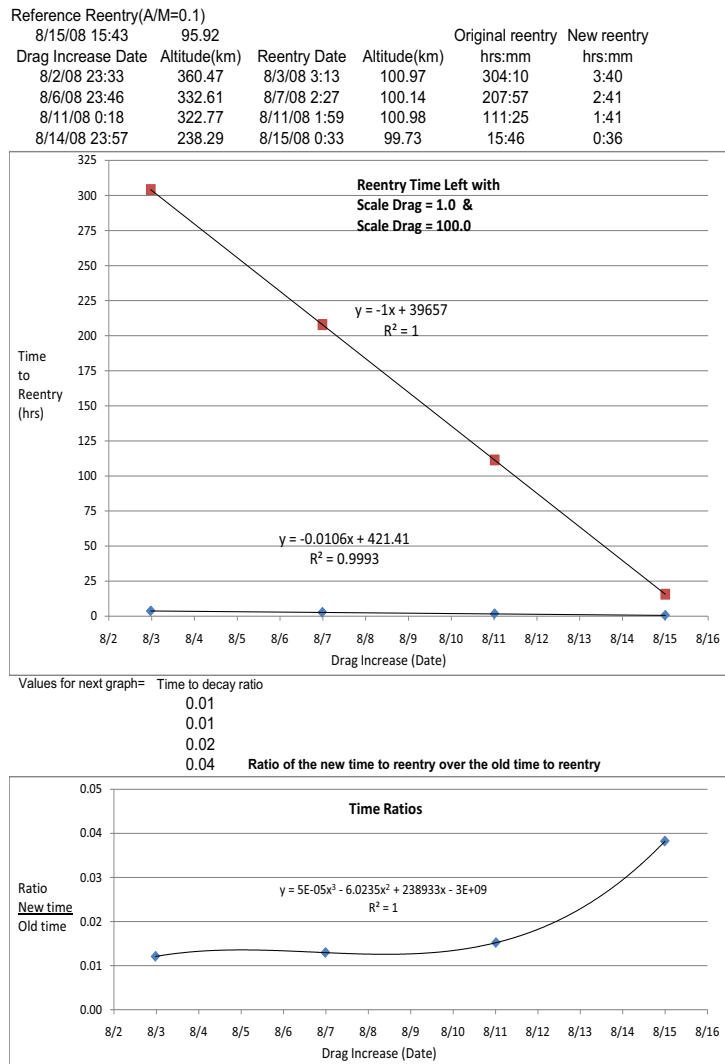


Figure 4.15: (Second) Predicted reentry times for ISS orbit; Original vs. New Time to Decay plot; New over Original Time to Decay Ratio plot.

Another observation is that in the extreme scale increase of 100, the ratios of time left to reentry were in the single percent digits, (see Figure 4.15) and in the scale increase of 10, shown in Figure 4.13, the time left to reentry ratios were in the low teens.

4.2.3 *Terrasar-X Orbit Reentry.* The last set of simulations for this study explore the effects of the same drag scale increases used in the previous 2 sets. This type of orbit will show what kind of an effect the increase in inclination will have on the patterns shown before by the increases in drag.

For the Terrasar-X element set, the first scale increase was set 3.5 days prior to reference reentry and the rest were spread out in 24 hour intervals.

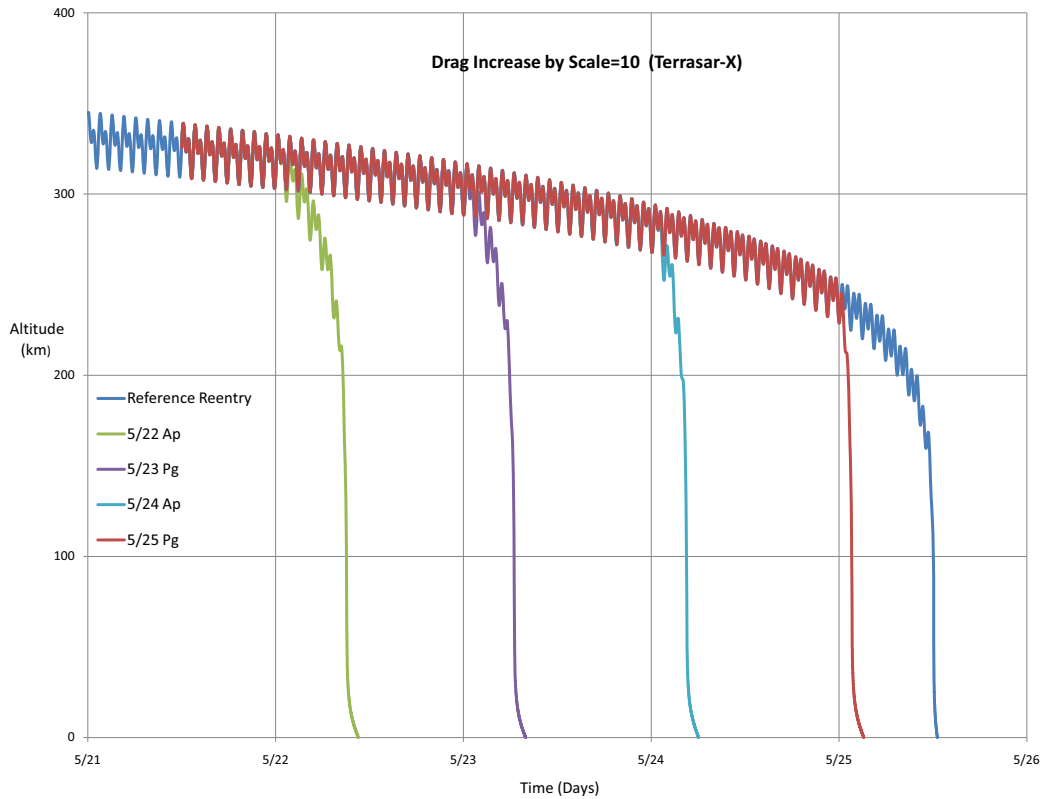


Figure 4.16: Terrasar-X reentry predictions due to drag increase at several points in the orbit path.

Figure 4.16 shows the same behavior as the 2 previous sets of simulations, where new time to reentry drops as you get closer to reference reentry from almost 9 hours to 96 minutes, depicted in Figure 4.17:

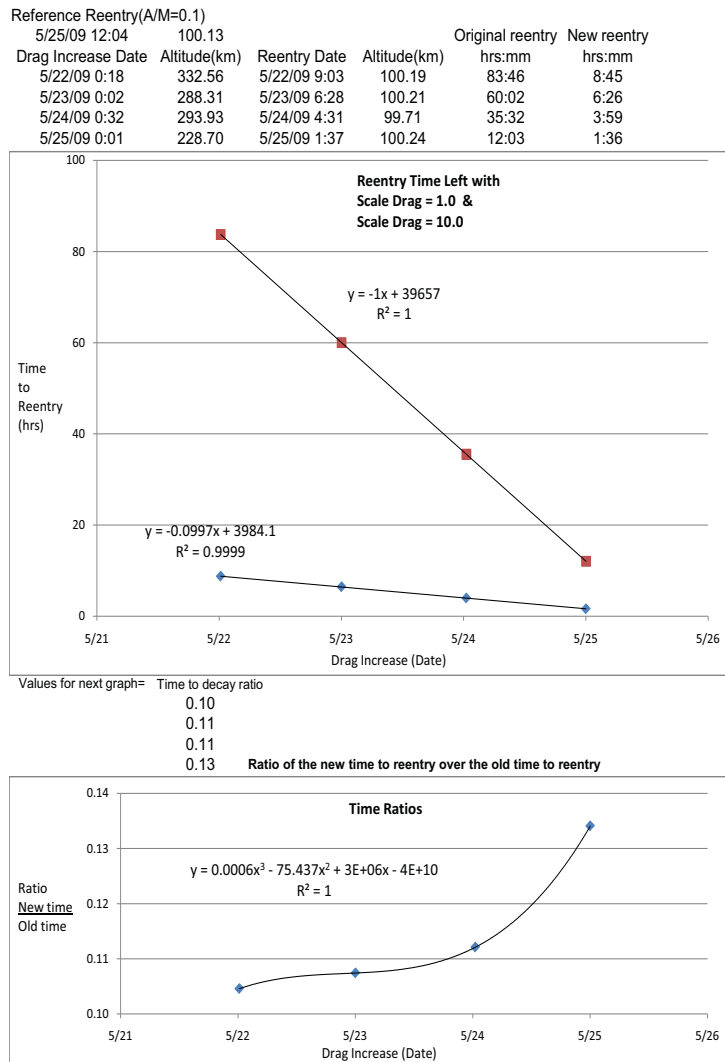


Figure 4.17: Predicted reentry times for ISS orbit; Original vs. New Time to Decay plot; New over Original Time to Decay Ratio plot.

One last time the drag scale was increased to 100 and the same conduct from the previous simulations was observed. The reentry path dramatically accelerated towards reentry.

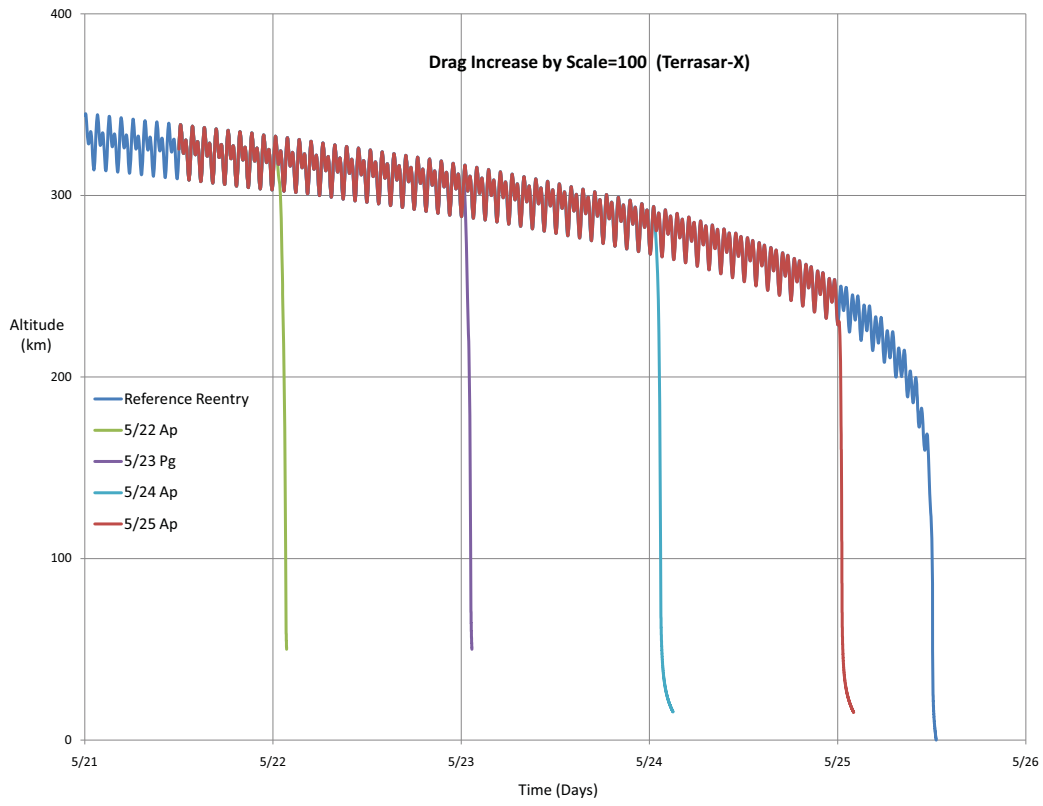


Figure 4.18: Terrasar-X Reentry predictions due to extreme drag increase at several points in the orbit path.

Similar results were observed as depicted in Figure 4.19 and again the time to reentry ratios in the bottom graph of Figure 4.19 show them to be in the single digit percentile.

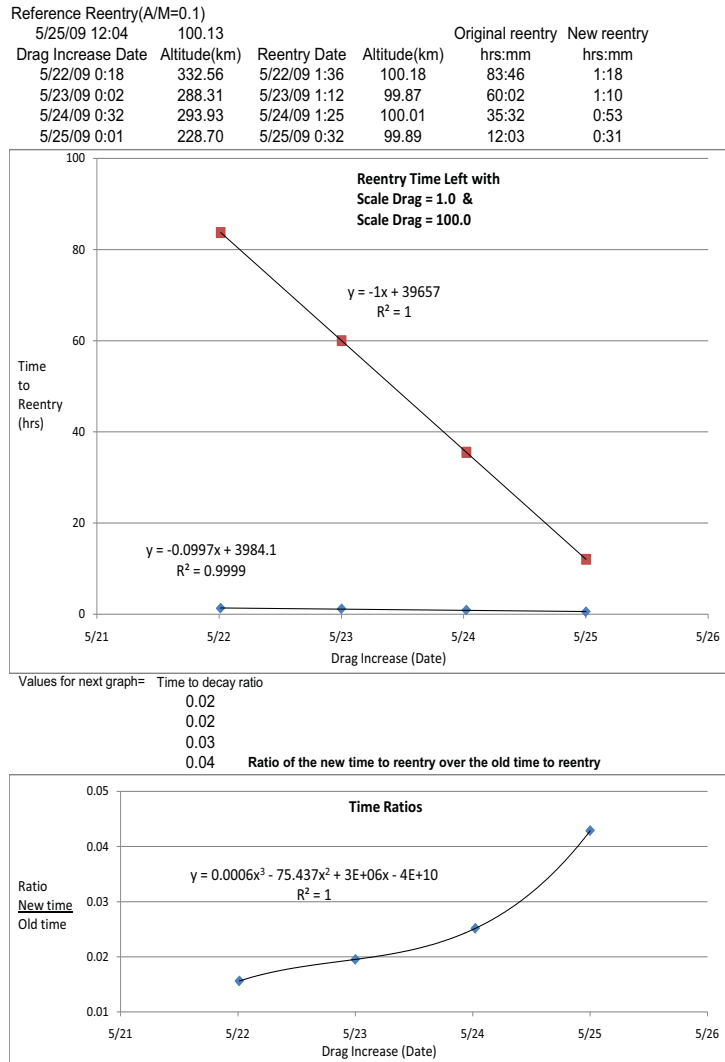


Figure 4.19: (Second) Predicted reentry times for ISS orbit; Original vs. New Time to Decay plot; New over Original Time to Decay Ratio plot.

4.2.4 Drag Increase Conclusion. This study has established making an object reenter through the use of drag is achievable with the appropriate increase in drag. It was observed that the ratio of the new time to reentry over the old time to reentry seemed to be inversely proportional to the scale of drag increase. Also, the drag increase shows a linear relationship to the time left to reentry.

4.3 Reentry Prediction with a Single Increase to A/M at Several Points in Orbit Path

In order to investigate more closely what the increase in surface area would do to the reentry path of an object the A/M ratio was manipulated in STK. All 3 orbits previously used in the studies were used for this study. There were 3 points chosen in the path of the reference reentry where the A/M ratio was increased from 0.1 to 1.0. The furthest point away from the reentry time was simulated first and all ten atmospheric models were used for the plotted propagations.

4.3.1 Debris Variability Change. The first element set propagated was the Debris set. The first set of simulations increased the A/M ratio at the 57 hour point before the reference reentry. Figure 4.20 shows the reentry prediction paths, with the larger A/M ratio, by all atmospheric models against the reference reentry. It displays a rapid descent in altitude with all the reentry predictions close to each other.

4.3.1.1 First A/M Increase. In Figure 4.21, the new reentry predictions are shown without the reference reentry to hone in on their variability spread. The time spread between the earliest prediction and the latest one was just over 2 hours. It is starting to become clear that the time prediction's uncertainty is decreasing greatly. The original 57 hours left to reentry decreased to about 6 hours and the original reentry time prediction spread of 2 days (from Figure 4.2), has dropped to a forced reentry spread of 2 hours.

Furthermore, the fact that the reentry time has dropped to nearly 2 hours indicates the reentry locations are a bit more than a revolution apart. Thus, Figure 4.22 shows 4 reentry points off the trend-line but 6 of them start to expose a gain in precision. At this point you are able to predict the location of the reentry within a ring around the earth where you essentially would want to land it or not.

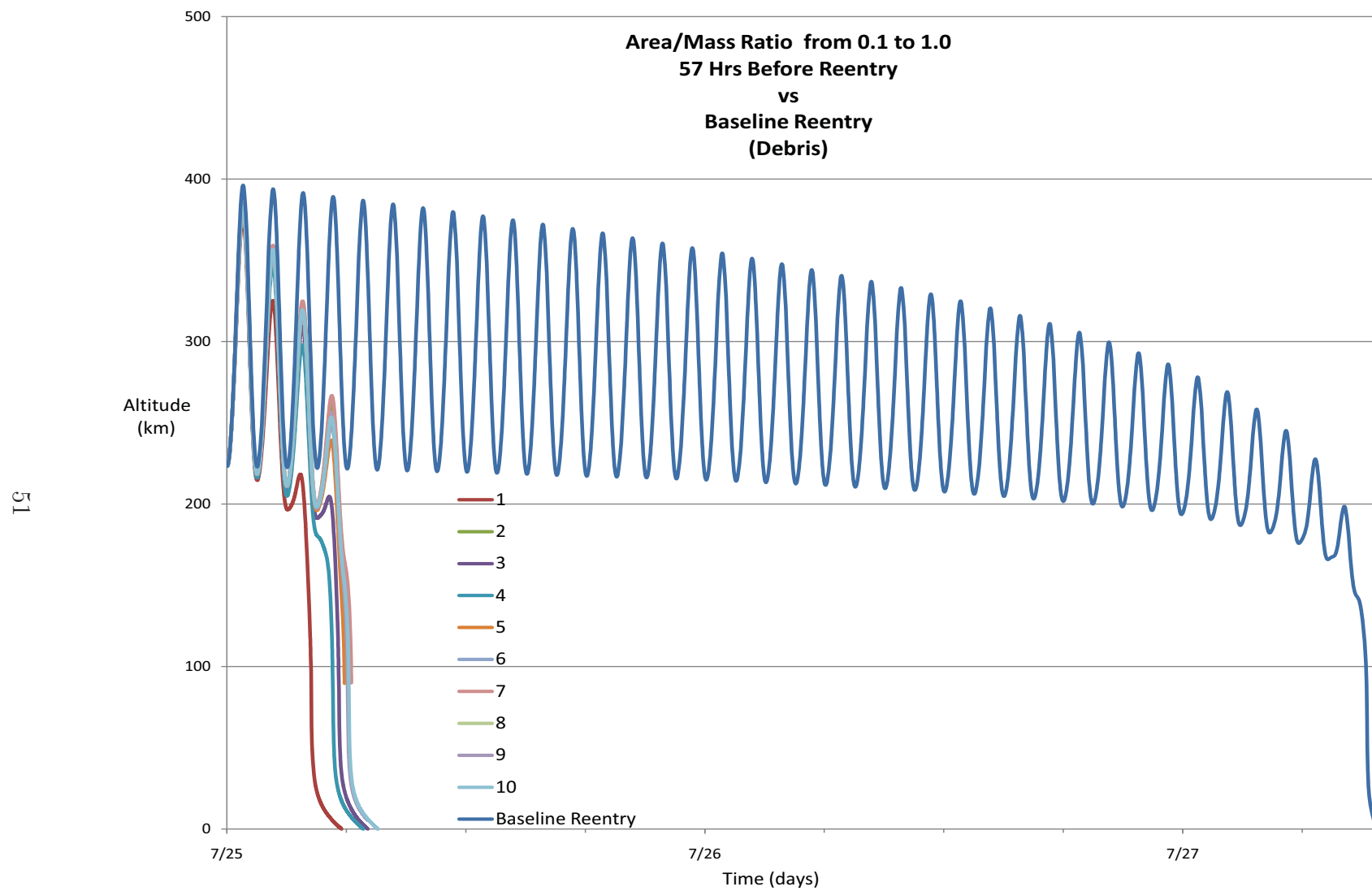


Figure 4.20: Debris orbit reentry predictions by ten atmospheric models with a single A/M increase 57 hours prior to original reentry.

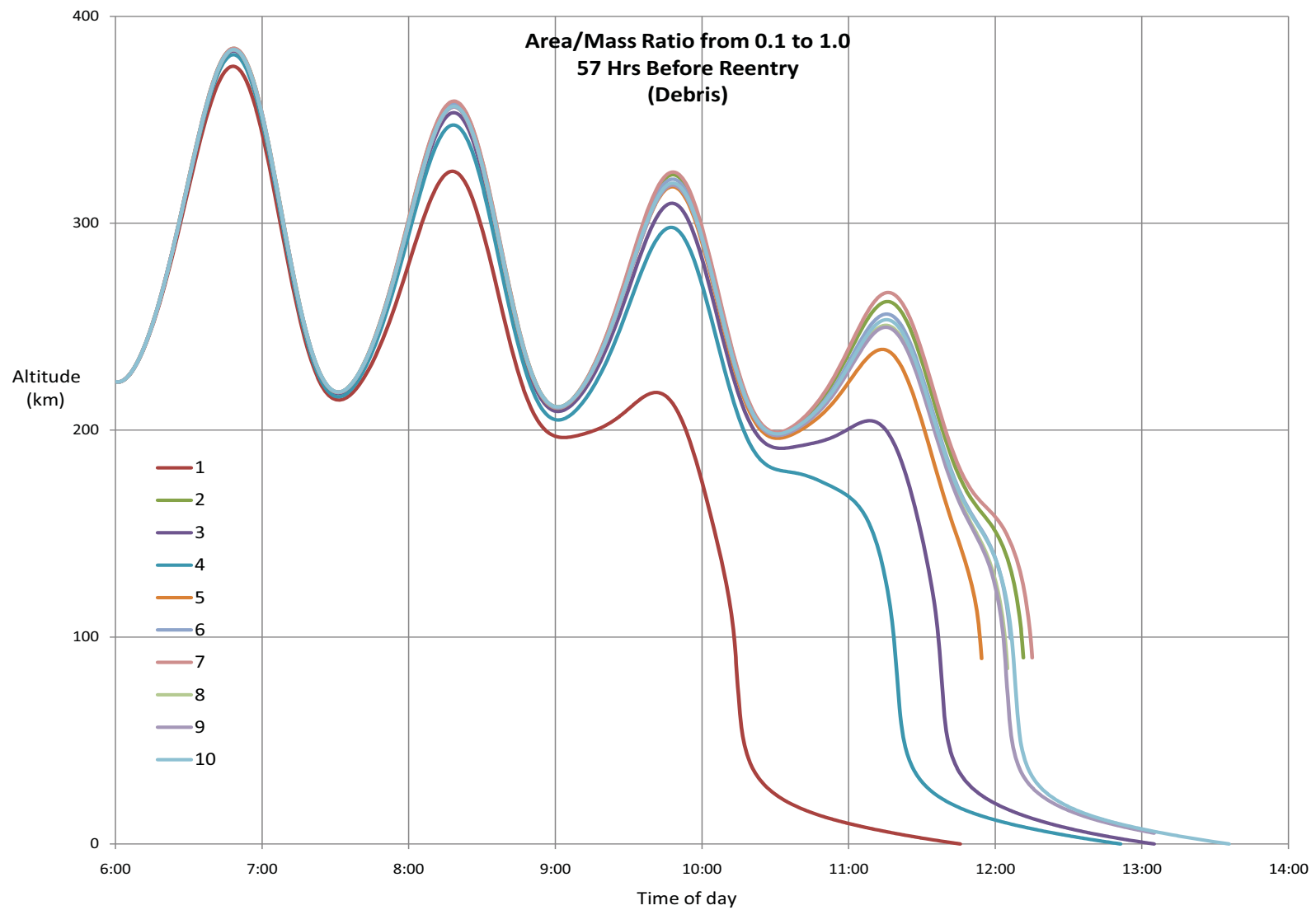


Figure 4.21: Homed in Debris orbit reentry predictions by ten atmospheric models with a single A/M increase 57 hours prior to original reentry.

A/M Scale Increase Point 57 hrs
Reentry Time Spread (hrs:mm:ss) 2:01:20

Sorted by Date				
Atmospheric Model	Reentry Time	Latitude (deg)	Longitude (deg)	Altitude (km)
1	7/25/08 10:13	-0.37	199.75	99.89
4	7/25/08 11:18	57.92	80.14	99.90
3	7/25/08 11:36	20.89	164.84	100.85
5	7/25/08 11:53	-35.65	200.02	100.66
9	7/25/08 12:03	-57.72	246.93	99.78
8	7/25/08 12:04	-58.21	251.73	99.70
6	7/25/08 12:06	-58.42	267.17	100.63
10	7/25/08 12:06	-58.11	271.56	100.53
2	7/25/08 12:10	-52.35	297.28	99.96
7	7/25/08 12:14	-43.24	313.65	99.08

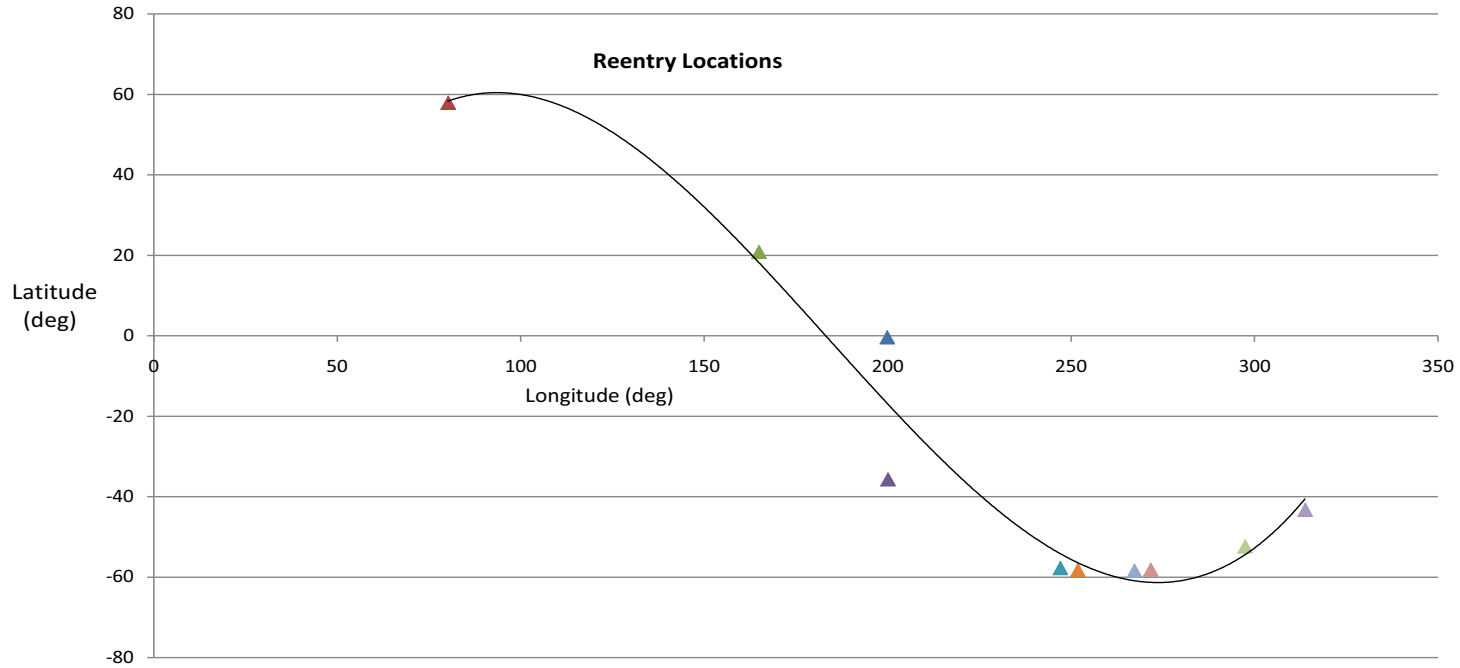


Figure 4.22: Summarized predicted Debris orbit reentry times and locations by ten atmospheric models with a single A/M increase 57 hours prior to original reentry.

4.3.1.2 Second A/M Increase. The second point of A/M ratio increase for the debris element set began 24 hours before the reference reentry. The purpose is to be closer to reentry in order to look for a precision gain in the time and location of the reentry prediction.

Figure 4.23 shows the reference orbit altitude of the object as it heads for reentry along with the rest of the predictions. The same behavior from the previous simulation is observed, that is, all ten projections with the A/M ratio increase are reentered much quicker and the predictions are even closer together. The time to reentry drops from 24 hours to about 3 hours.

In fact, the reentry time spread has dropped to 45 minutes. Through a closer look at the reentry time spread, there seems to be a point that is enough separated from the group to be considered an outlier. By removing this outlier the reentry time spread lowers to 16 minutes. This can clearly be seen in Figure 4.24 where the prediction using Atmospheric Model Number 1 is about half an hour before the rest of the predictions.

The drop in time variability drives to a much better reentry location spread. Figure 4.25 shows a plot of the latitude and longitude of each reentry point and it is clear that the path of reentry is much more desirable than before.

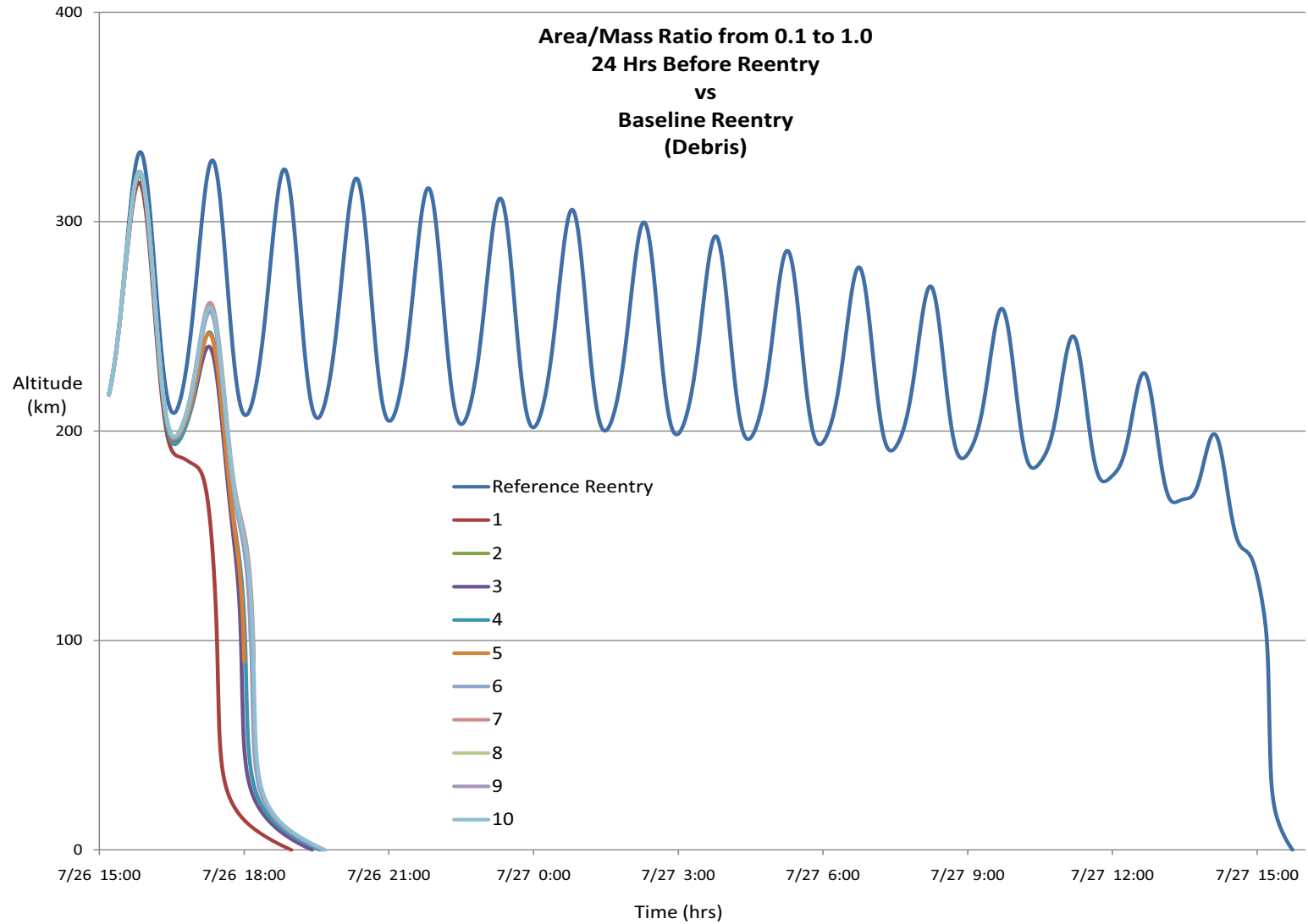


Figure 4.23: Debris orbit reentry predictions by ten atmospheric models with a single A/M increase 24 hours prior to original reentry.

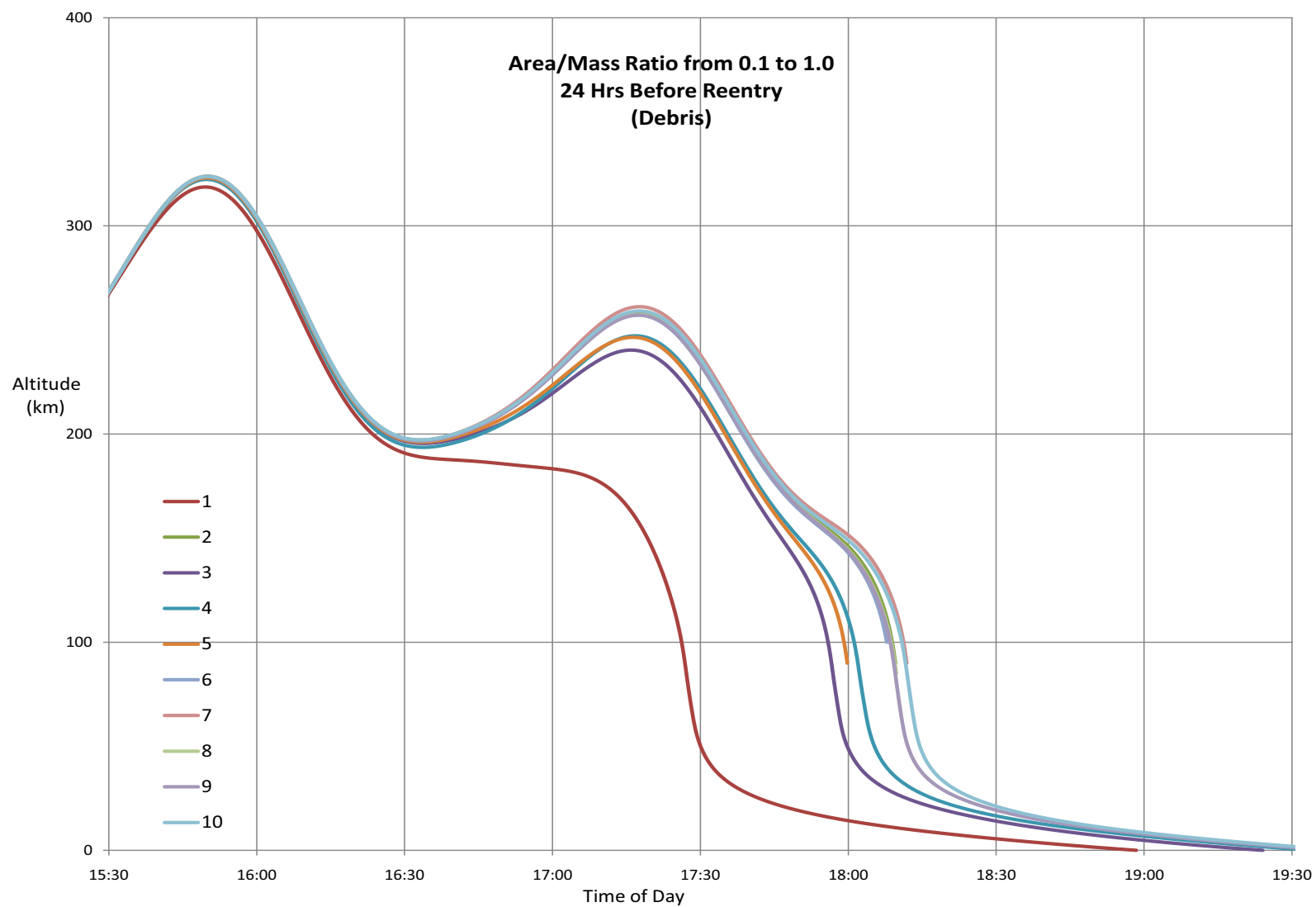


Figure 4.24: Homed in Debris orbit reentry predictions by ten atmospheric models with a single A/M increase 24 hours prior to original reentry.

A/M Scale Increase Point 24 hrs
Reentry Time Spread (hrs:mm:ss) 0:45:10

Sorted by Date				
Atmospheric Model	Reentry Time	Latitude (deg)	Longitude (deg)	Altitude (km)
1	7/26/08 17:26	55.08	23.00	100.80
3	7/26/08 17:56	-37.96	105.03	99.98
5	7/26/08 17:59	-46.91	116.53	101.02
4	7/26/08 18:01	-52.28	127.39	99.67
6	7/26/08 18:08	-58.31	171.59	99.95
9	7/26/08 18:08	-57.81	177.21	99.46
8	7/26/08 18:09	-57.66	178.44	100.07
2	7/26/08 18:09	-57.55	179.29	100.34
10	7/26/08 18:11	-54.75	192.89	100.06
7	7/26/08 18:11	-54.27	194.48	99.99

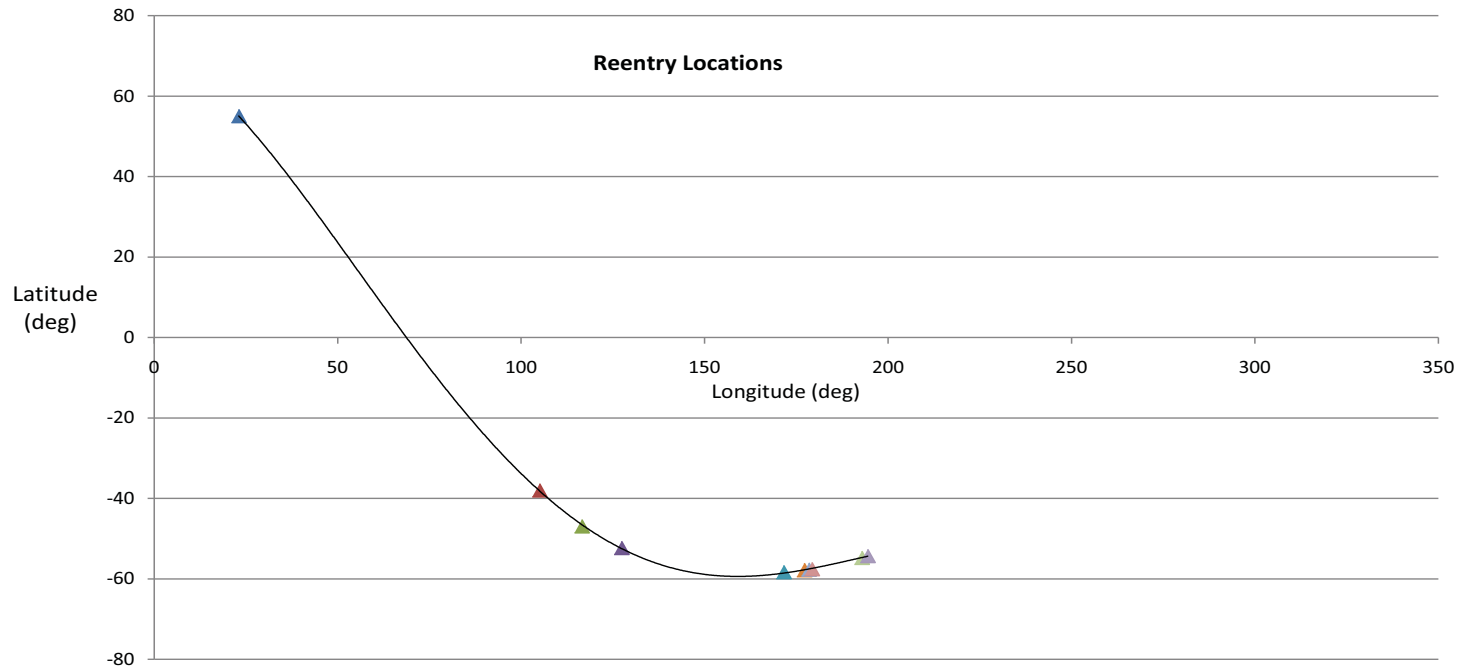


Figure 4.25: Summarized predicted Debris orbit reentry times and locations by ten atmospheric models with a single A/M increase 24 hours prior to original reentry.

4.3.1.3 Third A/M Increase. The last increase in A/M ratio was chosen to be 10 hours before reentry. It is expected to have the best effect out of all previous points since it is the closest one to the actual reentry.

The same behavior from the previous plots is observed in this simulation. The simulations with the A/M increase dramatically drop in altitude as shown in Figure 4.26. The time until reentry is decreased from 10 hours to about 1 hour and the reentry time spread is now down to about 20 minutes. Once more, if we take out the first reentry prediction out of the equation, the spread comes down to about 12 minutes.

Figure 4.28 shows a tightening of the reentry location spread and the point that seems to be an outlier is apparent. Taking out this point, which is the prediction by Atmospheric Model Number 1, makes the reentry path cover 36 degrees in latitude and just 40 degrees in longitude.

Once all 3 A/M increase simulations were performed, a plot displaying reference time left to reentry as a function of the time prediction spreads was produced. Subsequently, Excel was used to generate a best fit trendline along with its respective formula. The trendline equation has the units of days since dates were used for all the calculations in the simulations.

These first set of simulations were propagated with the debris element set. These simulations showed a glimpse of a trend. The trend seems to be that a quadratic relationship exists between the time left to reentry and the predicted time of reentry spread.

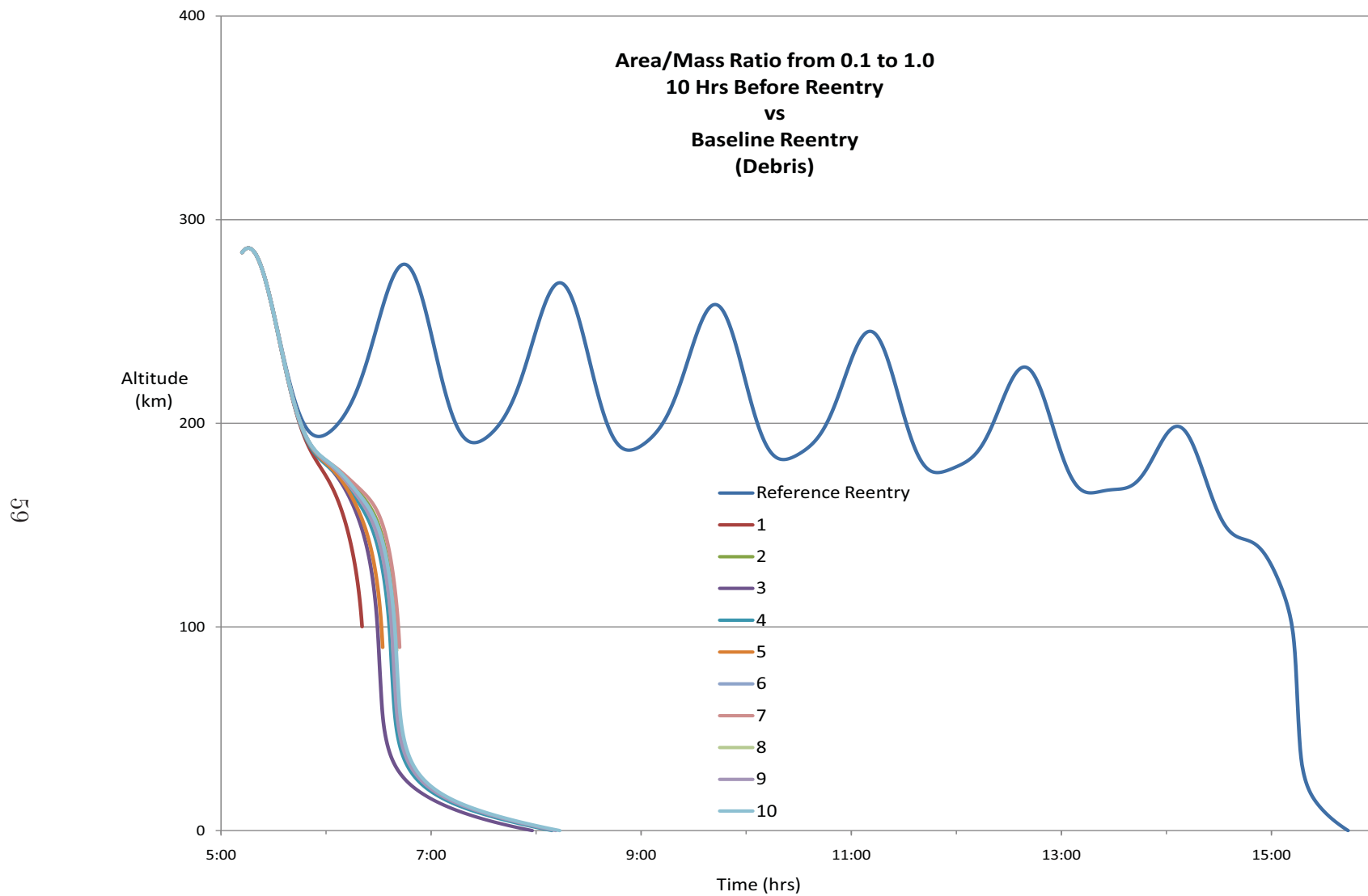


Figure 4.26: Debris orbit reentry predictions by ten atmospheric models with a single A/M increase 10 hours prior to original reentry.

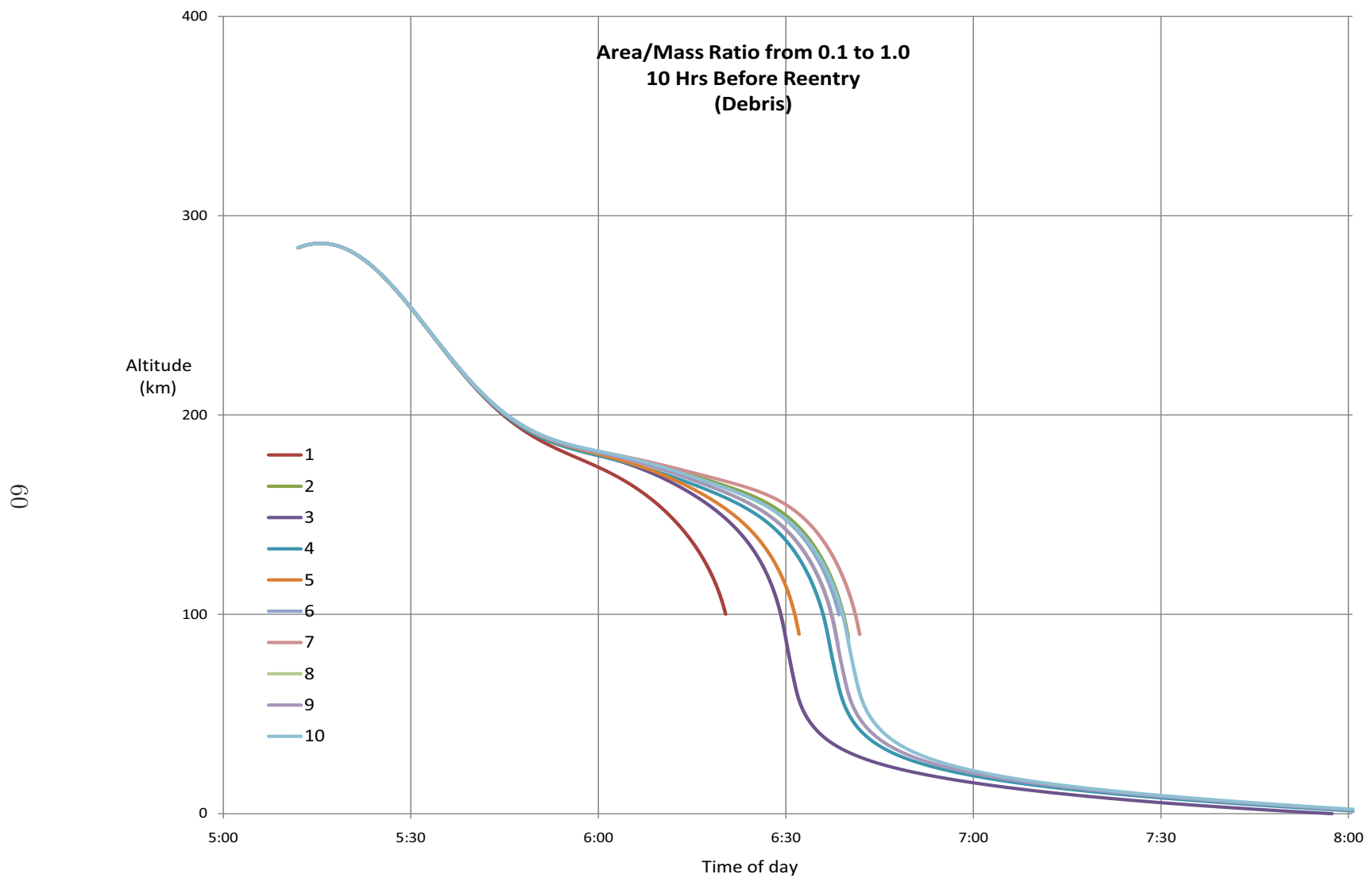


Figure 4.27: Homed in Debris orbit reentry predictions by ten atmospheric models with a single A/M increase 10 hours prior to original reentry.

A/M Scale Increase Point 10 hrs
Reentry Time Spread (hrs:mm:ss) 0:20:50

Sorted by Date

Atmospheric Model	Reentry Time	Latitude (deg)	Longitude (deg)	Altitude (km)
1	7/27/08 6:20	-13.79	58.97	100.12
3	7/27/08 6:29	16.98	76.11	100.06
5	7/27/08 6:31	24.90	81.24	99.08
4	7/27/08 6:36	39.52	93.89	99.40
8	7/27/08 6:37	43.37	98.54	100.21
9	7/27/08 6:37	43.36	98.52	99.32
6	7/27/08 6:38	46.58	103.21	100.02
10	7/27/08 6:39	47.93	105.47	100.94
2	7/27/08 6:39	48.32	106.16	100.48
7	7/27/08 6:41	52.92	116.27	99.53

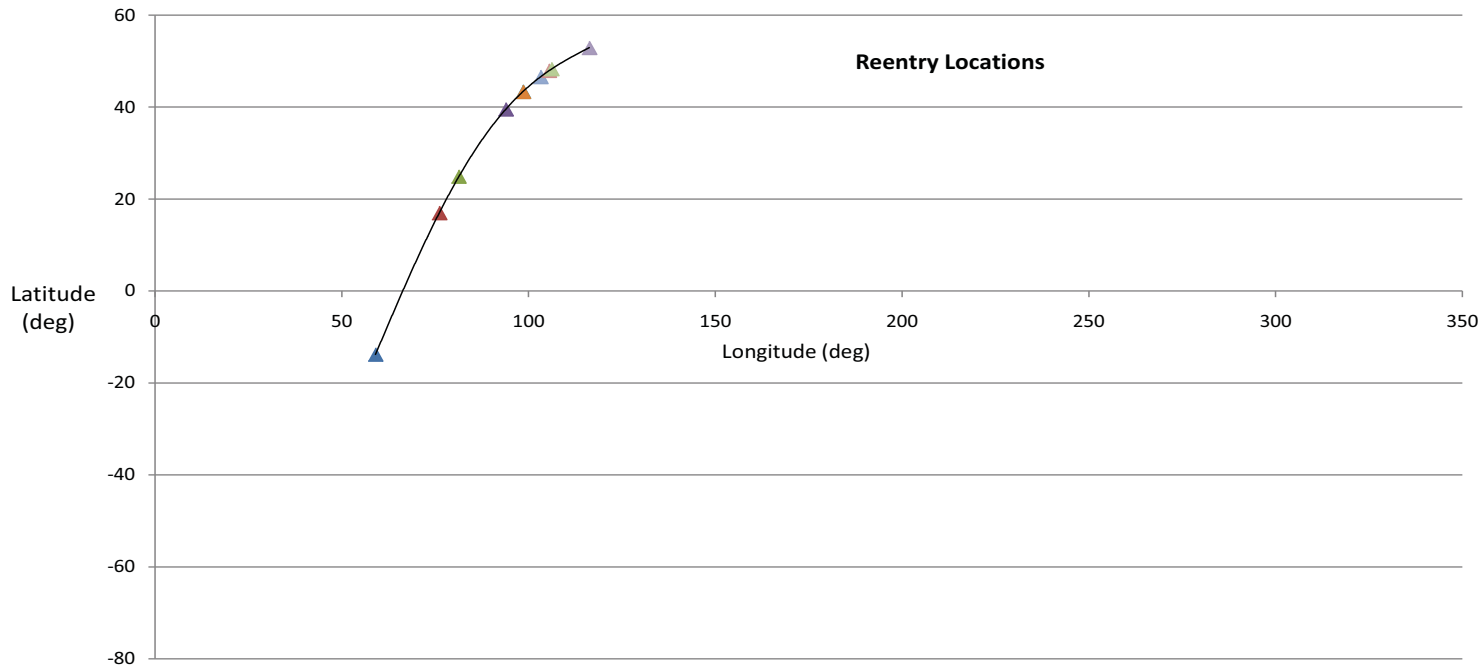


Figure 4.28: Summarized predicted Debris orbit reentry times and locations by ten atmospheric models with a single A/M increase 10 hours prior to original reentry.

Reentry Spread with A/M Increase from 0.1 to 1.0

Reference Reentry in MSISE 1990 with A/M= 0.1	Time 7/27/08 15:12	Altitude(km) 99.39
---	-----------------------	-----------------------

Drag Increase Point in Hrs Before Reference Reentry	Atmospheric Model	Reentry Time	Altitude (km)	Time Spread hrs:mm:ss
10	1 (earliest)	7/27/08 6:20	100.12	0:20:50
	9(reference)	7/27/08 6:37	99.32	
	7 (latest)	7/27/08 6:41	99.53	
24	1 (earliest)	7/26/08 17:26	100.80	0:45:10
	9(reference)	7/26/08 18:08	99.99	
	7 (latest)	7/26/08 18:11	99.46	
57	1 (earliest)	7/25/08 10:13	99.89	2:01:20
	9(reference)	7/25/08 12:03	99.08	
	7 (latest)	7/25/08 12:14	99.78	

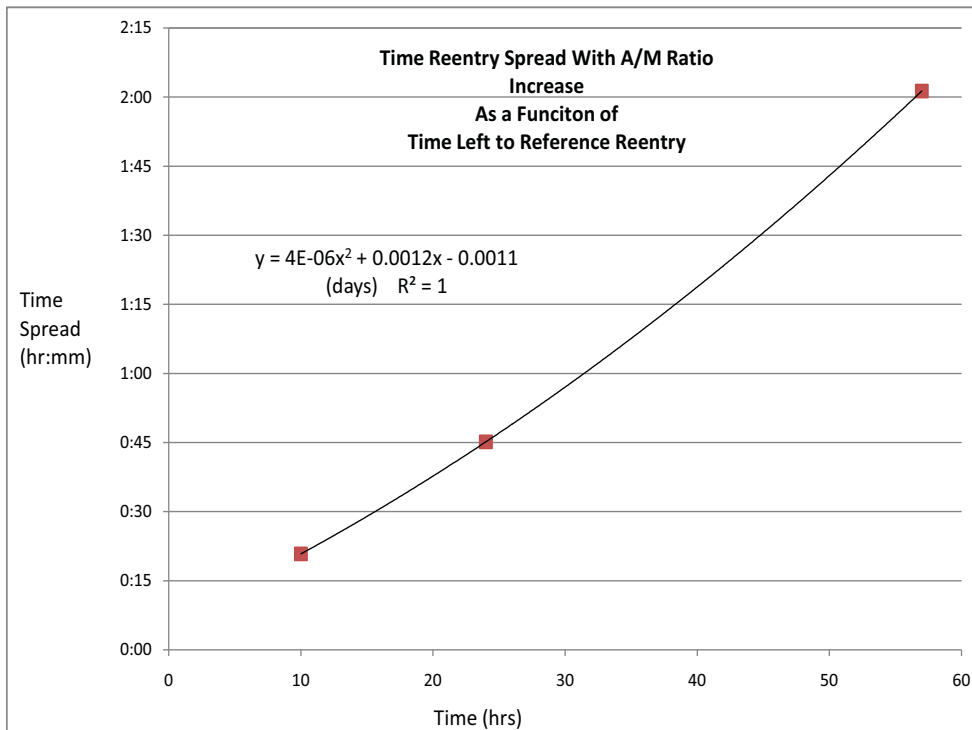


Figure 4.29: Summarized Debris orbit reentry time spreads with a single A/M increase at 57, 24, and 10 hours prior to original reentry.

4.3.2 ISS Element Variability Change. The second set of simulations for this study used the ISS orbit element set. The first point of A/M ratio increase was set 7.5 days prior to reference reentry. The change in A/M dropped the time left to reentry to less than 19 hours but, had a time reentry spread of over 7 hours. The reentry location spread was useless since the time prediction spread would put it just about anywhere in the world. Still, 7 of the predictions were within a trendline.

The next A/M ratio increase was set for 24 hours before reference reentry, decreasing the time to reentry to less than 3 hours. As in the previous subsection this one dropped the time reentry spread to 43 minutes. Also, like the previous set of simulations, the spread seems to have an outlier prediction. Subtracting it, gives a reentry time spread of 12 minutes. Once more, the location spread is very manageable, not counting the outlier point which is half an hour before the rest of the 9 points.

The last A/M ratio increase was set 10 hours prior to the reference reentry. As expected, this one gave the lowest reentry time spread at 14 minutes. When omitting the prediction by Atmospheric Model Number 1, the time drops down to 7 minutes. Also, the reentry location path spreads over 17 degrees in latitude and 28 degrees in longitude. To see further details mentioned above please see Figures C.1 through C.9 in Appendix C.

The same quadratic relationship that was observed in the debris simulations on Figure 4.29 between the time of reentry spread and the reference time left to reentry is observed in the plot on Figure 4.30:

Reentry Spread with A/M Increase from 0.1 to 1.0

Reference Reentry in MSISE 1990 with A/M= 0.1	Time 8/17/08 0:01	Altitude(km) 99.31
---	----------------------	-----------------------

Drag Increase Point in Hrs Before Reference Reentry	Atmospheric Model	Reentry Time	Altitude (km)	Time Spread hrs:mm:ss
10	1 (earliest)	8/16/08 15:15	103.96	0:15:00
	9(reference)	8/16/08 15:26	95.07	
	4 (latest)	8/16/08 15:30	91.86	
24	1 (earliest)	8/16/08 2:19	101.20	0:43:00
	9(reference)	8/16/08 2:50	101.09	
	7 (latest)	8/16/08 3:02	103.64	
180	1 (earliest)	8/10/08 0:15	106.42	7:11:00
	9(reference)	8/10/08 6:54	98.32	
	2 (latest)	8/10/08 7:26	99.71	

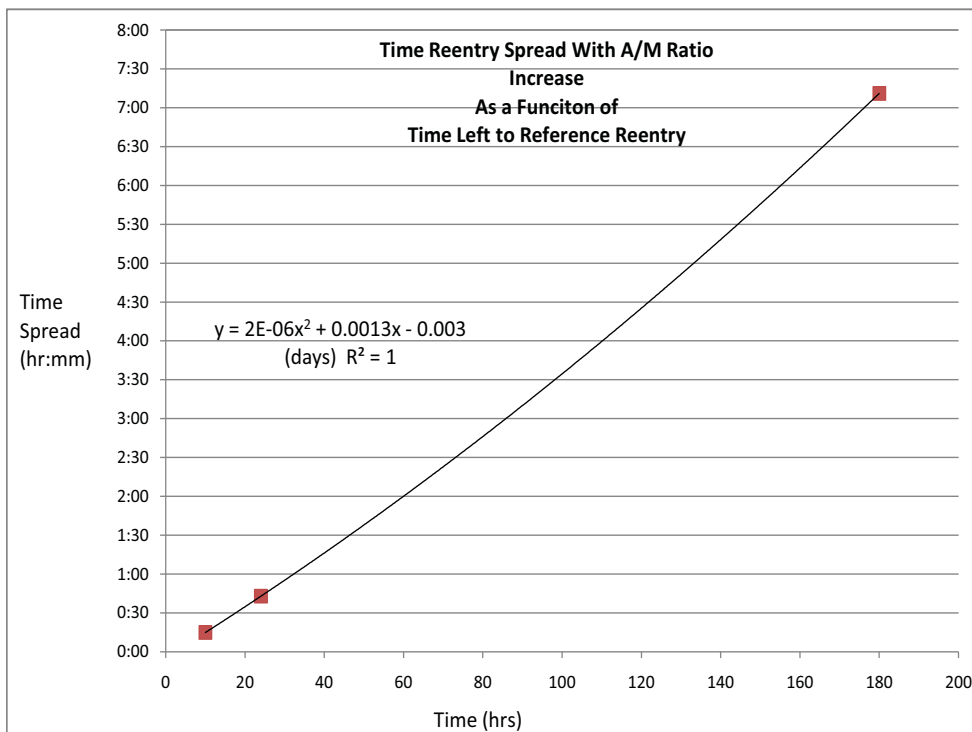


Figure 4.30: Summarized ISS orbit reentry time spreads with a single A/M increase at 180, 24, and 10 hours prior to original reentry.

4.3.3 Terrasar-X Element Variability Change. The last set of simulations for this section was performed using an element set from the Terrasar-X satellite. This element set not only has a circular orbit but it is also retrograde. The first point of A/M ratio increase was set 3 days before the reference reentry and decreased the time left to reentry to about 5.5 hours. It had a reentry spread of over 3 hours. This prediction spread was very poor on the location of reentry since only 4 of the predictions fell on a trendline.

The following point of A/M increase was set 24 hours prior to the reference reentry. The reentry time spread was lowered to less than 3 hours. The reentry time spread also decreased to 48 minutes. There was only 1 reentry point that was not on the trendline. It was half an hour off the rest of the predictions. When taking this point off, the reentry time drops to 27 minutes and the reentry locations have a spread of half a revolution.

The last point of A/M increase was 10 hours prior to reentry. The time left to reentry was shrunk down to 45 minutes. The actual reentry time spread was of less than 13 minutes. Finally, the reentry location path covered 51.3 degrees in latitude and only 10.1 degrees in longitude due to its high inclination. One last time, the time reentry spreads as a function of time left to reference reentry showed a quadratic relationship that Excel solved with units of days. Further details are in Figures C.10 through C.18 in Appendix C.

4.3.4 Conclusion of Reentry Variability Due to A/M Change. This study established that A/M ratio manipulation will dramatically change the time left to reentry. In addition, a great increase in precision of the predicted reentry is obtained when the manipulation is set closer to the natural reentry time. This would be done for objects where predicting the place and time of reentry are critical. Finally, the relationship between time reentry spread and time left to reentry seemed to be quadratic. Upon a closer look the relationship is actually much more linear than quadratic.

Reentry Spread with A/M Increase from 0.1 to 1.0

Reference Reentry in MSISE 1990 with A/M= 0.1	Time 4/19/09 17:20	Altitude(km) 100.44
---	-----------------------	------------------------

Drag Increase Point in Hrs Before Reference Reentry	Atmospheric Model	Reentry Time	Altitude (km)	Time Spread hrs:mm:ss
10	5 (earliest)	4/19/09 8:39	99.89	0:12:40
	9(reference)	4/19/09 8:45	99.85	
	3 (latest)	4/19/09 8:52	100.78	
24	6 (earliest)	4/18/09 19:57	99.82	0:48:14
	9(reference)	4/18/09 20:10	98.66	
	3 (latest)	4/18/09 20:45	100.93	
72	6 (earliest)	4/17/09 0:19	99.79	3:05:58
	9(reference)	4/17/09 1:01	101.64	
	3 (latest)	4/17/09 3:25	101.57	

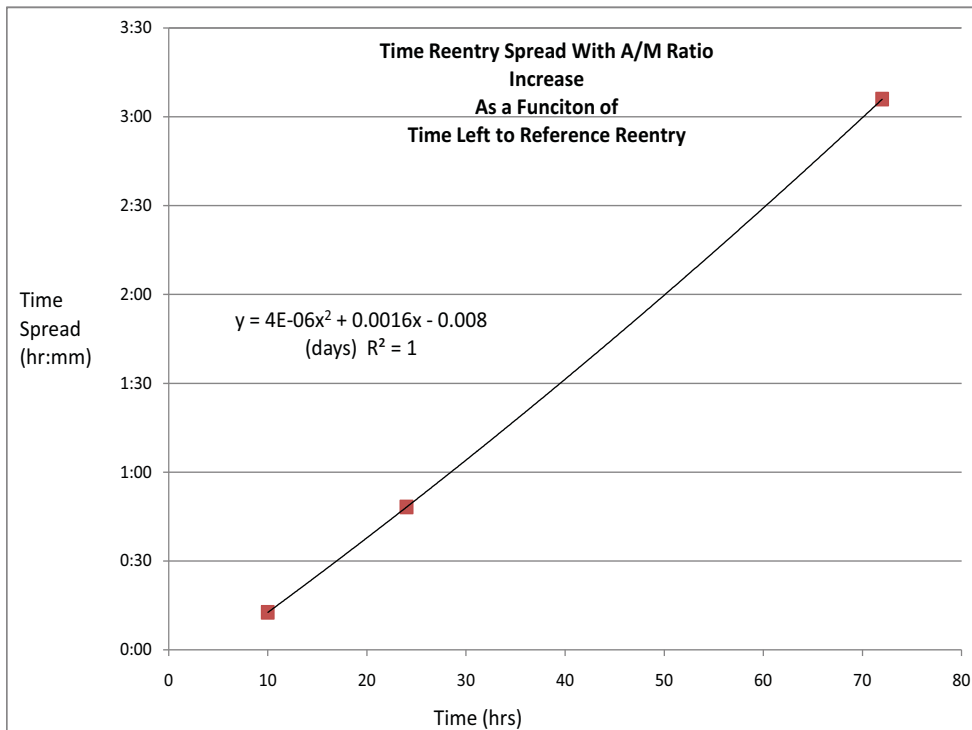


Figure 4.31: Summarized Terrasar-X orbit reentry time spreads with a single A/M increase at 72, 24, and 10 hours prior to original reentry.

4.4 Reentry Prediction Change by A/M Manipulation at a Single Point

The purpose of this study is to specifically explore how the reentry time prediction changes as we hold steady the atmospheric model and the point where the A/M manipulation happens. This section only uses the debris element set to do the study.

Figure 4.32 displays the reentry paths with A/M ratios between 0.01 to 1.0. It can be clearly seen that as you increase the A/M ratio the time left on orbit decreases. For a closer look at an expanded view of the reentries with A/M ratios between 0.1 and 1.0 please see Appendix C, Figure C.19. Also, Figure C.20 shows what all reentry paths look like compared with an object that has an A/M of 0.001. Excel is limited to an amount of points that it is capable of plotting, therefore, only the last 10 days of data were used in the path of the object with A/M of 0.001.

By observing the plots in Figure 4.33, it is clear there is an exponential relationship between the A/M ratio and the time left to reentry. This seems to stem from the fact that the atmospheric density is a factor in the acceleration equation 3.1. The relationship is better depicted by the comparison of the time to reentry as a function of A/M plot against the neutral atmospheric density plot shown in Figure 4.34.

This is important, it shows that for an order of magnitude increase in A/M ratio an order of magnitude drop in time left to reentry is obtained. Hence, for a Delta II rocket body with a length of 6 meters, a diameter of 2.4 meters, and a gross mass of 950 kilograms, the maximum A/M ratio possible would be 0.015. Therefore, if this object was in an orbit similar to the one from the USA 193 debris, instead of lasting ~45 days in orbit, it would take a balloon parachute of ~13.5 meters in diameter to make the rocket body reenter within 5 days.

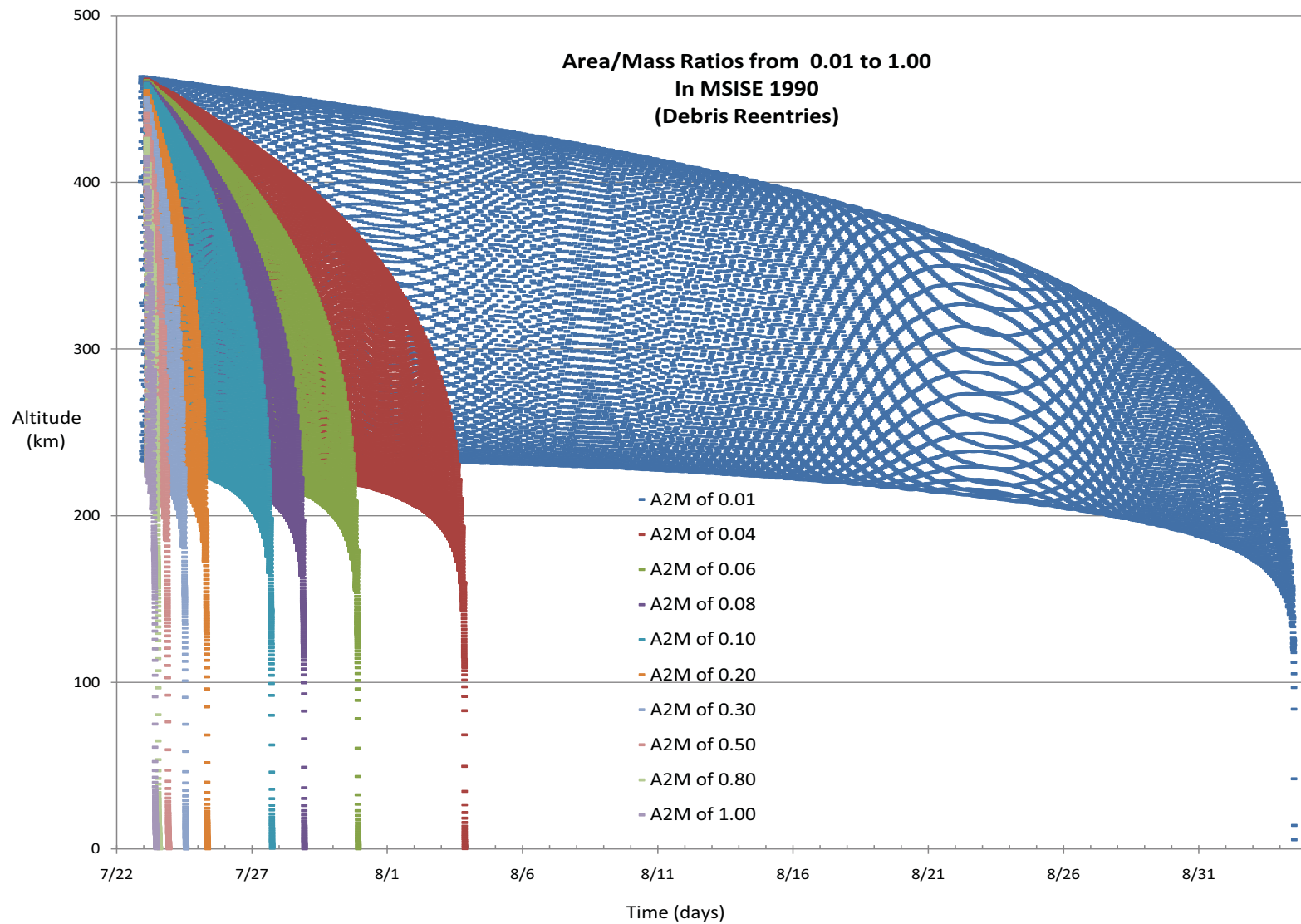


Figure 4.32: Reentry predictions as A/M changes between 0.01 and 1.00 at a single point in orbit path.

Propogation Sart	7/22/08 19:26	379 (km)	with MSISE 1990
Area to Mass ratio (m ² /kg)	Reentry Date	Altitude (km)	Time to reentry (days)
0.001	3/18/09 3:28	101	238.33
0.010	9/3/08 10:02	97	42.61
0.040	8/3/08 18:10	101	11.95
0.060	7/30/08 19:42	101	8.01
0.080	7/28/08 19:57	100	6.02
0.100	7/27/08 15:12	99	4.82
0.200	7/25/08 5:45	103	2.43
0.300	7/24/08 10:27	101	1.63
0.500	7/23/08 19:08	103	0.99
0.800	7/23/08 10:28	97	0.63
1.000	7/23/08 7:39	104	0.51

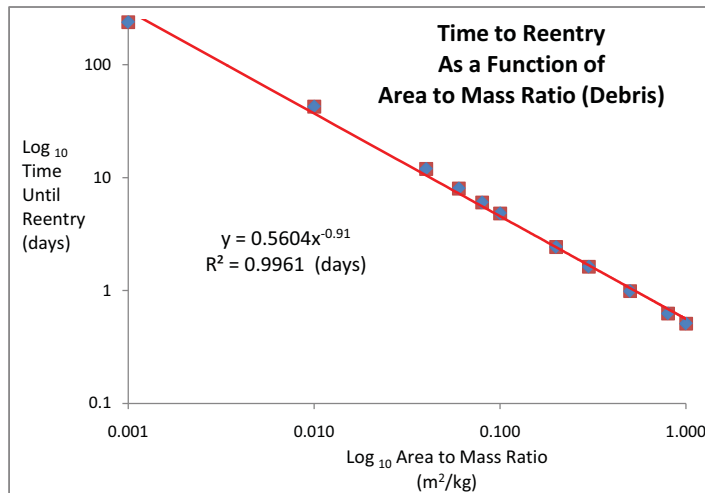
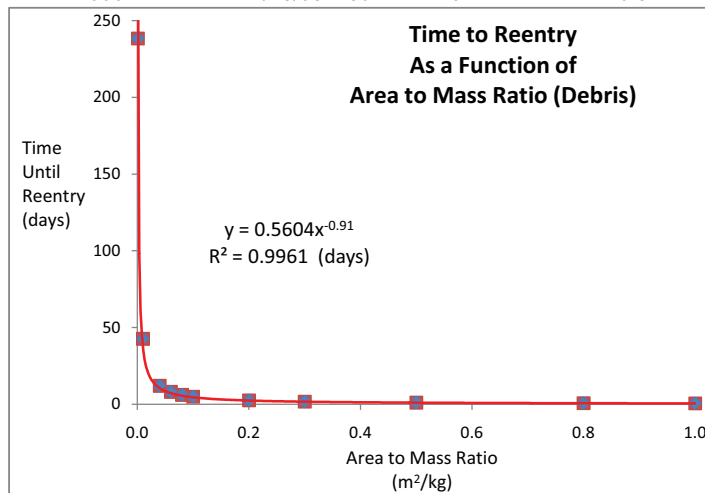
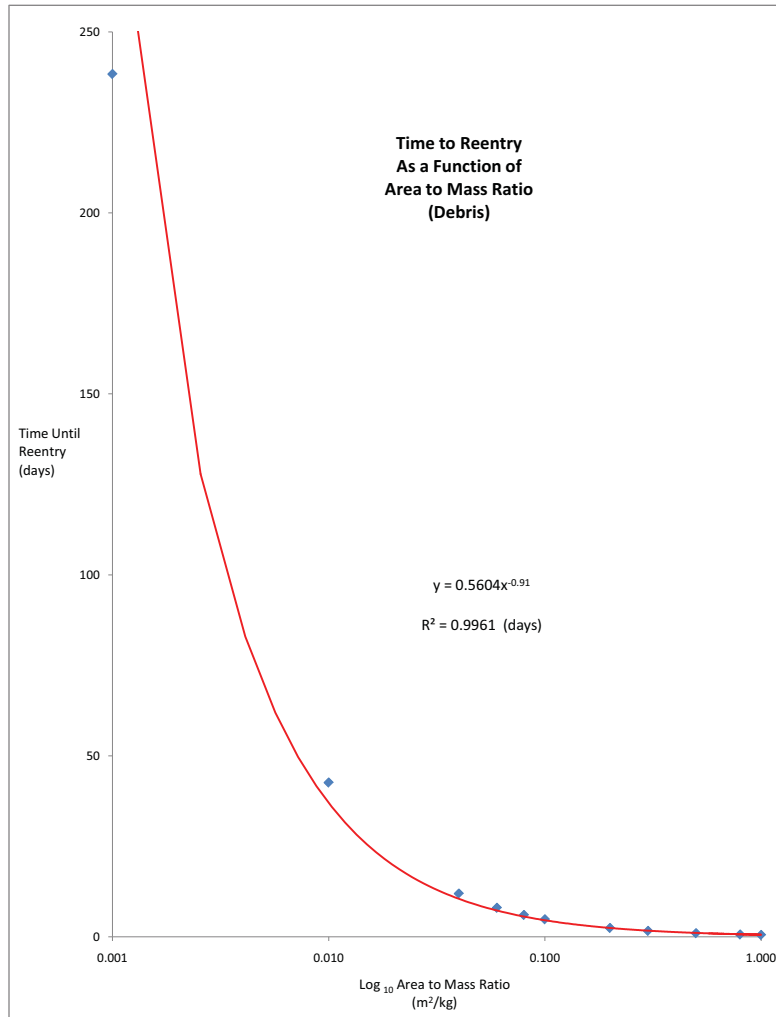
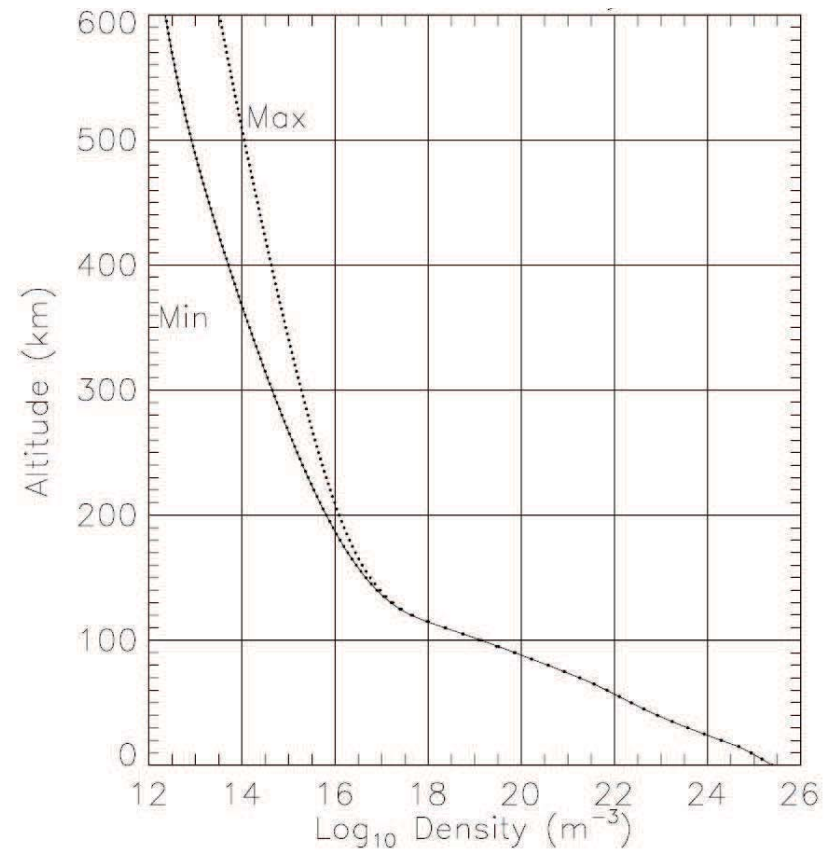


Figure 4.33: Summarized reentry prediction times as A/M changes between 0.001 and 1.000 at a single point in orbit path.



(a) Time to reentry as a function of A/M.



(b) Neutral Atmosphere (density). [30]

Figure 4.34: Comparison: Time to reentry as a function of A/M vs Neutral Density profile.

V. Conclusions and Recommendations

Here are the summarized conclusions of the studies as well as proposed schemes for a solution. The main proposed idea is to produce a system that will increase the objects cross-sectional area. Consequently, this area increase would raise the object's drag and decrease its orbital lifetime along with gaining control over the general area where it lands.

5.1 *Atmospheric Unpredictability*

The first study confirmed how the atmospheric instability affected any predicted reentry that was more than a few days away as it is known in practice [38]. It also brought to the front the need to better our atmospheric modeling capabilities when it comes to modeling objects in LEO. These capabilities have increased in quality with the new NRLMSISE 00, but there is still much room for improvement as we continually learn more about our atmosphere's changing nature.

5.2 *Drag Increase by a Factor*

The second study proved that the increase in drag has the effect of a faster decay. The study wasn't able to conclude whether there is any difference in the effect between drag increase at apogee or perigee. It was observed that the ratio between the new time to reentry over the old time to reentry was inversely proportional to the scale increase in drag.

5.3 *Decrease Variability in Reentry Prediction and Manipulation of A/M*

The third study demonstrated a quadratic relationship between the time left to reentry and the predicted time of reentry spread, but upon further scrutiny the behavior is basically linear. Moreover, the third and fourth studies corroborated that the increase in the A/M will decrease the orbital lifetime of the object. This will make it possible for objects to reenter sooner. It is important to remember all studies

were done using orbital element sets that have altitudes not much greater than 500 kilometers (the lower end of LEO orbits). This was set with the purpose that any object that could use the system being proposed would have a periapsees low enough to the earth where it can make use of the “thicker” atmospheric density.

Not only can a system that increases the object’s A/M be brought down sooner, it will consequently gain precision in the predicted reentry time. It was confirmed that the reentry prediction decreases greatly in variability as it comes closer to the actual reentry. Therefore, when forcing an object to reenter, you automatically gain precision in the predicted reentry time. Along with variability reduction in time of reentry, the next benefit is an actual decrease in variability of the predicted reentry location.

All simulations decreased their variability in location by setting their A/M increase closer to reference reentry. Even the prediction with the A/M increase one day out gave about a one revolution variability, or what it amounts to a “ring possibility” of reentering around the earth. This ring maybe enough of a prediction for the reentering object if it is known to have minimal chances of survival. It was also shown that even more precision may be gained if the A/M increase is postponed to be closer to actual reentry.

For this reason, it is also suggested the development of software that can solve for a needed cross-sectional area (or balloon size) given a desired window of reentry. The software would need inputs such as the object’s physical properties and its orbital parameters. It would require a robust dynamic atmospheric model. The inspiration for this idea came from the fourth study, where it was concluded that the time to reentry has a relationship that is exponential to changes in A/M. It was determined that this behavior was due to the density of the Neutral Atmosphere. This is because atmospheric density is a factor in the object’s acceleration due to drag.

5.4 *Parachute Proposal*

The proposed approach to increasing the A/M is through the on-orbit inflation of a balloon. The orbiting object will carry an attached package that, when signaled, will activate and simply open a compartment where a bag will be exposed. This bag will be deployed as it is inflated and will start acting as a parachute. Another idea for increasing the A/M would be through the deployment of a sail. The problem with this idea is that it would probably need a more sophisticated system for deployment and require an attitude control system.

5.4.1 Design Parameters. It is desirable to make the apparatus as cheap and simple as possible. It is well known that the more complicated an object becomes, the more things that can go wrong with it. Therefore, from the inception of the idea, simplicity in design must be aggressively followed.

A minimum amount of functions in the apparatus is a must while minimizing moving parts. The single most complicated idea at this point would be the desire to have its own power supply. The goal is for the system to have autonomy and be able to come into action when needed. If it has its own power source, it may be able to force the reentry of a malfunctioned satellite.

Keeping the design simple will add robustness and drive to a low-mass end-product. This will keep the cost down for launch, while a separate power source will provide the system with versatility to go on different orbiting objects. The list would include satellites, rocket-bodies, platforms, and any big enough pieces of debris where it may be used.

5.4.2 Prototype Use. A satellite parachute prototype would probably be better used on a fuel tank which will already be left in orbit such as the one from a Delta II rocket body second stage. It may also be used on experimental satellites.

Then again, the use of the prototype on a more simple object such as a rocket body could constitute faster deployment. The reason for this is that its power source

may not be as complicated as one that has to make sure the prototype survives until the end of a satellite's mission. It does mean that some modifications must be made to the launch system (rocket body). It must be kept in mind that this is to further the cause of increasing our knowledge, experience, and practical expertise of a new system that will help alleviate the debris problem in space and further protect the precious resource that is our limited orbital space.

5.4.3 Further Research Needed. Pageos I, Echo I, and Echo II satellites proved that balloons are capable of surviving for long periods of time up in space even when they are intercepted by micrometeors. Still, a small collision probability assessment must be performed since there is a considerable larger amount of manmade debris in space.

Many of the reports from the missions of the balloon satellites may be exploited to benefit this project. It is important to remember that these systems are expected to go through a higher level of stress than previous systems did. The reason for this is because their capability to decrease the orbital lifetime of objects will be tested.

As a final note, it is important to realize that the simulations only varied the A/M and kept the coefficient of drag constant. This is not entirely accurate. When increasing the geometry of the object, the coefficient of drag is also affected. Therefore, the effect of the increase in surface area should actually be greater.

Appendix A. Orbital Element Sets

A.1 Orbital Element Sets Used For Simulations

The following figures provide the orbital element sets that were used as the beginning points for the simulations.

They give a quick description and international designator of the orbiting object from which they were acquired along with the web address where the elements were obtained.

The last figure in this Appendix is a set of keys to decipher element sets. The bottom key is the one to be used for the element sets presented.

International Designator 2006-057

2006-057A

USA 193 is an American military satellite that was launched from Vandenberg AFB at 21:00 UT on 2006 December 14. It is a highly classified spacecraft, owned and operated by the National Reconnaissance Office (NRO). No further details are available.

Debris SCC number 29651

The satellite was destroyed on Feb 21, 2008.

Accessed on 23 July 2008 at 1647 ET

From

<http://celestrak.com/NORAD/elements/usa-193-debris.txt>

USA 193 DEB

1	32601U	06057BY	08204.81039892	.00270106	32405-4	65292-3	0	2673
2	32601	58.5124	127.6791	0168670	250.1491	108.2035	15.75949212	22370

Figure A.1: Orbital element set for Debris orbit.

International Designator 1998-067

1998-067A

ISS-ZARYA is a Russian-built first module of the International Space Station (ISS) that was launched by a Proton-K rocket from Baikonur at 06:40 UT. The ISS is also known by the Russian acronym, MKS standing for the transliterated Mezhdunarodnii Kosmicheskii Stantsii. It will require 43 rocket launches, including about 35 Shuttles, over at least a five year period to complete the 16-country, 60 m x 24 m x 21.5 m, 454-ton, 110-kW, and >\$50 billion ISS (or whatever its eventual name/acronym may turn out to be). ZARYA ("Dawn") module has a mass of 27 tons and will contribute power, attitude control, fuel, and command/control coordination to the other 33 (USA 18, Russia 9, Japan 3, ESA 2, and Canada 1) modules. No definitive information is currently available regarding ISS's scientific, commercial, or military vision. It is likely that some or all of the science payload now housed in the 140-ton Mir station may be transferred to the ISS in the event of having to disassemble and deorbit Mir; the orbital parameters of the two are similar. Initial orbital parameters of ISS-ZARYA were period 92 min, apogee 396 km, perigee 384 km, and inclination 51.6 deg.

SCC number 25544

Accessed on 30 Jul 08 at 1234 ET

From <http://celestrak.com/NORAD/elements/stations.txt>

ZARYA

1	25544U	98067A	08211.87215691	.00006360	00000-0	50579-4	0	9514
2	25544	51.6417	156.9681	0010004	11.4376	39.1422	15.72722297	555256

Figure A.2: Orbital element set for ISS orbit.

International Designator 2007-026

2007-026A

TERRASAR-X is a German (DLR) Synthetic Aperture Radar that was launched by a Dnepr rocket from Baikonur at 02:14 UT on 2007 June 15. It will map the Earth and oceans at a rate of one million square-km/day, provide scientific data such as sea ice coverage, vegetation/crop estimates, and military reconnaissance information, all at 1.0-m resolution.

The initial orbital parameters were period 95 min, apogee 510 km, perigee 507 km, and inclination 97.5°.

Accessed on 2 December 2008 at 13:36 ET

From

<http://celestrak.com/satcat/2007/2007-026.asp#A>
<http://celestrak.com/NORAD/elements/resource.txt>

TERRASAR-X

1	31698U	07026A	08337.19636624	.000000629	00000-0	33137-4	0	6377
2	31698	97.4442	341.4278	0001424	77.7037	52.2730	15.19157484	8136

Figure A.3: Orbital element set Terrasar-X orbit.

Figure A.4: Orbital element set keys.

Appendix B. STK Propagator Inputs

B.1 Set Up Inputs for Simulations

The following figures are the propagator inputs used for the initial runs of the simulations of all three orbits.

It is important to remember that the inputs changed as different simulations were required by the different studies or to have the propagator produce better results.

Such changes included A/M ratio manipulations, integrator time step manipulation and atmospheric model type changes.

Educational Use Only
Satellite-MSISE_1990

Propagator Initial Conditions

Propagator Name = HPOP
Orbit Epoch = 22 Jul 2008 19:26:00.000000000

Position - J2000 - x = -4138831.51430963
Position - J2000 - y = 5341288.19322933
Position - J2000 - z = 17736.34682893
Velocity - J2000 - x = -3226.12586528
Velocity - J2000 - y = -2367.10813792
Velocity - J2000 - z = 6530.86213070

Mass = 1000.000

Gravity File Name = C:\Program Files\AGI\STK 8\STKData\CentralBodies\Earth\WGS84_EGM96.grv
MaxDegree = 50 MaxOrder = 50
Include Solid Tides? No
Include Ocean Tides? No

Include Drag? Yes
Drag Coefficient = 2.0000
Area/Mass Ratio = 0.1000
Atmos density model = MSISE 1990
Use Flux File? Yes
Flux Filename = C:\Program Files\AGI\STK 8\DynamicEarthData\SpaceWeather-v1.2.txt
Use Approximate Altitude for Drag? Yes
Use Apparent Sun for Drag? Yes

Include Solar Radiation Pressure? No
Include general relativity correction? No
Include albedo? No
Include thermal radiation pressure? No

Integrator = Runge-Kutta-Fehlberg 7-8
Relative Error Tolerance = 1.000000e-013
Integrator Step Size = Variable
Report On Fixed Step? Yes
Equations of Motion = VOP Universal Variables
Independent Variable = Time
Interpolation Method = Lagrangian VOP ($\mu = 3.9860044180000000e+014$)
Interpolation Order = 8
Integrator stops when altitude is below 0.0000 m
Computing partials? No

Figure B.1: STK propagator inputs for Debris orbit simulation.

Educational Use Only
Satellite-MSIS_1990

Propagator Initial Conditions

Propagator Name = HPOP
Orbit Epoch = 1 Aug 2008 15:21:00.000000000

Position - J2000 - x = -5193760.32542793
Position - J2000 - y = -1297506.48023412
Position - J2000 - z = 4076421.27492316
Velocity - J2000 - x = 4285.68711167
Velocity - J2000 - y = -5117.57790620
Velocity - J2000 - z = 3832.28596309

Mass = 1000.000

Gravity File Name = C:\Program Files\AGI\STK 8\STKData\CentralBodies\Earth\WGS84_EGM96.grv
MaxDegree = 50 MaxOrder = 50
Include Solid Tides? No
Include Ocean Tides? No

Include Drag? Yes
Drag Coefficient = 2.2000
Area/Mass Ratio = 0.1000
Atmos density model = MSISE 1990
Use Flux File? Yes
Flux Filename = C:\Program Files\AGI\STK 8\DynamicEarthData\SpaceWeather-v1.2.txt
Use Approximate Altitude for Drag? Yes
Use Apparent Sun for Drag? Yes

Include Solar Radiation Pressure? No
Include general relativity correction? No
Include albedo? No
Include thermal radiation pressure? No

Integrator = Runge-Kutta-Fehlberg 7-8
Relative Error Tolerance = 1.000000e-013
Integrator Step Size = Variable
Report On Fixed Step? Yes
Equations of Motion = Cowell
Independent Variable = Time
Interpolation Method = Lagrangian
Interpolation Order = 7
Integrator stops when altitude is below 0.000 m
Computing partials? No

Figure B.2: STK propagator inputs for ISS orbit simulation.

Educational Use Only
Satellite-Satellite1

Propagator Initial Conditions

Propagator Name = HPOP
Orbit Epoch = 2 Dec 2008 04:42:46.043136000

Position - J2000 - x = -4412479.14888076
Position - J2000 - y = 761502.76035328
Position - J2000 - z = 5231259.08903455
Velocity - J2000 - x = -5324.63669209
Velocity - J2000 - y = 2457.28610748
Velocity - J2000 - z = -4847.81515618

Mass = 1000.000

Gravity File Name = C:\Program Files\AGI\STK 8\STKData\CentralBodies\Earth\WGS84_EGM96.grv
MaxDegree = 50 MaxOrder = 50
Include Solid Tides? No
Include Ocean Tides? No

Include Drag? Yes
Drag Coefficient = 2.0000
Area/Mass Ratio = 0.1000
Atmos density model = MSISE 1990
Use Flux File? Yes
Flux Filename = C:\Program Files\AGI\STK 8\DynamicEarthData\SpaceWeather-v1.2.txt
Use Approximate Altitude for Drag? Yes
Use Apparent Sun for Drag? Yes

Include Solar Radiation Pressure? No
Include general relativity correction? No
Include albedo? No
Include thermal radiation pressure? No

Integrator = Runge-Kutta-Fehlberg 7-8
Relative Error Tolerance = 1.000000e-013
Integrator Step Size = Variable
Report On Fixed Step? No
Equations of Motion = VOP Universal Variables
Independent Variable = Time
Interpolation Method = Lagrangian VOP ($\mu = 3.9860044180000000e+014$)
Interpolation Order = 8
Integrator stops when altitude is below 0.0000 m
Computing partials? No

Figure B.3: STK propagator inputs for Terrasar-X orbit simulation.

Appendix C. Graphs From Chapter Four

C.1 Graphs From Section Three and Four of Chapter Four

Since the amount of figures in sections 3 and 4 of Chapter 4 were impeding a better reading flow for the thesis, they were moved to this appendix.

The graphs, along with their summaries, depict the predicted reentry paths of the different orbits.

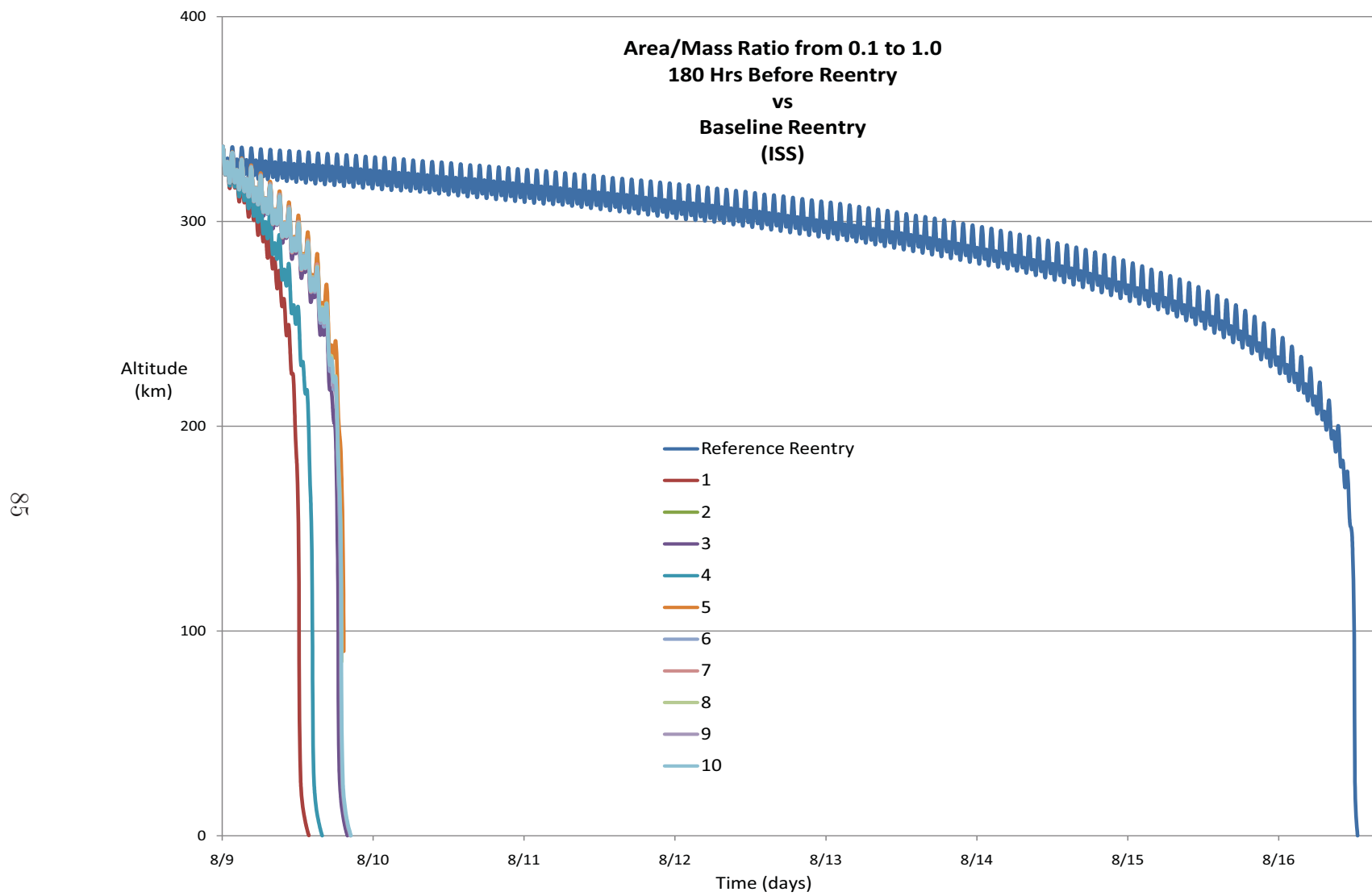


Figure C.1: ISS orbit reentry predictions by ten atmospheric models with a single A/M increase 180 hours prior to original reentry.

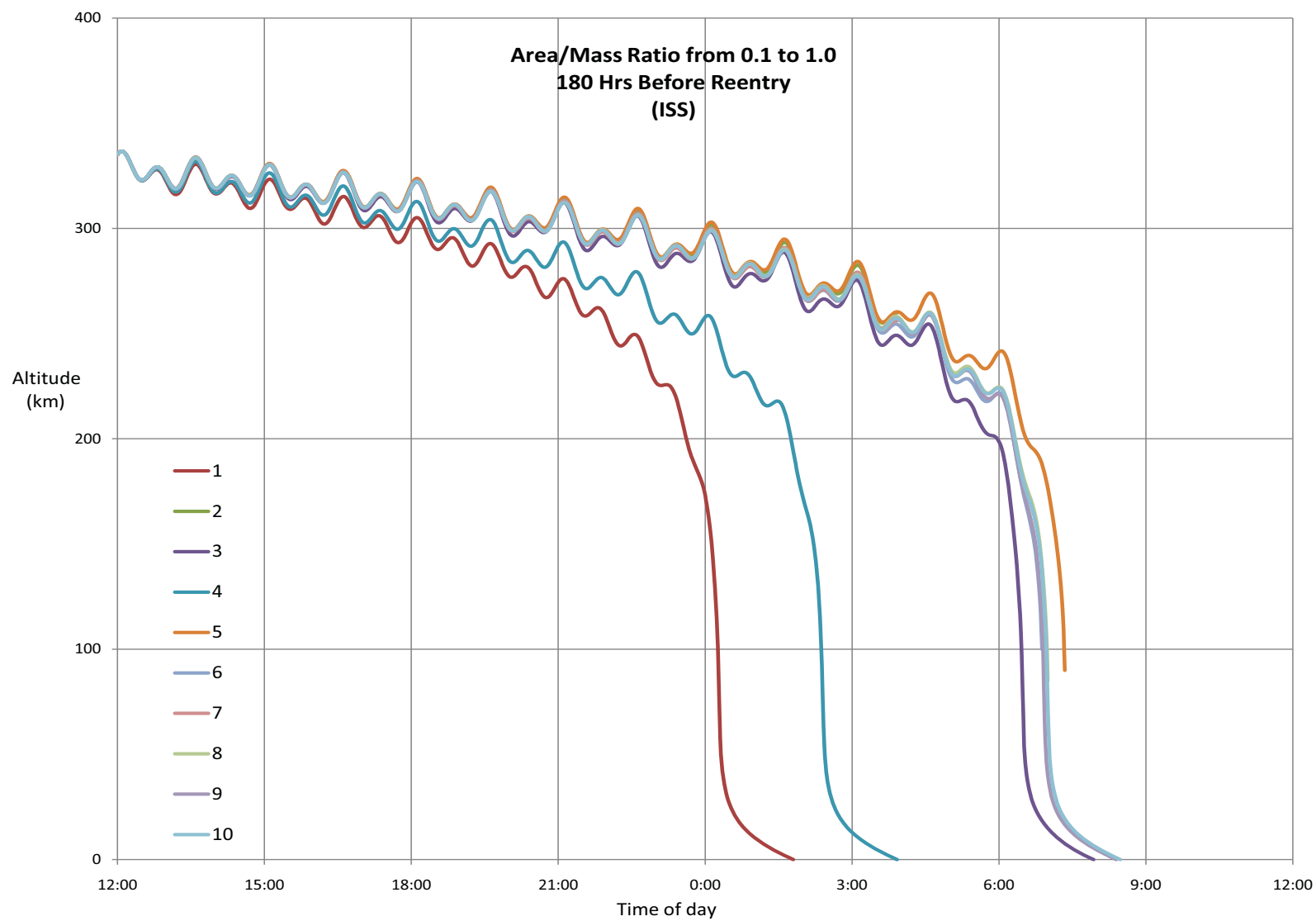


Figure C.2: Homed in ISS orbit reentry predictions by ten atmospheric models with a single A/M increase 180 hours prior to original reentry.

A/M Scale Increase Point 180 hrs
Reentry Time Spread (hrs:mm:ss) 7:11:00

Sorted by Date				
Atmospheric Model	Reentry Time	Latitude (deg)	Longitude (deg)	Altitude (km)
1	8/10/08 0:15	37.31	294.30	106.42
4	8/10/08 2:22	-51.07	41.53	104.65
3	8/10/08 6:28	2.36	234.51	97.07
6	8/10/08 6:52	-51.32	-30.05	99.95
9	8/10/08 6:54	-50.52	-23.44	98.32
10	8/10/08 6:58	-44.47	-1.99	100.41
8	8/10/08 6:59	-42.58	2.05	98.13
7	8/10/08 7:06	-21.82	28.12	99.16
5	8/10/08 7:20	18.28	58.24	99.71
2	8/10/08 7:26	36.18	76.83	101.45

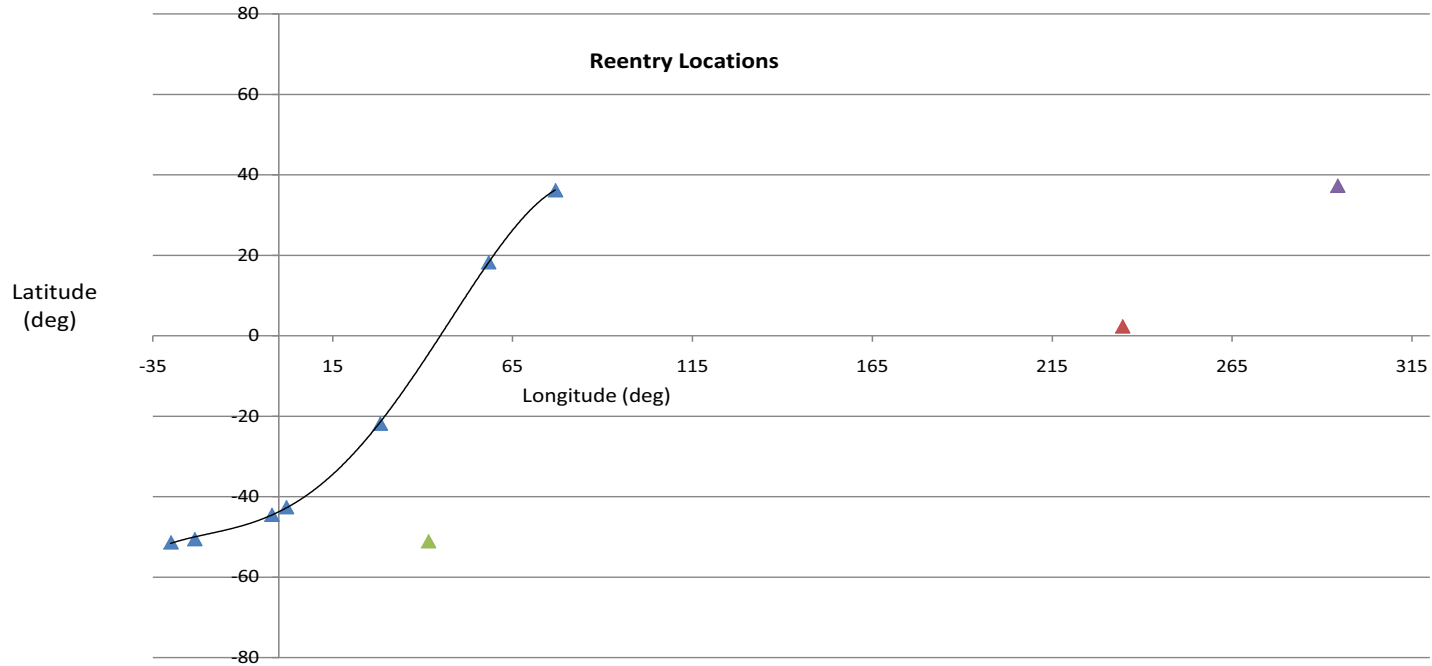


Figure C.3: Summarized predicted ISS orbit reentry times and locations by ten atmospheric models with a single A/M increase 180 hours prior to original reentry.

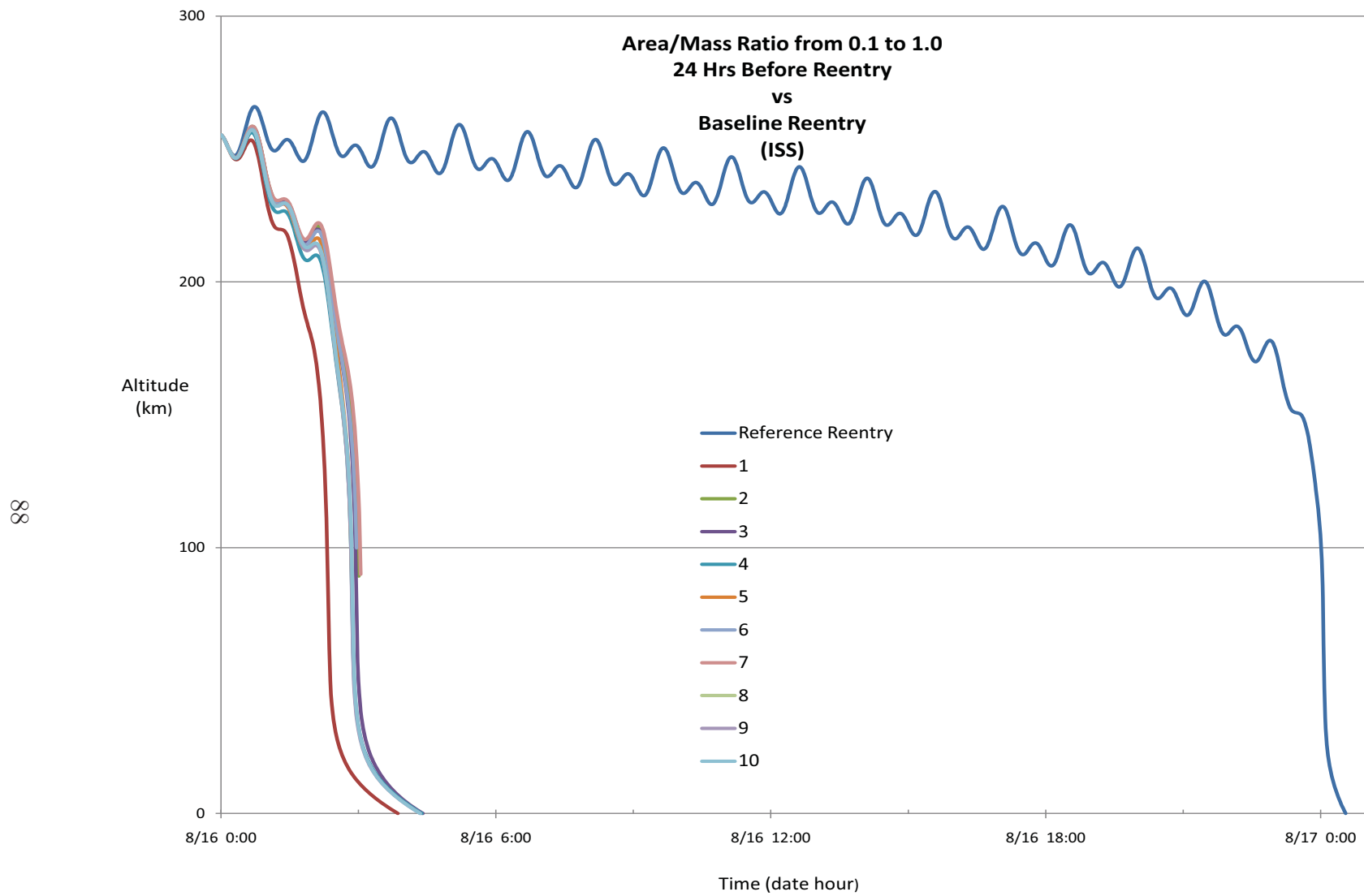


Figure C.4: ISS orbit reentry predictions by ten atmospheric models with a single A/M increase 24 hours prior to original reentry.

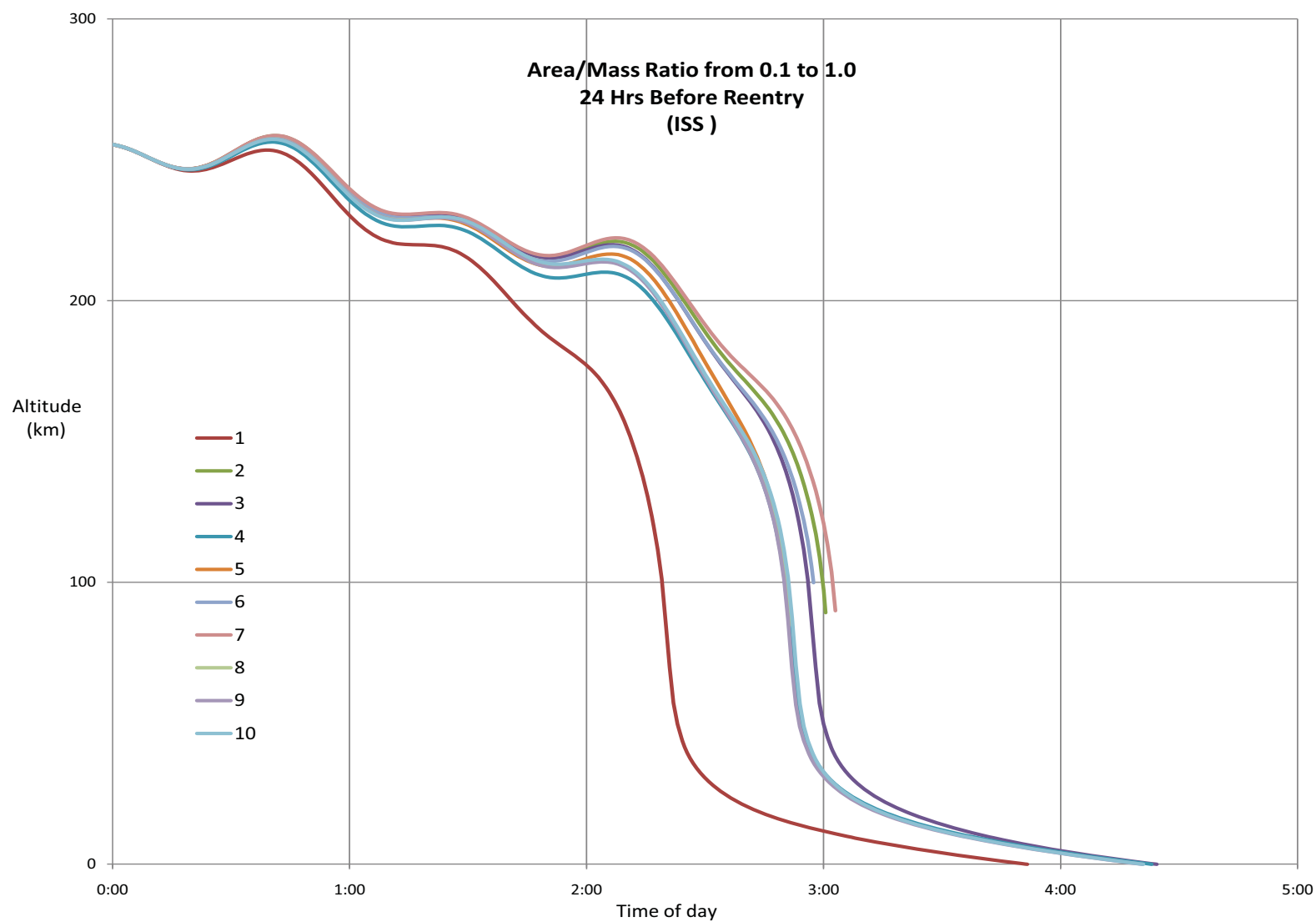


Figure C.5: Homed in ISS orbit reentry predictions by ten atmospheric models with a single A/M increase 24 hours prior to original reentry.

A/M Scale Increase Point 24 hrs
Reentry Time Spread (hrs:mm:ss) 0:43:00

Sorted by Date				
Atmospheric Model	Reentry Time	Latitude (deg)	Longitude (deg)	Altitude (km)
1	8/16/08 2:19	43.65	213.34	101.20
4	8/16/08 2:50	-45.11	306.56	102.37
8	8/16/08 2:50	-44.96	306.17	104.12
9	8/16/08 2:50	-44.93	306.09	101.09
5	8/16/08 2:51	-46.54	310.32	94.89
10	8/16/08 2:51	-46.78	311.03	101.84
3	8/16/08 2:56	-51.70	339.66	101.02
6	8/16/08 2:57	-51.55	349.05	99.90
2	8/16/08 3:00	-49.57	363.97	97.13
7	8/16/08 3:02	-46.48	375.05	103.64

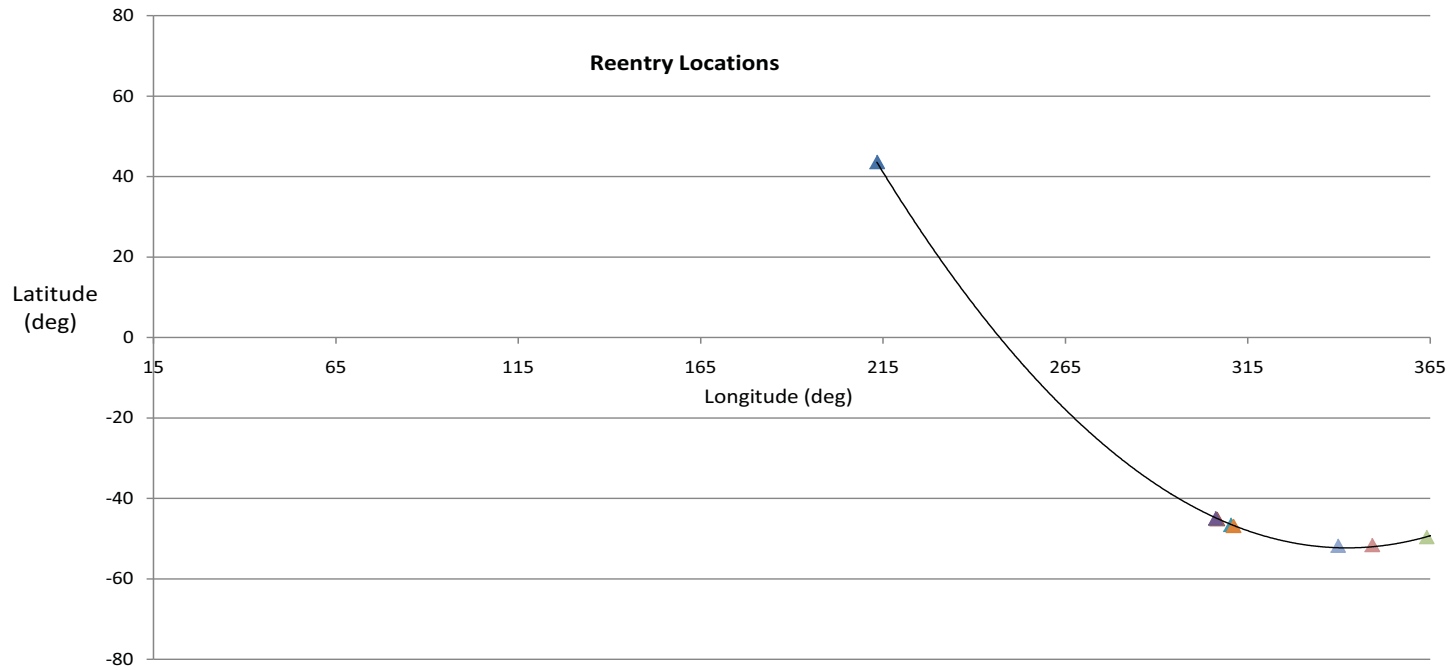


Figure C.6: Summarized predicted ISS orbit reentry times and locations by ten atmospheric models with a single A/M increase 24 hours prior to original reentry.

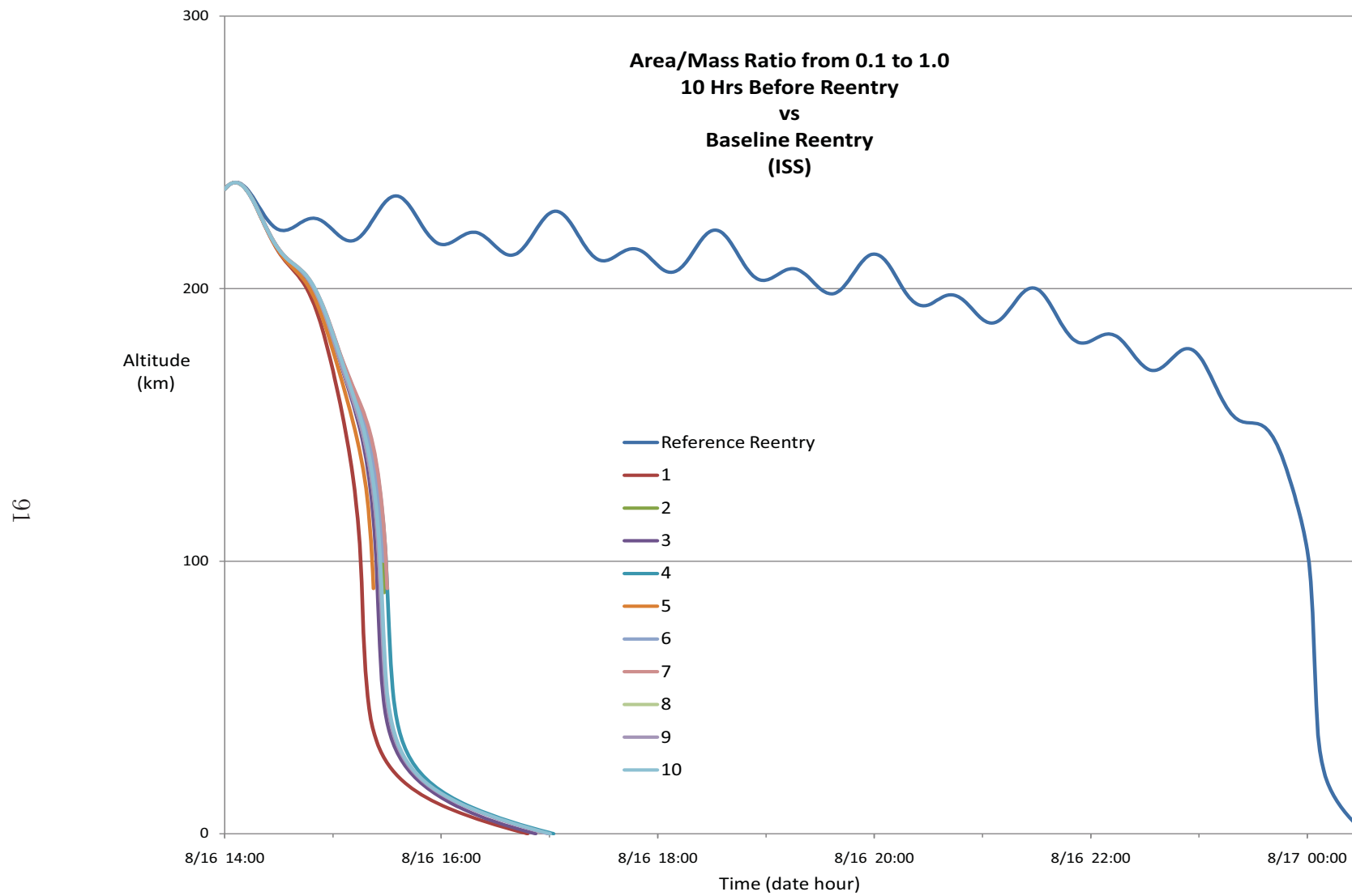


Figure C.7: ISS orbit reentry predictions by ten atmospheric models with a single A/M increase 10 hours prior to original reentry.

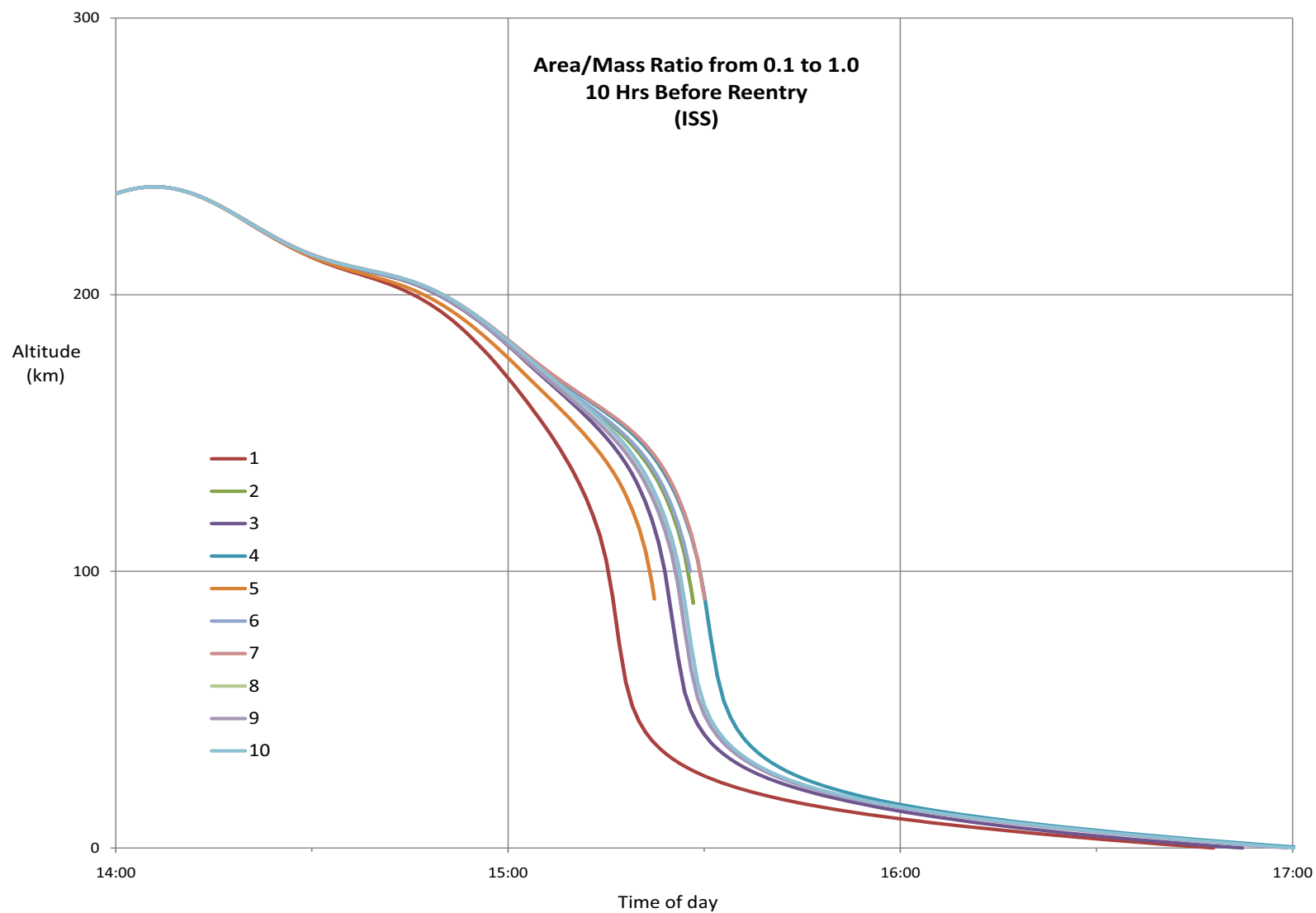


Figure C.8: Homed in ISS orbit reentry predictions by ten atmospheric models with a single A/M increase 10 hours prior to original reentry.

A/M Scale Increase Point 10 hrs
Reentry Time Spread (hrs:mm:ss) 0:14:00

Sorted by Date				
Atmospheric Model	Reentry Time	Latitude (deg)	Longitude (deg)	Altitude (km)
1	8/16/08 15:15	8.36	251.30	103.96
5	8/16/08 15:22	29.66	269.58	95.62
3	8/16/08 15:24	35.29	276.29	100.01
8	8/16/08 15:26	40.30	283.83	95.52
9	8/16/08 15:26	40.30	283.84	95.07
10	8/16/08 15:26	40.44	284.07	102.71
2	8/16/08 15:27	42.79	288.46	106.05
6	8/16/08 15:27	44.57	292.34	99.98
4	8/16/08 15:29	46.77	298.09	104.11
7	8/16/08 15:29	46.73	297.98	104.27

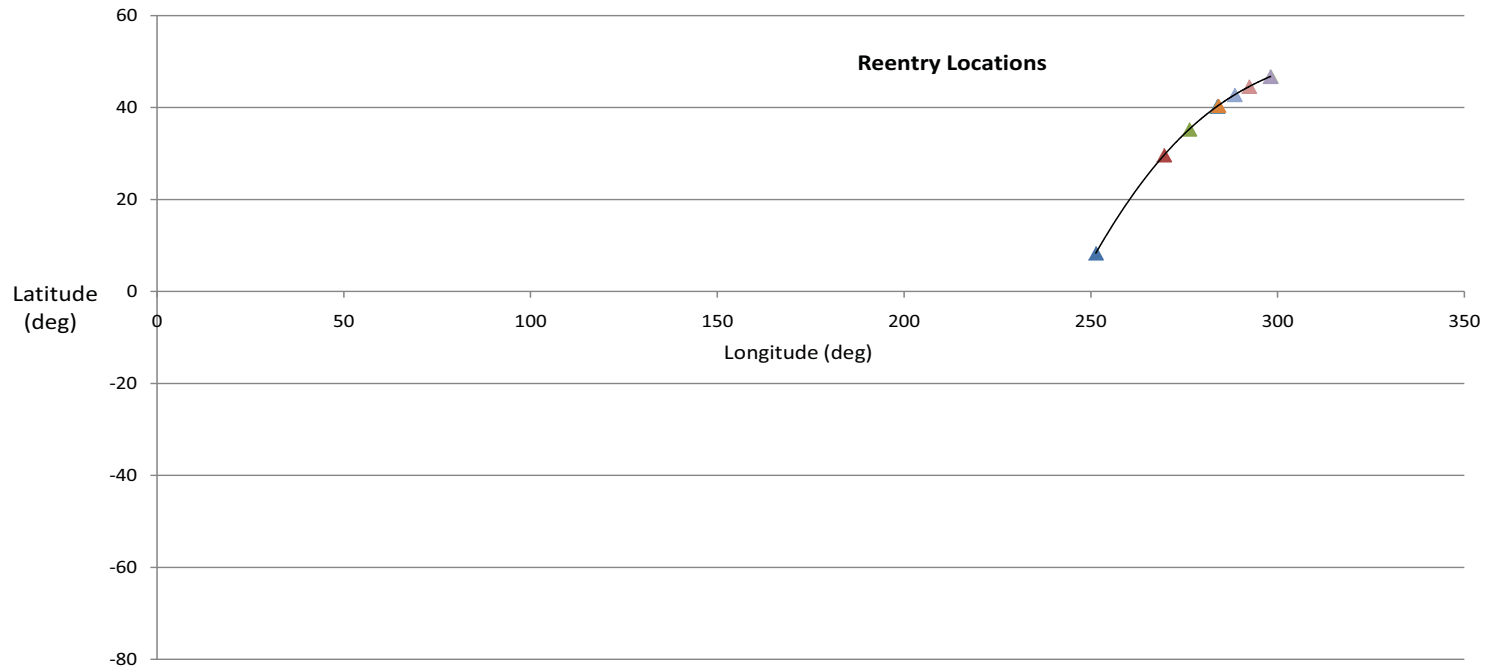


Figure C.9: Summarized predicted ISS orbit reentry times and locations by ten atmospheric models with a single A/M increase 10 hours prior to original reentry.

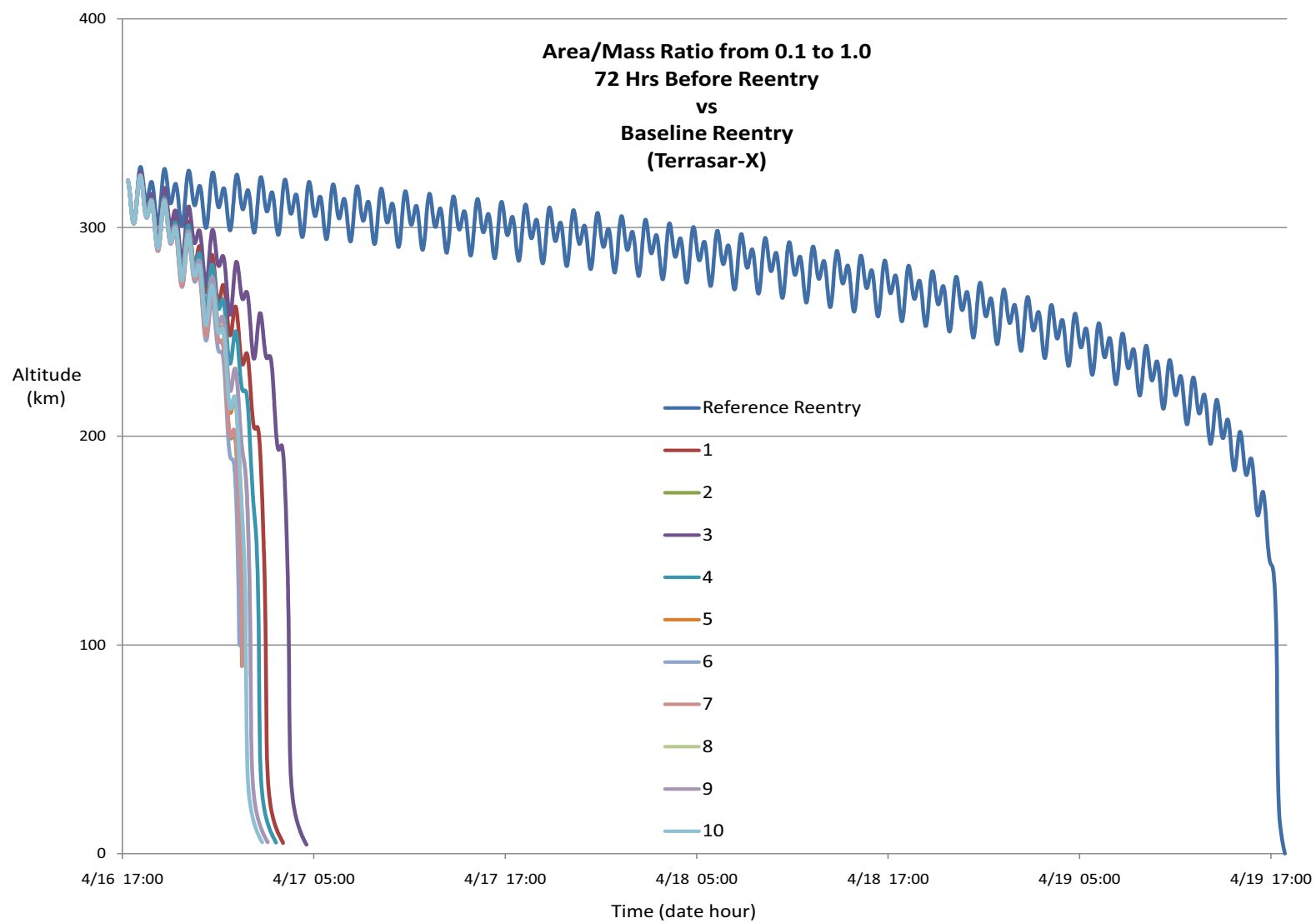


Figure C.10: Terrasar-X orbit reentry predictions by ten atmospheric models with a single A/M increase 72 hours prior to original reentry.

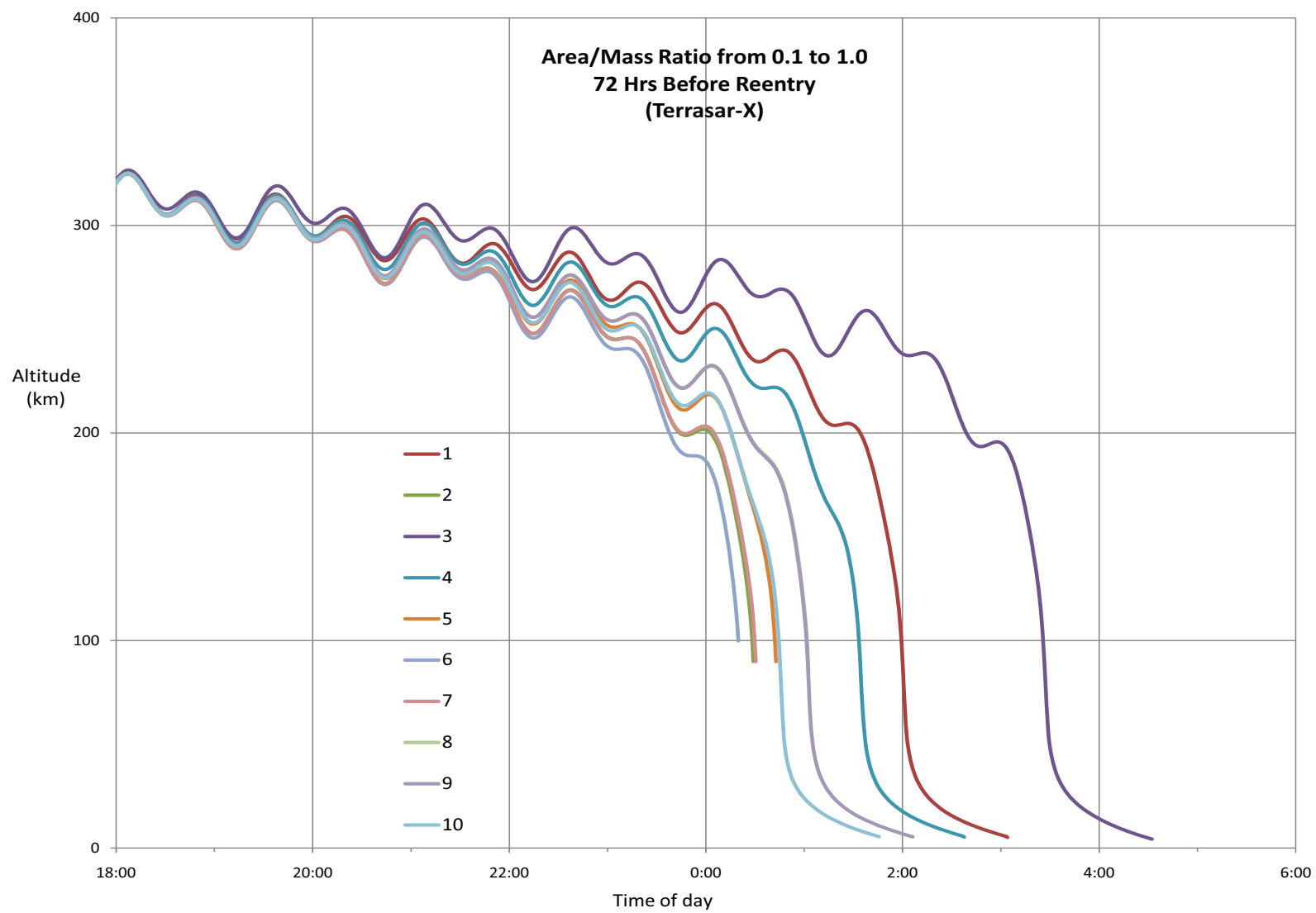


Figure C.11: Homed in Terrasar-X orbit reentry predictions by ten atmospheric models with a single A/M increase 72 hours prior to original reentry.

A/M Scale Increase Point 72 hrs
Reentry Time Spread (hrs:mm:ss) 3:06:00

Sorted by Date				
Atmospheric Model	Reentry Time	Latitude (deg)	Longitude (deg)	Altitude (km)
6	4/17/09 0:19	31.21	238.86	100.23
2	4/17/09 0:28	-2.51	231.98	100.08
7	4/17/09 0:29	-8.65	230.81	100.92
5	4/17/09 0:42	-57.63	217.16	97.81
10	4/17/09 0:44	-67.61	210.09	97.76
9	4/17/09 1:01	-44.57	51.28	101.64
8	4/17/09 1:01	-42.66	50.69	99.51
4	4/17/09 1:33	80.19	348.35	102.11
1	4/17/09 1:59	-6.70	208.69	101.83
3	4/17/09 3:25	7.59	188.91	101.57

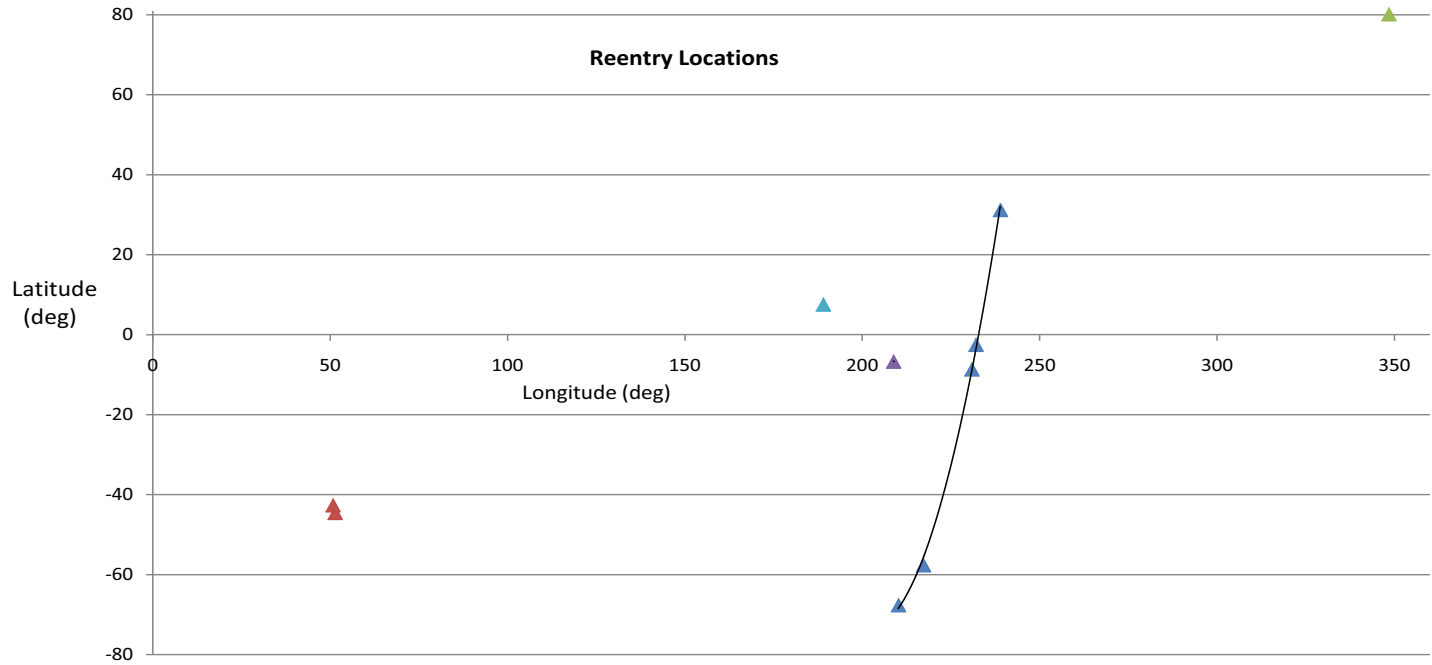


Figure C.12: Summarized predicted Terrasar-X orbit reentry times and locations by ten atmospheric models with a single A/M increase 72 hours prior to original reentry.

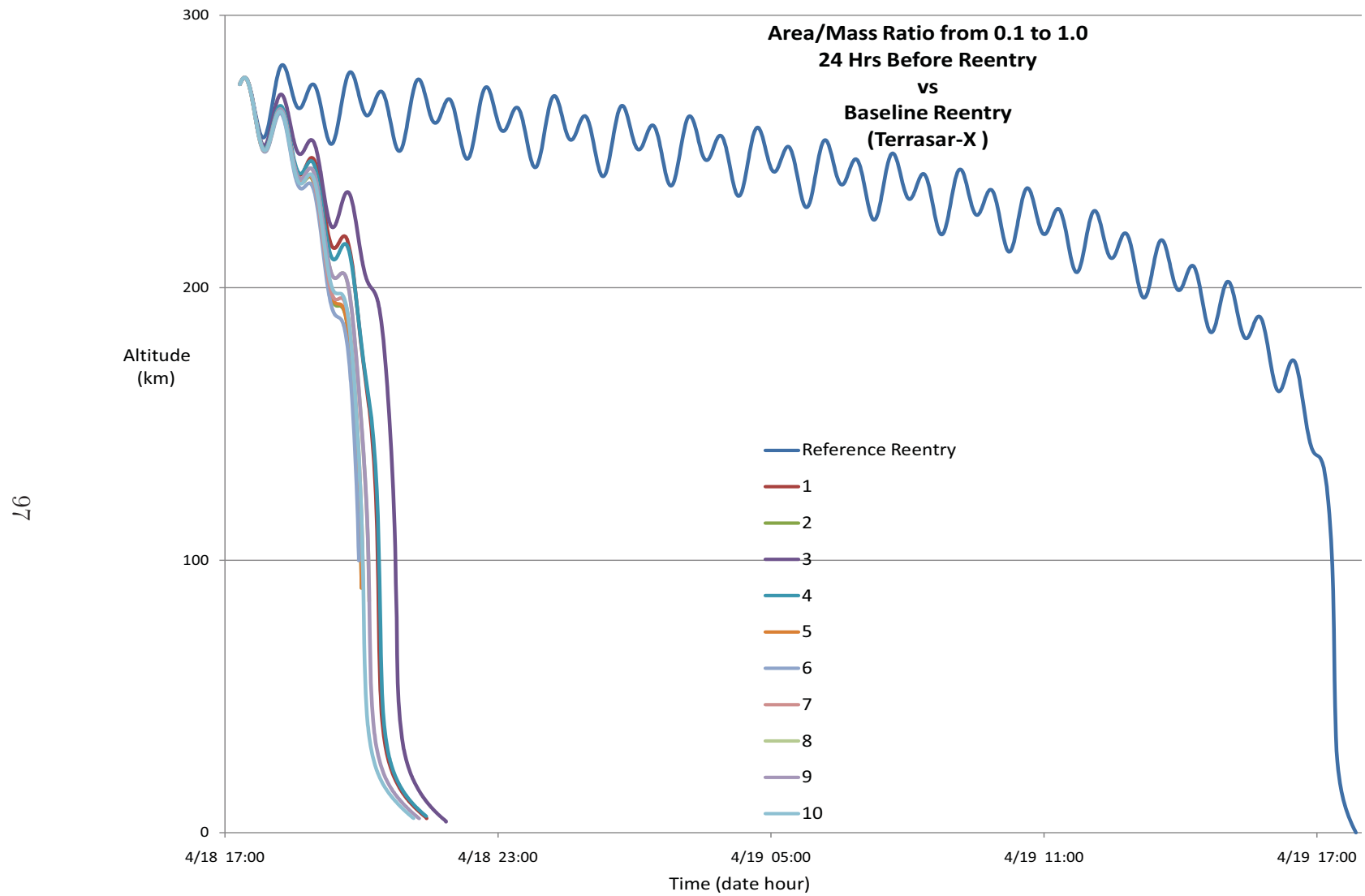


Figure C.13: Terrasar-X orbit reentry predictions by ten atmospheric models with a single A/M increase 24 hours prior to original reentry.

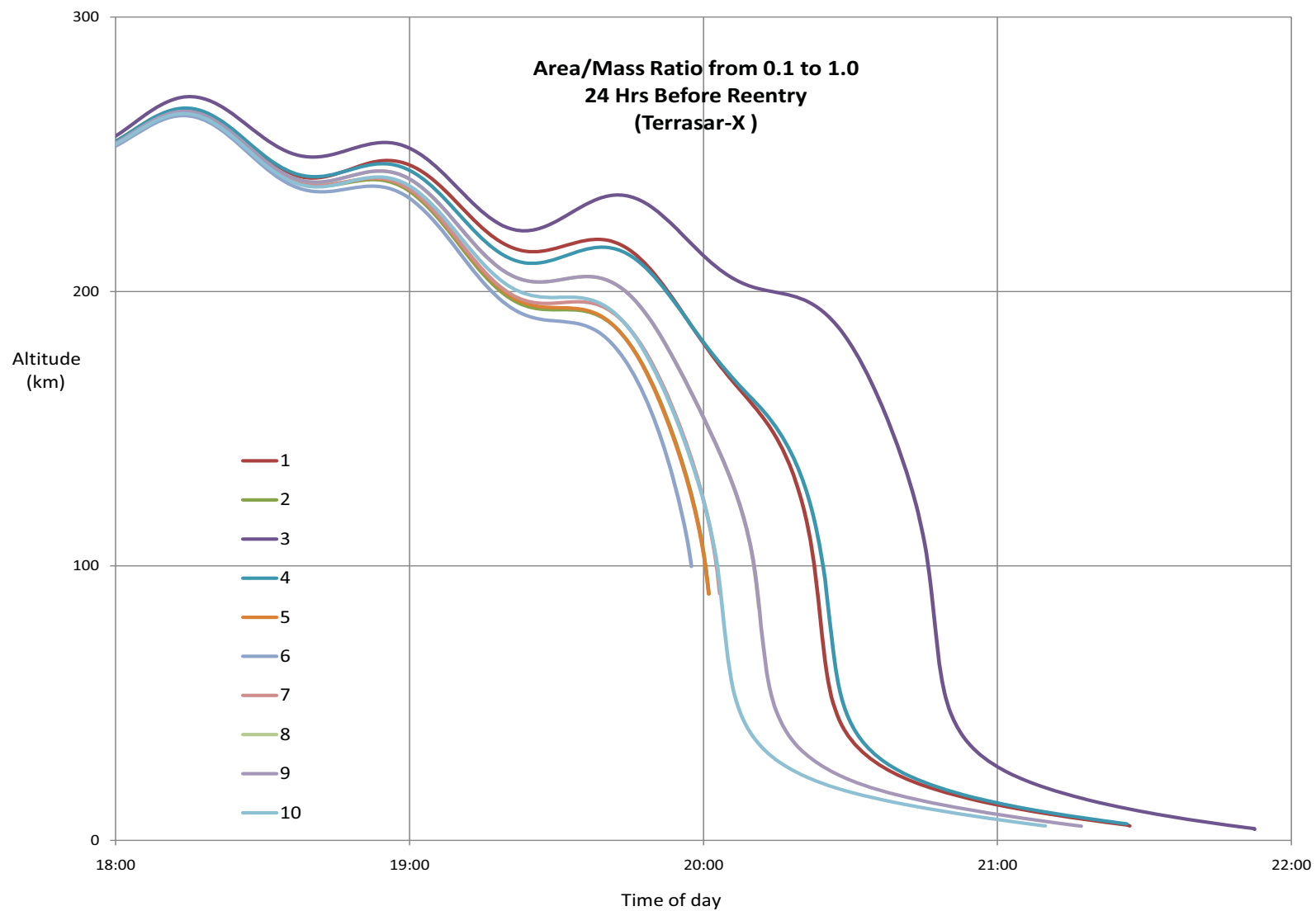


Figure C.14: Homed in Terrasar-X orbit reentry predictions by ten atmospheric models with a single A/M increase 24 hours prior to original reentry.

A/M Scale Increase Point 24 hrs
Reentry Time Spread (hrs:mm:ss) 0:48:14

Sorted by Date				
Atmospheric Model	Reentry Time	Latitude (deg)	Longitude (deg)	Altitude (km)
6	4/18/09 19:57	33.31	305.00	99.82
2	4/18/09 20:00	21.82	302.39	99.53
5	4/18/09 20:00	21.82	302.39	99.60
7	4/18/09 20:02	12.50	300.50	98.24
10	4/18/09 20:02	12.35	300.47	100.43
8	4/18/09 20:10	-17.27	294.75	101.89
9	4/18/09 20:10	-18.52	294.50	98.66
1	4/18/09 20:22	-67.21	276.16	98.23
4	4/18/09 20:24	-73.83	267.29	99.64
3	4/18/09 20:45	-18.96	110.64	100.93

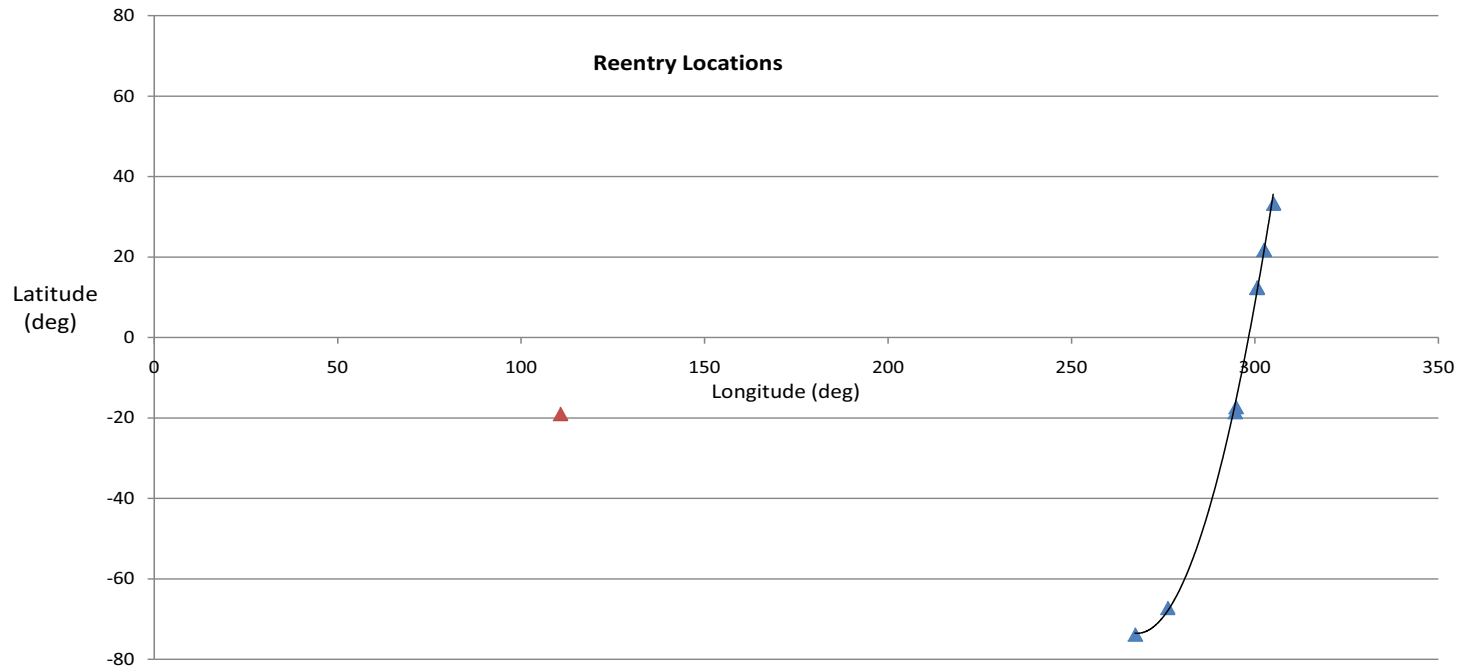


Figure C.15: Summarized predicted Terrasar-X orbit reentry times and locations by ten atmospheric models with a single A/M increase 24 hours prior to original reentry.

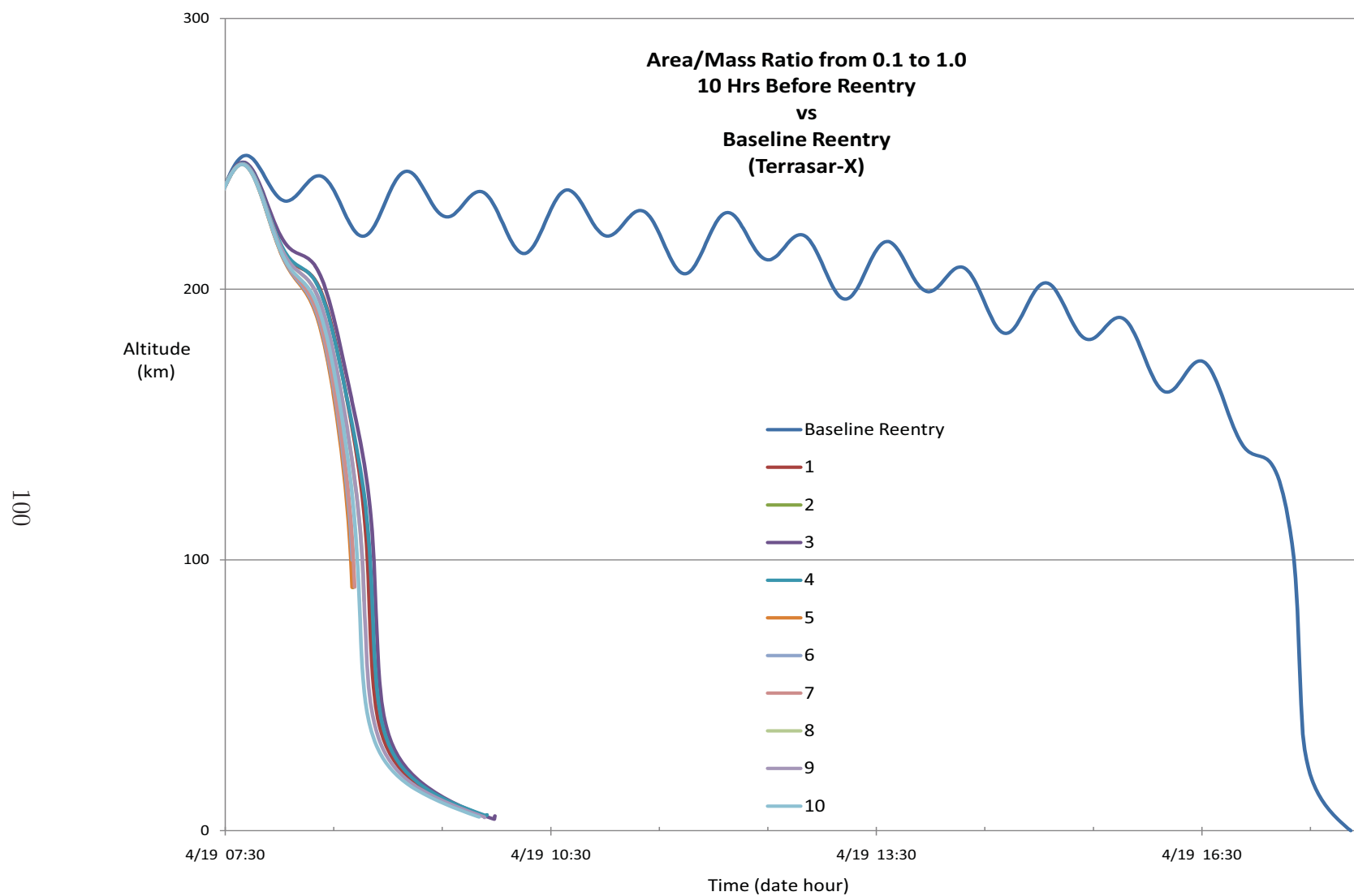


Figure C.16: Terrasar-X orbit reentry predictions by ten atmospheric models with a single A/M increase 10 hours prior to original reentry.

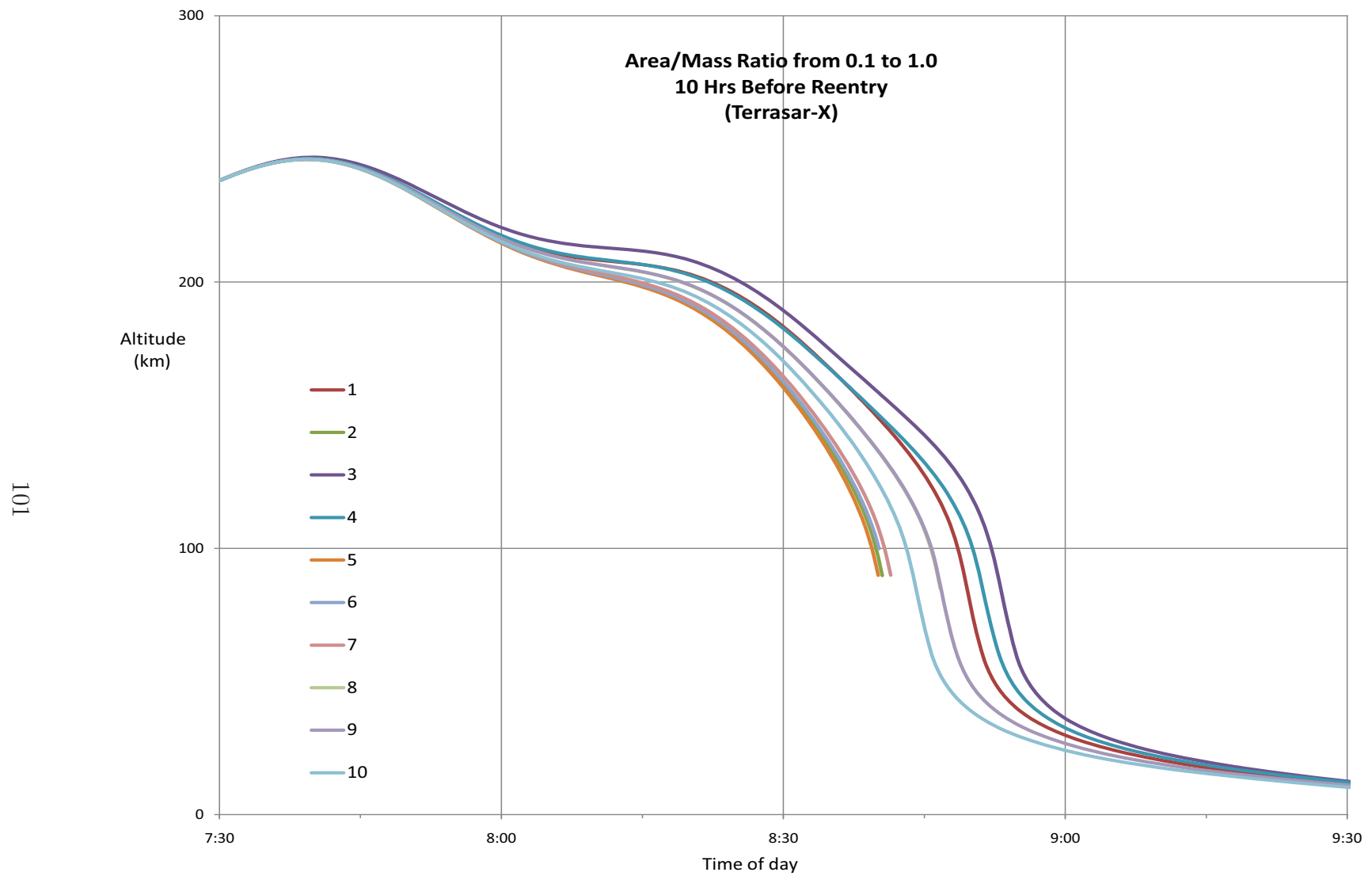


Figure C.17: Homed in Terrasar-X orbit reentry predictions by ten atmospheric models with a single A/M increase 10 hours prior to original reentry.

A/M Scale Increase Point 10 hrs
Reentry Time Spread (hrs:mm:ss) 0:12:40

Sorted by Date				
Atmospheric Model	Reentry Time	Latitude (deg)	Longitude (deg)	Altitude (km)
5	4/19/09 8:39	-27.71	293.62	99.89
2	4/19/09 8:39	-26.33	293.32	101.32
6	4/19/09 8:40	-25.00	293.03	100.96
7	4/19/09 8:40	-22.34	292.45	100.08
10	4/19/09 8:43	-12.76	290.51	100.14
8	4/19/09 8:45	-1.96	288.44	99.25
9	4/19/09 8:45	-1.93	288.43	99.85
1	4/19/09 8:48	8.83	286.38	101.88
4	4/19/09 8:50	15.73	285.04	100.54
3	4/19/09 8:52	23.54	283.41	100.78



Figure C.18: Summarized predicted Terrasar-X orbit reentry times and locations by ten atmospheric models with a single A/M increase 10 hours prior to original reentry.

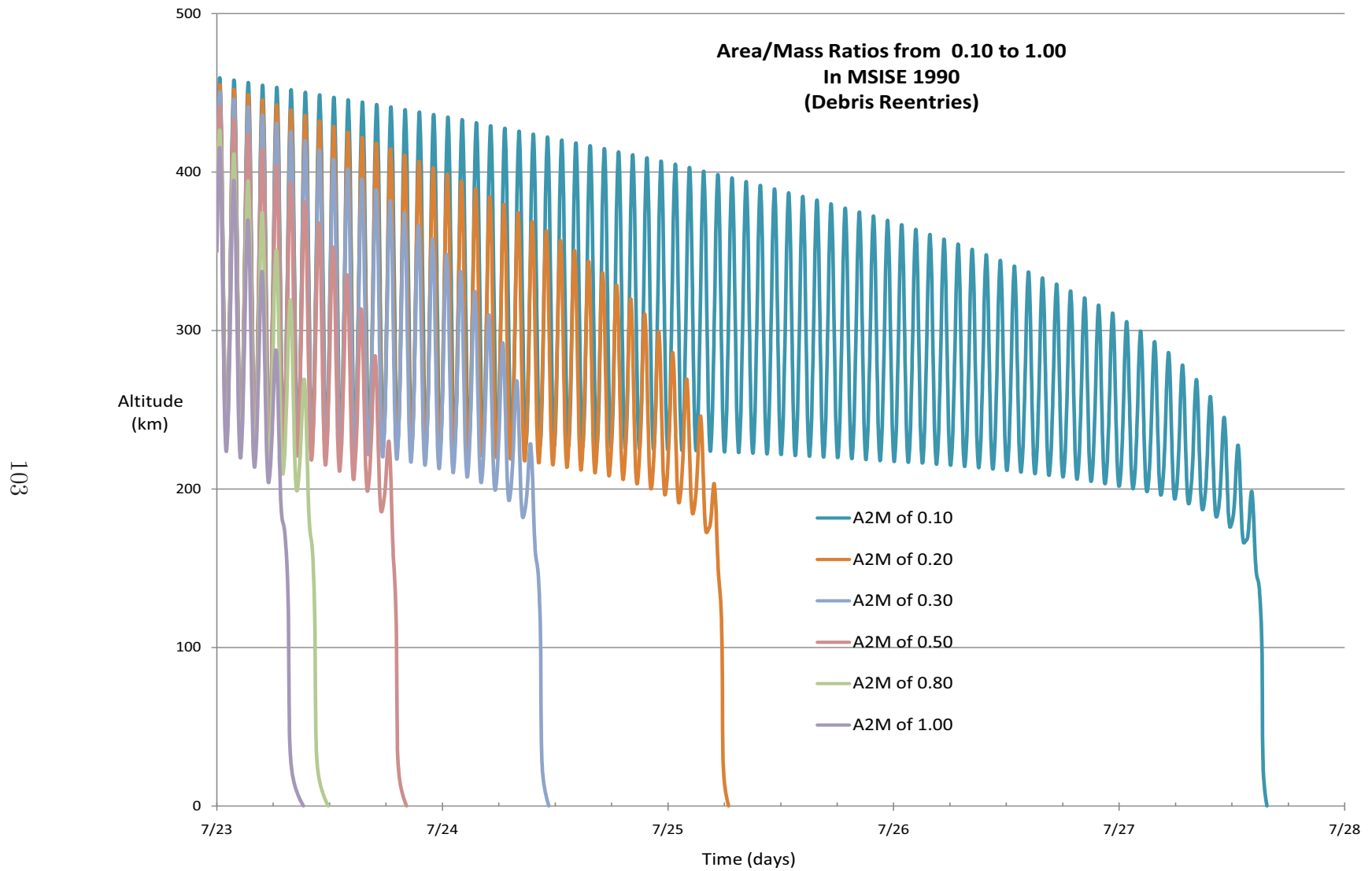


Figure C.19: Homed in Reentry predictions as A/M changes between 0.10 and 1.00 at a single point in orbit path.

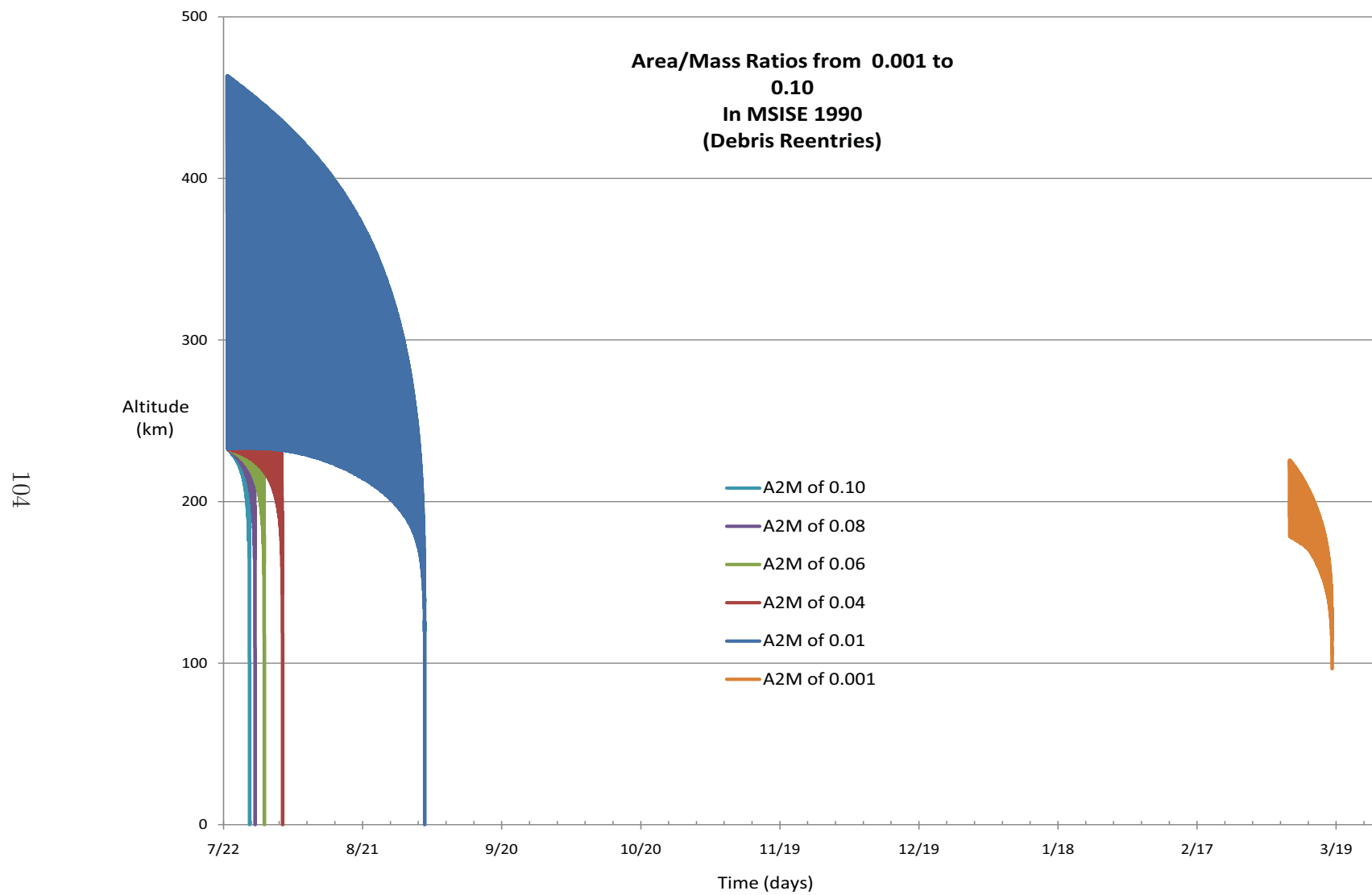


Figure C.20: All reentry predictions as A/M changes between 0.001 and 1.000 at a single point in orbit path.

Bibliography

1. “DoD To Engage Decaying Satellite”. *US Department of Defense News Release*, 14 February 2008.
2. “Russia: US Satellite Shot a Weapons Test”. *The Associated Press*, 16 February 2008.
3. “US satellite shoot-down part of space arms race: Russia”. *Agence France-Presse, AFP*, 17 February 2008.
4. <http://nssdc.gsfc.nasa.gov/nmc/masterCatalog.do?sc=1964-004A>. Technical report, National Aeronautics and Space Administration, 1964.
5. *Interagency Report on Orbital Debris*. Technical report, The White House, Washington D.C., 1995.
6. *Technical Report on Space Debris*. Technical report, United Nations, New York, 1999.
7. “DoD Succeeds In Intercepting Non-Functioning Satellite”. *US Department of Defense News Release*, 20 February 2008.
8. *IADC Space Debris Mitigation Guidelines*. Inter-Agency Space Debris Coordination Committee, September 2007.
9. *Process for Limiting Orbital Debris*. 8719.14. National Aeronautics and Space Administration, Washington, DC 20546, 2 edition, August 2007.
10. *Handbook For Limiting Orbital Debris*. 8719.14. National Aeronautics and Space Administration, Washington, DC 20546, baseline edition, July 2008.
11. *NASA Procedural Requirements for Limiting Orbital Debris*. National Aeronautics and Space Administration, 2008.
12. “Neither Perpendicular nor Parallel”. *NASA-JPL-UCSD-JSC*, 2008.
13. *Note verbale dated 19 December 1978 from the Permanent Representative of Canada to the United Nations addressed to the Secretary-General*. Technical report, United Nations, General Assembly, Committee on The Peaceful Uses of Outer Space A/AC.105/236, 78-3263, 22 December 1978.
14. “Satellite Debris Analysis Indicates Hydrazine Tank Hit”. *US Department of Defense News Release*, 25 February 2008.
15. *U.S Standard Atmosphere 1976*. National Oceanic and Atmospheric Administration, National Aeronautics and Space Administration, USAF, October 1976.
16. http://grin.hq.nasa.gov/ABSTRACTS/GPN_2000-001896.html. “Test inflation of a PAGEOS satellite in a blimp hangar at Weeksville, North Carolina”. *NASA*, 1965.

17. Carmen Pardini, Paula H. Krisko, Toshiya Hanada. *Benefits and Risks of Using Electrodynamic Tethers to De-Orbit Spacecraft*. Report IAC-06-B6.2.10, Inter-Agency Space Debris Coordination Committee, October 2006.
18. Dr. Russell P. Patera, Dr. William H. Ailor. "The Realities of Reentry Disposal". *Advances in Astronautical Sciences*, 99:1059–1071, February 1998.
19. Esker, David. *Galileo's Square-Cube Law*, chapter 1. <http://dinosaurtheory.com>, 2008.
20. Galileo Galilei, Translated by Henry Crew and Alfonso de Salvio of Northwestern University. *Dialogues Concerning TWO NEW SCIENCES*. Macmillan, 1914.
21. Hansen, James R. *Spaceflight Revolution*. NASA Langley Research Center, 1995.
22. Hedin, A. E. "MSIS Model 1986". NASA, 2009.
23. Hedin, A. E. "NRLMSISE-00: A New Empirical Model of the Atmosphere". *US Naval Research Laboratory*, 2009.
24. <http://www.orbitaldebris.jsc.nasa.gov/reentry/recovered.html>. *Recovered Objects*. Technical report, National Aeronautics and Space Administration, 2005.
25. Kunihiro Tatsuzawa (College of International Relations, Ritsumeikan University). *Settlement of Claim between Canada and the Union of Soviet Socialist Republics for Damage Caused by Cosmos 954*. Technical report, Chuogakuin University Local Autonomy Research Center, Space Law, Database 3-2-2 Legal Texts Number 1, 2 April 1981.
26. J.C. Liou, N.L. Johnson and N.M. Hill. "Stabilizing the Future LEO Debris Environment with Active Debris Removal". *Orbital Debris Quarterly News*, 12(4):12, October 2008.
27. Jr., Dewey L. Clemmons. *The Echo 1 Inflation System*, NASA TN D-2194. Technical report, National Aeronautics and Space Administration, June 1964.
28. McGuire, Dr. Robert. "About Atmospheric Models at SPDF". NASA, 2009.
29. Myers, Steven Lee. "Look Out Below. The Arms Race in Space May Be On". *The New York Times*, 9 March 2008.
30. Olsen, Richard Christopher. *Introduction to the Space Environment*. Naval Postgraduate School, January 2003.
31. Shanker, Thom. "An Errant Satellite Is Gone, but Questions Linger". *The New York Times*, 22 February 2008.
32. Simmon, Robert. "Unusual Activity during the Solar Minimum". *Earth Observatory website*, NASA, 2005.
33. Tascione, Thomas F. *Introduction To The Space Environment*. Krieger Publishing Company, second edition edition, 1994.

34. Teichman, Louis A. *The Fabrication and Testing of Pageos 1*, NASA TN D-4596. Technical report, National Aeronautics and Space Administration, June 1968.
35. W. David Compton, Charles D. Benson. *Living and Working in Space - A History of Skylab*. Scientific and Technical Information Branch, NASA, Washington DC, 1983, SP-4208.
36. Weiss, Gus W. *The Life and Death of Cosmos 954*. Technical report, U.S. Central Intelligence Agency, Reproduced at National Archives, Sprin 1978. Studies in Intelligence.
37. Wertz, James R. and Wiley J. Larson. *Space Mission Analysis and Design*. Microcosm Press, 2007.
38. Wiesel, Dr. William E. *Spaceflight Dynamics*. McGraw-Hill, 1995.

NONPRINT FORM

1. Type of Product: CD	2. Operating System/Version: Windows	3. New Product or Replacement: New Product	4. Type of File: Excel, PDF, Text files
5. Language/Utility Program: N/A			
6. # of Files/# of Products: 2 PDF 6 Text 188 Excel	7. Character Set:	8. Disk Capacity: 700 MB	
	9. Compatibility: ISO 9660	10. Disk Size:	
11. Title: Satellite Reentry Control Via Surface Area Amplification			
12. Performing Organization: Air Force Institute of Technology Graduate School of Engineering and Management (AFIT/ENY) 2950 Hobson Way WPAFB OH 45433-7765	13. Performing Report #: AFIT-GSS-ENY-09-M01	14. Contract #:	
		15. Program Element #:	
16. Sponsor/Monitor: AFIT/ENY	17. Sponsor/Monitor # Acronym:	19. Project #:	
	18. Sponsor/Monitor #:	20. Task #:	
		21. Work Unit #:	
22. Date: 26 March 2009		23. Classification of Product: UNCLASSIFIED	
24. Security Classification Authority:		25. Declassification/Downgrade Schedule:	
26. Distribution/Availability: UNLIMITED			

27. Abstract:

CD contains text set up files, data Excel files used for plots associated with the AFIT Master's thesis "Satellite Reentry Control Via Surface Area Amplification" written by Captain Salvador Aleman. It also includes the PDF format of the thesis itself. The thesis was completed on Mar of 2009.

28. Classification of Abstract:

UNCLASSIFIED

29. Limitation of Abstract:

N/A

30. Subject Terms:

Reentry Control, Natural Decay,
Surface Area Amplification,
Debris Reentry

30a. Classification of Subject Terms:

UNCLASSIFIED

31. Required Peripherals:**32. # of Physical Records:****33. # of Logical Records:****34. # of Tracks:****35. Record Type:****36. Color:****37. Recording System:****38. Recording Density:****39. Parity:****40. Playtime:****41. Playback
Speed:****42. Video:****43. Text:****44. Still
Photos:****45. Audio:****46. Other:****47. Documentation/Supplemental Information:**

AFIT Master's Thesis "Satellite Reentry Control Via Surface Area Amplification", Mar 2009

48. Point of Contact and Telephone Number:

Dr. William E. Wiesel
William.Wiesel@afit.edu
(937) 785-3636 ext 4312

REPORT DOCUMENTATION PAGE				Form Approved OMB No. 074-0188	
<p>The public reporting burden for this collection of information is estimated to average 1 hour per response, including the time for reviewing instructions, searching existing data sources, gathering and maintaining the data needed, and completing and reviewing the collection of information. Send comments regarding this burden estimate or any other aspect of the collection of information, including suggestions for reducing this burden to Department of Defense, Washington Headquarters Services, Directorate for Information Operations and Reports (0704-0188), 1215 Jefferson Davis Highway, Suite 1204, Arlington, VA 22202-4302. Respondents should be aware that notwithstanding any other provision of law, no person shall be subject to a penalty for failing to comply with a collection of information if it does not display a currently valid OMB control number.</p> <p>PLEASE DO NOT RETURN YOUR FORM TO THE ABOVE ADDRESS.</p>					
1. REPORT DATE (DD-MM-YYYY) 26-03-2009		2. REPORT TYPE Master's Thesis		3. DATES COVERED (From - To) October 2007- March 2009	
4. TITLE AND SUBTITLE Satellite Reentry Control Via Surface Area Amplification				5a. CONTRACT NUMBER	
				5b. GRANT NUMBER	
				5c. PROGRAM ELEMENT NUMBER	
6. AUTHOR(S) Salvador Aleman, Captain, USAF				5d. PROJECT NUMBER	
				5e. TASK NUMBER	
				5f. WORK UNIT NUMBER	
7. PERFORMING ORGANIZATION NAMES(S) AND ADDRESS(S) Air Force Institute of Technology Graduate School of Engineering and Management (AFIT/ENY) 2950 Hobson Way WPAFB OH 45433-7765				8. PERFORMING ORGANIZATION REPORT NUMBER AFIT-GSS-ENY-09-M01	
9. SPONSORING/MONITORING AGENCY NAME(S) AND ADDRESS(ES) Air Force Institute of Technology / ENY				10. SPONSOR/MONITOR'S ACRONYM(S)	
				11. SPONSOR/MONITOR'S REPORT NUMBER(S)	
12. DISTRIBUTION/AVAILABILITY STATEMENT APPROVED FOR PUBLIC RELEASE; DISTRIBUTION UNLIMITED					
13. SUPPLEMENTARY NOTES					
14. ABSTRACT This project endeavors to find whether it is feasible to use an increase in surface area as a way of increasing the drag on an orbiting object, thus decreasing its orbital lifetime. The surface area increase can be achieved by an apparatus that deploys a balloon. The balloon will act as a parachute that will decrease the potential energy of the object through atmospheric drag. This is most effective by objects that reach the Low Earth altitudes of less than 500 kilometers, where an object is encountering a firmer atmospheric density. The project is carried out through propagating three different element sets to reentry using STK®. The orbital paths generated by the software are then graphed in Excel® and presented. The analysis is divided into four main studies. The first study focuses on confirming the effects the atmospheric instability has on the long term predictions of a natural decay. The second study explores how an increase in the scale of the drag, at different points in the orbital path, affects the reentry time. The third study investigates a specific increase of area to mass ratio (A/M) at different points in the trajectory. This is to survey changes in the variability of the reentry time prediction and how the reentry location's variability is altered. To finish off, the last study examines how A/M manipulation affects the reentry time prediction. The project discovered that an increase in A/M decreases the variability in reentry prediction. Furthermore, it discerns the exponential relationship between the time to reentry and the A/M.					
15. SUBJECT TERMS Reentry Control, Surface Area Amplification, Natural Decay, Debris Reentry					
16. SECURITY CLASSIFICATION OF:			17. LIMITATION OF ABSTRACT UU	18. NUMBER OF PAGES 128	19a. NAME OF RESPONSIBLE PERSON Dr. William E. Wiesel, Professor, ENY
REPORT U	ABSTRACT U	c. THIS PAGE U			19b. TELEPHONE NUMBER (Include area code) (719) 785-3636 ext 4312 William.Wiesel@afit.af.mil